UNIVERSITY OF CALGARY

A Comparison Between Numerically Calculated and Formula Based Scattering Coefficients for Anisotropic Media

by

Ayman Suleiman

A THESIS

SUBMITTED TO THE FACULTY OF GRADUATE STUDIES

IN PARTIAL FULFILLMENT OF THE REQUIREMENTS FOR THE

DEGREE OF MASTER OF SCIENCE

DEPARTMENT OF GEOSCIENCE

CALGARY, ALBERTA

September, 2007

Abstract

A numerically based program TAVRT (Tilted Anisotropic Viscoelastic Reflection and Transmission), which calculates scattering coefficients for generally anisotropic media with arbitrary tilt, is tested for isotropic, VTI and monoclinic anisotropic media. The results agree with those of the scattering coefficients calculated via analytical formulae found in the literature. TAVRT is also tested for the HTI case and the results are in good agreement with those calculated using the Seismic Unix program program refRealAziHTI (Rüger, 2001; Stockwell, 1997) which computes the exact scattering coefficients numerically for interfaces between two HTI media having the same symmetry plane.

Formulae for SH-wave scattering coefficients for an interface between two tilted VTI media with angles φ_1 and φ_2 about the x_2-axis have been derived and their results matched very well those of TAVRT.

The program TAVRT can be used to have more confidence about new derived exact and approximate scattering coefficient and group velocity formulae. It can be also used to study more complex anisotropic media.

For tilted VTI media, it is found that the scattering coefficients vary with tilt, but are unaffected by the sign of the tilt angle of the lower medium, i.e., the scattering coefficient for an interface between two tilted VTI media with angles φ_1 and φ_2 and the scattering coefficient for an interface between two tilted VTI media with angles

φ_1 and $-\varphi_2$ are equal.

For tilted VTI media at pre-critical angles of incidence, the magnitude of the reflection coefficient is inversely proportional to the absolute value of the tilt angle of the upper medium. The magnitude of the transmission coefficient is directly proportional to the absolute value of the tilt angle of the upper medium.

In general, the angle of incidence and the angle of reflection are different for tilted VTI media.

Acknowledgements

I would like to thank my supervisor, Professor Edward S. Krebes, for proposing this very interesting research topic. His insightful guidance and encouragements as well as his excellent course on seismic wave propagation helped me achieve many academic and industrial goals. I also wish to thank Professor Edward S. Krebes for correcting my original draft and for his diligent proof reading my thesis.

I also would like to thank my teacher (during my undergraduate studies) and friend Dr. Youcef Bouzidi for his help, support and the many fruitful discussions regarding my thesis.

I also would like to thank Cathy Hubbell, the Geoscience Grad Program Administrator, for the wonderful job she is doing. She always goes out of her way to help students.

I would like to thank my friends Dr. Ziad Abu-Sara and Dr. Mohammed Shehata for their input to my thesis presentation and their support.

I would like to thank my friends Awni Jaradat, Mohammed Al-Samri and Abdulatif Al-Barnawi for being there for me when I needed help and support.

I would like to thank my wife for her love, patience, support, and encouragement.

Dedication

To

my parents: Ahmad and Lubna,

my wife Faiza,

and my kids: Ahmad and Aness.

Table of Contents

List of Tables

List of Figures

List of Abbreviations

Below are listed the important abbreviations used in the text.

HTI	Horizontal transverse isotropy
Im(z)	Imaginary part of the complex number z
P	Compressional mode
qP	Quasi-P
qSH	Quasi-SH
qSV	Quasi-SV
Re(z)	Real part of the complex number z
SH	Vertical shear mode-wave (polarized in plane of propagation)
SV	Horizontal shear-wave mode (polarized orthogonal to propagation plane)
TAVRT	Tilted Anisotropic Viscoelastic Reflection and Transmission
TI	Transverse isotropy
VTI	Vertical transverse isotropy
P1P1	reflection coefficient for the case “incident qP in medium 1 / reflected qP in med 1”
V2P1	transmission coefficient for the case “incident qSV in medium 2 – transmitted qP in medium 1”
H1P1	reflection coefficient for the case “incident qSH in medium 1 – reflected qP in medium 1”

List of Symbols

Below are listed a glossary of symbols and references to equations using them.

Symbol	In equation	Description
σ_{ij}	(2.1)	Stress tensor
$\boldsymbol{\sigma}$	(2.26)	Stress column vector
$\boldsymbol{f}$	(2.1)	Body force
$\boldsymbol{u}$	(2.1)	Displacement vector
ρ	(2.1)	Density
c_{ijkl}	(2.2)	Fourth-order stiffness tensor
$\boldsymbol{C}$	(2.23)	Stiffness matrix
e_{kl}	(2.2)	Second-order strain tensor
$\boldsymbol{e}$	(2.27)	Strain column vector
λ	(2.28)	Lamé's λ constant
μ	(2.28)	Lamé's μ constant
V_{P0}	(2.31)	Velocity of P-wave propagating in the symmetry-axis direction
V_{S0}	(2.31)	Velocity of S-wave propagating in the symmetry-axis direction
ϵ	(2.31)	Thomsen's ϵ parameter
γ	(2.31)	Thomsen's γ parameter
δ	(2.31)	Thomsen's δ parameter

Symbol	In equation	Description
a_{ij}	(2.35)	Direction cosines
$\boldsymbol{M}$	(2.35)	Rotation matrix
$\boldsymbol{U}$	(2.38)	Polarization vector
$\boldsymbol{s}$	(2.39)	Slowness vector
$\boldsymbol{k}$	(2.39)	Wavenumber vector
$\boldsymbol{n}$	(2.39)	Unit vector in the direction of $\boldsymbol{s}$ and $\boldsymbol{k}$
ω	(2.39)	Angular frequency
$\boldsymbol{D}$	(2.44)	Differential-operator matrix
$\boldsymbol{G}$	(2.51)	Christoffel matrix
$\nabla \cdot \boldsymbol{a}$	(2.10)	Divergence of the vector $\boldsymbol{a}$
$\boldsymbol{a}^T$	(2.20)	Transpose of the array $\boldsymbol{a}$
v	(2.39)	Phase velocity
$\boldsymbol{V_E}$	(2.56)	Energy velocity vector
$\boldsymbol{V_G}$	(2.78)	Group velocity vector
$\boldsymbol{d}$	(4.1)	Unit polarization vector
x_1, x_2 ,x_3	(2.1)	Cartesian coordinates
K	(2.6)	Kinetic energy density
$\boldsymbol{I}$	(2.10)	Energy flux vector
W	(2.11)	Potential energy density
E	(2.13)	Total energy density

Chapter 1

Introduction

1.1 Background

The kinetic and dynamic properties of wave propagation in anisotropic media have been the subject of many publications (Daley and Hron (1977), Thomsen (1986), Graebner (1992), Rüger (2001), Carcione (2001), Tsvankin (2005)). However these publications focus on simple anisotropic models such as vertical transverse isotropy (VTI) and horizontal transverse isotropy (HTI), because of their simplicity and abundance in nature. Unfortunately, simple models become invalid for more complicated anisotropic media such as tilted transverse isotropy (TTI) and thin layered media with a multi-fracture orientation system. Consequently the study of more complex anisotropic models becomes necessary.

1.2 Objectives of the Thesis

In 2001, Professor E.S. Krebes developed a theory and a code for the numerical calculation of scattering coefficients at a flat interface between two generally anisotropic media (with up to 21 medium parameters) that can be oriented (tilted) in any arbitrary direction. He called the program TAVRT which stands for "Tilted Anisotropic Viscoelastic Reflection and Transmission". Despite its name, TAVRT does not yet treat the viscoelastic case as it stands. Because TAVRT has not yet been fully tested, the main objective of the thesis is to test the validity of TAVRT program by comparing its results with the results of, as many as possible, existing scattering coefficients analytical formulae.

1.3 Structure of the Thesis

The thesis is composed of seven chapters. Chapter 1 introduces and gives the motivation and objectives of this research. Chapter 2 is devoted to providing some background material on wave propagation in anisotropic, homogeneous and elastic media. Chapter 3 treats the analytical solution of the scattering coefficient problem in anisotropic media, used to validate the results obtained numerically by TAVRT. Chapter 4 presents the theory behind the TAVRT code. Chapter 5 presents the derivation of analytical formulae for the reflection and transmission coefficients of an SH-wave propagating in a VTI medium tilted with an angle φ about the x_2-axis. It then investigates the effect of the tilt on the scattering coefficients. Chapter 6 compares the numerical results obtained by TAVRT and those obtained via the formula based scattering coefficients. The comparison is done for isotropic, VTI, tilted VTI, and monoclinic media. For HTI media, the comparison is done between the results obtained by the program TAVRT and those obtained by the Seismic Unix program refRealAziHTI (Rüger, 2001; Stockwell, 1997). Finally, chapter 7 concludes the present research and gives some recommendations for future work.

1.4 Contributions of the Thesis

The contributions of this thesis are:

- A presentation of the daunting theory of the scattering coefficient computation in generally anisotropic (with up to 21 medium parameters) and oriented (tilted) in any arbitrary direction in an easy way.

- A derivation of SH-wave scattering coefficients formulae for an interface between two tilted VTI media with angles φ_1 and φ_2 about the x_2-axis.

- Checked and re-derived the theory behind TAVRT.

- Modifications of TAVRT:

  - Converted TAVRT into a MATLAB function
  - The coordinate transformation of the stiffness matrix is done now outside TAVRT
  - The input parameters were all over the code and now they are passed as input function arguments

- Implementation of codes to calculate the :

  - Exact scattering coefficients for interfaces between two isotropic media
  - Exact scattering coefficients for interfaces between two VTI media
  - Exact SH reflection and transmission coefficients for interfaces between two tilted VTI media with angles φ_1 and φ_2 about the x_2-axis

- The conversion of the Seismic Unix program refRealAziHTI (Rüger, 2001; Stockwell, 1997) to MATLAB.

- Investigated the effect of tilt on the SH reflection and transmission coefficients for interfaces between two tilted VTI media with angles φ_1 and φ_2 about the x_2-axis.

- The testing of TAVRT for isotropic, VTI, tilted VTI, HTI and monoclinic media.

- Chapters 1 to 4 are mostly a review of known material while chapters 5 and 6 are essentially new.

Chapter 2

Review of Anisotropic Wave Propagation

In general, anisotropy is the dependence of the physical properties of a medium on the direction. Thomsen (2002) defined seismic anisotropy as “the dependence of seismic velocity upon angle”. This is a simple but yet accurate definition of seismic anisotropy. A seismic wave produced by a point source travels through different directions of an anisotropic medium with different velocities which produces a non-spherical wavefront.

Heterogeneity is the dependence of the physical properties of a medium on the position. Heterogeneity on the small scale (smaller than the seismic wavelength) appears as anisotropy on the large scale (Thomsen, 2002).

Anisotropy can be caused by the preferred orientation of anisotropic mineral grains or the preferred orientation of the shapes of isotropic minerals. It can be also caused by a stack of isotropic layers having thicknesses smaller than the seismic wavelength, in which case the stack of layers can be treated as a single anisotropic medium (Backus, 1962) . Another common cause of anisotropy is the existence of fractures and cracks (Thomsen, 1986) in a material.

This chapter is devoted to providing some background material on wave propagation in anisotropic, homogeneous and elastic media. The main idea of this chapter is that, for anisotropic, homogeneous and elastic media, the direction of the wave vector and the direction of energy flow (the ray direction) do not coincide, which means that the phase velocity is generally different from the energy velocity. The energy velocity vector is identical to the group velocity vector and has the same direction as the energy flux vector.

2.1 Equation of Motion and Hooke's Law

The equation of motion for a general anisotropic and heterogenous medium comes from the application of Newton's second law to a volume element ΔV within a continuum (Krebes, 2001) . It is given by

$$\frac{\partial \sigma_{ij}}{\partial x_j} + f_i = \rho \frac{\partial^2 u_i}{\partial t^2}, \qquad i = 1, 2, 3 \tag{2.1}$$

where σ_{ij} is the stress tensor, x_1, x_2 and x_3 are the cartesian coordinates, $\boldsymbol{f} = (f_1, f_2, f_3)$ is the body force, ρ is the density and $\boldsymbol{u} = (u_1, u_2, u_3)$ is the displacement vector. The summation convention is used in equation 2.1 and in the remainder of the thesis, i.e., if a term contains a doubly-repeated index, then a sum is performed over that index (unless otherwise indicated).

Notice that the equation of motion (2.1) depends on two unknowns: the stress tensor σ_{ij} and the displacement $\boldsymbol{u}$. Therefore, to solve it for the displacement $\boldsymbol{u}$, we need to find a relation that links the two unknowns. It is reasonable to consider the stress resulting from a seismic wave experiment to be small, which allows us to treat sedimentary rock as a linear elastic material. Under this condition, the relationship between the stress and strain is linear and is given by the generalized Hooke law

$$\sigma_{ij} = c_{ijkl} e_{kl} \qquad i, j = 1, 2, 3 \tag{2.2}$$

where c_{ijkl} is the fourth-order stiffness tensor and e_{kl} is the second-order strain tensor.

The stress σ_{ij} produces the strain e_{kl}. The dimensions of stress are force per unit area. The strain e_{kl} describes the change of shape of a medium under stress and is defined by

$$e_{kl} = \frac{1}{2}\Big(\frac{\partial u_k}{\partial x_l} + \frac{\partial u_l}{\partial x_k}\Big) \tag{2.3}$$

The stress and strain tensors are symmetric, i.e., $\sigma_{ij} = \sigma_{ji}$ and $e_{kl} = e_{lk}$. Another convenient form of Hooke's law is given as follows (Krebes, 2001):

$$\sigma_{ij} = c_{ijkl}\frac{\partial u_l}{\partial x_k} = c_{ijkl}\frac{\partial u_k}{\partial x_l} \qquad i, j = 1, 2, 3 \tag{2.4}$$

Hooke's law given by equation 2.2 holds for the general case of a linearly elastic, heterogenous and anisotropic medium but doesn't hold for a dissipative (anelastic) medium (Krebes, 2001).

Replacing the stress tensor in the equation of motion 2.1 by its definition given in equation 2.4, we obtain the equation of motion for a generally anisotropic, elastic and homogeneous medium:

$$c_{ijkl}\frac{\partial^2 u_k}{\partial x_j \partial x_l} + f_i = \rho\frac{\partial^2 u_i}{\partial t^2} \tag{2.5}$$

2.2 Conservation of Energy

We can derive a conservation of energy for the equation of motion of equation 2.1 by taking its dot product with the velocity vector $\dot{\boldsymbol{u}}$ (Krebes, 2001), and we have

$$\frac{\partial \sigma_{ij}}{\partial x_j}\dot{u}_i + f_i\dot{u}_i = \frac{\partial K}{\partial t} \tag{2.6}$$

where K is known as the kinetic energy density and is defined as follows:

$$K = \frac{1}{2}\rho\Big(\frac{\partial u_i}{\partial t}\Big)^2 \tag{2.7}$$

Applying the rule for the differentiation of a product, we can write the first term of the left hand side of equation 2.6 as follows:

$$\frac{\partial \sigma_{ij}}{\partial x_j}\dot{u}_i = \frac{\partial}{\partial x_j}\big(\sigma_{ij}\dot{u}_i\big) - \sigma_{ij}\frac{\partial \dot{u}_i}{\partial x_j} \tag{2.8}$$

Letting "$,j$" denote partial differentiation with respect to x_j, the last term in equation 2.8, can be written as follows:

$$\sigma_{ij}\dot{u}_{i,j} = \frac{1}{2}\big(\sigma_{ij}\dot{u}_{i,j} + \sigma_{ij}\dot{u}_{i,j}\big) = \frac{1}{2}\big(\sigma_{ij}\dot{u}_{i,j} + \sigma_{ji}\dot{u}_{j,i}\big) = \frac{1}{2}\sigma_{ij}\big(\dot{u}_{i,j} + \dot{u}_{j,i}\big) = \sigma_{ij}\dot{e}_{ij} \tag{2.9}$$

where the symmetry of the stress tensor was used in the next-to-last step. Substituting equations 2.8 and 2.9 into equation 2.6, we get:

$$\frac{\partial K}{\partial t} + \frac{\partial W}{\partial t} = -\boldsymbol{\nabla}\cdot\boldsymbol{I} + \boldsymbol{f}\cdot\frac{\partial \boldsymbol{u}}{\partial t} \tag{2.10}$$

where $\boldsymbol{I}$ is the intensity, or the energy flux vector, given as follows:

$$I_j = -\sigma_{ij}\frac{\partial u_i}{\partial t} \tag{2.11}$$

and W is the potential energy density or the strain energy density, given implicitly as follows:

$$\frac{\partial W}{\partial t} = \sigma_{ij}\frac{\partial e_{ij}}{\partial t} \tag{2.12}$$

The effects of body forces, e.g., gravity, on the propagation of seismic waves is usually negligible, hence we can write equation 2.10 as follows:

$$\frac{\partial E}{\partial t} = -\boldsymbol{\nabla}\cdot\boldsymbol{I} \tag{2.13}$$

where $E = K + W$ is the total energy density. Equation 2.13 is usually known as the equation of the continuity for the energy density (Krebes, 2001).

2.3 Strain Energy Density

So far, we have not given an explicit general formula for the strain energy density W. All we know is its rate of change given by equation 2.12. Assume that the strain energy density W is a function of all the strain components as follows (Krebes, 2001):

$$W = W\big(e_{11}, e_{12}, \cdots, e_{33}\big) \tag{2.14}$$

Applying the chain rule we have:

$$\frac{\partial W}{\partial t} = \frac{\partial W}{\partial e_{11}}\frac{\partial e_{11}}{\partial t} + \frac{\partial W}{\partial e_{12}}\frac{\partial e_{12}}{\partial t} + \cdots + \frac{\partial W}{\partial e_{33}}\frac{\partial e_{33}}{\partial t} = \frac{\partial W}{\partial e_{ij}}\frac{\partial e_{ij}}{\partial t} \tag{2.15}$$

From equations 2.12 and 2.15 we have

$$\sigma_{ij}\frac{\partial e_{ij}}{\partial t} = \frac{\partial W}{\partial e_{ij}}\frac{\partial e_{ij}}{\partial t} \tag{2.16}$$

For equation 2.16 to be true for all possible stress-strain fields, we must have

$$\sigma_{ij} = \frac{\partial W}{\partial e_{ij}}, \qquad i,j = 1,2,3 \tag{2.17}$$

To get a better insight on equation 2.17, we make the analogy with the notion of basic physics that states that the force is derived from the potential energy. In the context of elasticity theory we say that the stress tensor σ_{ij} is derived from the potential energy density W.

Substituting equation 2.2 into equation 2.17, we get

$$\frac{\partial W}{\partial e_{ij}} = c_{ijkl}e_{kl}, \qquad i,j = 1,2,3 \tag{2.18}$$

The explicit form of the strain energy density W can be obtained by integrating both sides of equation 2.18:

$$W = \frac{1}{2}c_{ijkl}e_{kl}e_{ij} \tag{2.19}$$

or

$$W = \frac{1}{2}\boldsymbol{e}^T \boldsymbol{C}\boldsymbol{e} \tag{2.20}$$

where $\boldsymbol{C}$ and $\boldsymbol{e}$ are defined in equations 2.23 and 2.27 below.

2.4 Symmetry of Stiffness Tensor

The second-order stress and strain tensors σ_{ij} and e_{kl} have $3^2 = 9$ components each, but only 6 of them are independent. This is due to the fact that σ_{ij} and e_{kl} are symmetric, which means that $\sigma_{ij} = \sigma_{ji}$ and $e_{kl} = e_{lk}$.

The stiffness tensor c_{ijkl} has the following symmetry properties:

$$\begin{array}{lll} c_{ijkl} = c_{jikl}, & \text{because} & \sigma_{ij} = \sigma_{ji} \\ c_{ijkl} = c_{ijlk}, & \text{because} & e_{ij} = e_{ij} \\ c_{ijkl} = c_{klij}, & \text{because} & \partial^2 W/\partial e_{ij}\partial e_{kl} = \partial^2 W/\partial e_{kl}\partial e_{ij} \end{array} \tag{2.21}$$

The second-order stiffness tensor c_{ijkl} has $3^4 = 81$ components, but because of the stiffness tensor symmetries, only 21 of them are independent. Therefore, only 21 medium parameters are required to describe the most general anisotropic medium, and we can represent the stiffness tensor c_{ijkl} by the following 6×6 symmetric matrix:

$$\boldsymbol{c} = \begin{pmatrix} c_{1111} & c_{1122} & c_{1133} & c_{1123} & c_{1113} & c_{1112} \\ c_{1122} & c_{2222} & c_{2233} & c_{2223} & c_{2213} & c_{2212} \\ c_{1133} & c_{2233} & c_{3333} & c_{3323} & c_{3313} & c_{3312} \\ c_{1123} & c_{2223} & c_{3323} & c_{2323} & c_{2313} & c_{2312} \\ c_{1113} & c_{2213} & c_{1113} & c_{2313} & c_{1313} & c_{1312} \\ c_{1112} & c_{2212} & c_{3312} & c_{2312} & c_{1312} & c_{1212} \\ \end{pmatrix} \tag{2.22}$$

By using the well known Voigt notation which relates each element c_{ijkl} of the

Table 2.1: Voigt Notation

ij	m
11	1
22	2
33	3
23	4
13	5
12	6

stiffness tensor to the c_{mn} of the 6×6 stiffness matrix (see table , we can rewrite equation 2.22 as follows

$$\boldsymbol{C} = \begin{pmatrix} c_{11} & c_{12} & c_{13} & c_{14} & c_{15} & c_{16} \\ c_{12} & c_{22} & c_{23} & c_{24} & c_{25} & c_{26} \\ c_{13} & c_{23} & c_{33} & c_{34} & c_{35} & c_{36} \\ c_{14} & c_{24} & c_{34} & c_{44} & c_{45} & c_{46} \\ c_{15} & c_{25} & c_{15} & c_{45} & c_{55} & c_{56} \\ c_{16} & c_{26} & c_{36} & c_{46} & c_{56} & c_{66} \end{pmatrix} \tag{2.23}$$

where $c_{ij} = c_{ji}$ and equation 2.2 can be rewritten as

$$\begin{pmatrix} \sigma_{11} \\ \sigma_{22} \\ \sigma_{33} \\ \sigma_{23} \\ \sigma_{13} \\ \sigma_{12} \end{pmatrix} = \begin{pmatrix} c_{11} & c_{12} & c_{13} & c_{14} & c_{15} & c_{16} \\ c_{12} & c_{22} & c_{23} & c_{24} & c_{25} & c_{26} \\ c_{13} & c_{23} & c_{33} & c_{34} & c_{35} & c_{36} \\ c_{14} & c_{24} & c_{34} & c_{44} & c_{45} & c_{46} \\ c_{15} & c_{25} & c_{15} & c_{45} & c_{55} & c_{56} \\ c_{16} & c_{26} & c_{36} & c_{46} & c_{56} & c_{66} \end{pmatrix} \begin{pmatrix} e_{11} \\ e_{22} \\ e_{33} \\ 2e_{23} \\ 2e_{13} \\ 2e_{12} \end{pmatrix} \tag{2.24}$$

or in a concise way as

$$\boldsymbol{\sigma} = \boldsymbol{C}\boldsymbol{e} \tag{2.25}$$

where $\boldsymbol{\sigma}$ and $\boldsymbol{e}$ are defined as follows:

$$\boldsymbol{\sigma} = (\sigma_1, \sigma_2, \sigma_3, \sigma_4, \sigma_5, \sigma_6)^T = (\sigma_{11}, \sigma_{22}, \sigma_{33}, \sigma_{23}, \sigma_{13}, \sigma_{12})^T \tag{2.26}$$

$$\boldsymbol{e} = (e_1, e_2, e_3, e_4, e_5, e_6)^T = (e_{11}, e_{22}, e_{33}, 2e_{23}, 2e_{13}, 2e_{12})^T \tag{2.27}$$

The stiffness matrix given by equation 2.23 represents the most general anisotropic model which is known as the triclinic model.

So far, triclinic models have not been used in seismological applications, because of the large number of independent parameters (Tsvankin, 2005) and because no geophysical survey can measure all these parameters (Thomsen, 2002).

The simplest stiffness matrix is the one for isotropic symmetry. While isotropic symmetry is very useful for understanding wave propagation, it fails to describe all the effects we see in the data we record (Thomsen, 2002). The stiffness matrix for isotropy contains only two independent elastic parameters, λ and μ, the well known Lamé constants, and is given by

$$\boldsymbol{C}^{(iso)} = \begin{pmatrix} \lambda+2\mu & \lambda & \lambda & 0 & 0 & 0 \\ \lambda & \lambda+2\mu & \lambda & 0 & 0 & 0 \\ \lambda & \lambda & \lambda+2\mu & 0 & 0 & 0 \\ 0 & 0 & 0 & \mu & 0 & 0 \\ 0 & 0 & 0 & 0 & \mu & 0 \\ 0 & 0 & 0 & 0 & 0 & \mu \end{pmatrix} \tag{2.28}$$

A more realistic but yet simple anisotropy model is the transversely isotropic (TI) symmetry known also as hexagonal symmetry or polar symmetry. This type of anisotropy has only one axis of rotational symmetry. It is called vertical transverse isotropy (VTI) when the axis of symmetry is vertical (with respect to the Earth's surface), horizontal transverse isotropy (HTI) when the axis of symmetry is horizontal and tilted transverse isotropy (TTI) when the axis of symmetry is tilted.

The TI stiffness matrix has the same form as the isotropic stiffness matrix but (in terms of the locations of the zero and non-zero elements) has five independent elastic parameters and is given, for the case of a VTI medium, by (Tsvankin, 2005)

$$\boldsymbol{C}^{(vti)} = \begin{pmatrix} c_{11} & c_{11} - 2c_{66} & c_{13} & 0 & 0 & 0 \\ c_{11} - 2c_{66} & c_{11} & c_{13} & 0 & 0 & 0 \\ c_{13} & c_{13} & c_{33} & 0 & 0 & 0 \\ 0 & 0 & 0 & c_{55} & 0 & 0 \\ 0 & 0 & 0 & 0 & c_{55} & 0 \\ 0 & 0 & 0 & 0 & 0 & c_{66} \end{pmatrix} \tag{2.29}$$

and for the case of HTI medium, by (Tsvankin, 2005)

$$\boldsymbol{C}^{(hti)} = \begin{pmatrix} c_{11} & c_{13} & c_{13} & 0 & 0 & 0 \\ c_{13} & c_{33} & c_{33} - 2c_{44} & 0 & 0 & 0 \\ c_{13} & c_{33} - 2c_{44} & c_{33} & 0 & 0 & 0 \\ 0 & 0 & 0 & c_{44} & 0 & 0 \\ 0 & 0 & 0 & 0 & c_{55} & 0 \\ 0 & 0 & 0 & 0 & 0 & c_{55} \end{pmatrix} \tag{2.30}$$

Thomsen (1986) suggested replacing the five independent elastic parameters for a VTI medium with two vertical velocities and three dimensionless anisotropy parameters, defined by

$$
\begin{aligned}
V_{P0} &\equiv \sqrt{c_{33}/\rho} \\
V_{S0} &\equiv \sqrt{c_{55}/\rho} \\
\epsilon &\equiv (c_{11} - c_{33})/(2c_{33}) \\
\gamma &\equiv (c_{66} - c_{55})/(2c_{55}) \\
\delta &\equiv ((c_{13} + c_{55})^2 - (c_{33} - c_{55})^2)/(2c_{33}(c_{33} - c_{55}))
\end{aligned}
\tag{2.31}
$$

where V_{P0} and V_{S0} are the vertical P wave and S wave velocities.

The most realistic simple anisotropy model is the orthorhombic symmetry model (Bakulin et al., 2000b). An orthorhombic medium is characterized by three mutually orthogonal planes of symmetry. For example, an orthorhombic medium can be used to model a set of thin horizontal layers with a set of parallel vertical fractures, and in this case one of the symmetry planes is horizontal and the other two are parallel and perpendicular to the fractures. The medium coordinate system has the symmetry planes as coordinate planes. If we choose the cartesian coordinate system to coincide with the medium coordinate system, the stiffness matrix will have nine independent parameters, as follows (Tsvankin, 2005)

$$
\boldsymbol{C}^{(ort)} = \begin{pmatrix}
c_{11} & c_{12} & c_{13} & 0 & 0 & 0 \\
c_{12} & c_{22} & c_{23} & 0 & 0 & 0 \\
c_{13} & c_{23} & c_{33} & 0 & 0 & 0 \\
0 & 0 & 0 & c_{44} & 0 & 0 \\
0 & 0 & 0 & 0 & c_{55} & 0 \\
0 & 0 & 0 & 0 & 0 & c_{66}
\end{pmatrix}
\tag{2.32}
$$

A symmetry model with one plane of mirror symmetry is known as the monoclinic system. Such a system can be formed, for example, by two systems of parallel vertical fractures, making between them an angle other than 0° or 90°. A monoclinic medium with $x_1 - x_3$ plane of symmetry has the following form for the stiffness matrix:

$$\boldsymbol{C}^{(mnc)} = \begin{pmatrix} c_{11} & c_{12} & c_{13} & 0 & c_{15} & 0 \\ c_{12} & c_{22} & c_{23} & 0 & c_{25} & 0 \\ c_{13} & c_{23} & c_{33} & 0 & c_{35} & 0 \\ 0 & 0 & 0 & c_{44} & 0 & c_{46} \\ c_{15} & c_{25} & c_{35} & 0 & c_{55} & 0 \\ 0 & 0 & 0 & c_{46} & 0 & c_{66} \end{pmatrix} \tag{2.33}$$

It is necessary to be able to define how the stiffness matrix transforms in an arbitrary cartesian coordinate system.

Let $\boldsymbol{C}$ be the stiffness matrix of a given medium, in the medium coordinate system (x_1, x_2, x_3), and let $\boldsymbol{C}'$ be the stiffness matrix of the same medium but in a different coordinate system (x_1', x_2', x_3'). It can be shown that (Mavko et al., 2003; Carcione, 2001)

$$\boldsymbol{C}' = \boldsymbol{M}\boldsymbol{C}\boldsymbol{M}^T \tag{2.34}$$

where

$$\boldsymbol{M} = \begin{pmatrix} a_{11}^2 & a_{12}^2 & a_{13}^2 & 2a_{12}a_{13} & 2a_{13}a_{11} & 2a_{11}a_{12} \\ a_{21}^2 & a_{22}^2 & a_{23}^2 & 2a_{22}a_{23} & 2a_{23}a_{21} & 2a_{21}a_{22} \\ a_{31}^2 & a_{32}^2 & a_{33}^2 & 2a_{32}a_{33} & 2a_{33}a_{31} & 2a_{31}a_{32} \\ a_{21}a_{31} & a_{22}a_{32} & a_{23}a_{33} & a_{22}a_{33} + a_{23}a_{32} & a_{21}a_{33} + a_{23}a_{31} & a_{22}a_{31} + a_{21}a_{32} \\ a_{31}a_{11} & a_{32}a_{12} & a_{33}a_{13} & a_{12}a_{33} + a_{13}a_{32} & a_{13}a_{31} + a_{11}a_{33} & a_{11}a_{32} + a_{12}a_{31} \\ a_{11}a_{21} & a_{12}a_{22} & a_{13}a_{23} & a_{12}a_{23} + a_{13}a_{22} & a_{13}a_{21} + a_{11}a_{23} & a_{11}a_{22} + a_{12}a_{21} \end{pmatrix} \tag{2.35}$$

where a_{ij} are the direction cosines defined as the cosine of the angle between the x_i'-axis and the x_j-axis.

2.5 Stability Conditions of Elastic Parameters

The strain energy density W provides the only constraints on the elastic parameters c_{ijkl} (Slawinski, 2003). These constraints, known also as the stability conditions, guarantee that the medium is stable; i.e., remains undeformed if energy is not expended.

We can write the strain energy density W of equation 2.19, in a concise way, as follows

$$W = \frac{1}{2}\big(\boldsymbol{e}^T \boldsymbol{C}\,\boldsymbol{e}\big) \tag{2.36}$$

where $\boldsymbol{C}$ is the stiffness matrix given in equation 2.23 and $\boldsymbol{e}$ is the strain vector shown in equation 2.27 (Slawinski, 2003).

Generally, the energy is positive unless the material is undeformed, in which case the strain energy density is null. This means that we have the following stability condition

$$\frac{1}{2}\big(\boldsymbol{e}^T \boldsymbol{C}\,\boldsymbol{e}\big) > 0 \qquad \text{for all } \boldsymbol{e}\text{, with } \boldsymbol{e} \neq 0 \tag{2.37}$$

Equation 2.37 means that for the medium to be stable, the stiffness matrix $\boldsymbol{C}$ should be positive-definite.

2.6 Christoffel Equation

Consider the plane wave

$$\boldsymbol{u} = \boldsymbol{U}\, e^{i\omega(\boldsymbol{s}\cdot\boldsymbol{x}-t)} = \boldsymbol{U}\, e^{i(\boldsymbol{k}\cdot\boldsymbol{x}-\omega\, t)} \tag{2.38}$$

as a trial solution for equation 2.1, where $\boldsymbol{U} = (U_1, U_2, U_3)$ is the polarization vector, ω is the angular frequency and $\boldsymbol{s}$ and $\boldsymbol{k}$ are the slowness and wavenumber vectors defined by

$$\boldsymbol{s} = \frac{\boldsymbol{n}}{v} \quad \text{and} \quad \boldsymbol{k} = \frac{\omega}{v}\boldsymbol{n} \tag{2.39}$$

where $\boldsymbol{n}$ is a unit vector in the direction of $\boldsymbol{s}$ and $\boldsymbol{k}$, i.e. the direction of wave propagation, and v is the velocity of wave propagation, also known as the phase velocity.

The time derivative of the displacement vector, i.e. the particle velocity, is given as follows:

$$\dot{\boldsymbol{u}} = \partial_t \boldsymbol{u} = -i\,\omega\,\boldsymbol{u} \tag{2.40}$$

which means that the following replacement can be made in mathematical manipulations involving plane harmonic waves:

$$\partial_t \rightarrow -i\,\omega \tag{2.41}$$

The spatial derivative of the displacement vector is given as follows:

$$\partial_j \boldsymbol{u} = i\,k\,n_j\,\boldsymbol{u} = i\,\omega\,s_j\,\boldsymbol{u}, \quad j = 1, 2, 3 \tag{2.42}$$

which means that the following replacement can be made in mathematical manipulations involving plane harmonic waves:

$$\partial_j \rightarrow i\,k\,n_j, \quad j = 1, 2, 3 \tag{2.43}$$

Let $\boldsymbol{D}$ be the differential-operator matrix defined as follows (Carcione, 2001):

$$\boldsymbol{D} = \begin{pmatrix} \partial_1 & 0 & 0 & 0 & \partial_3 & \partial_2 \\ 0 & \partial_2 & 0 & \partial_3 & 0 & \partial_1 \\ 0 & 0 & \partial_3 & \partial_2 & \partial_1 & 0 \end{pmatrix} \tag{2.44}$$

The differential-operator matrix $\boldsymbol{D}$ can be replaced by (Carcione, 2001):

$$\boldsymbol{D} \rightarrow i\,k \begin{pmatrix} n_1 & 0 & 0 & 0 & n_3 & n_2 \\ 0 & n_2 & 0 & n_3 & 0 & n_1 \\ 0 & 0 & n_3 & n_2 & n_1 & 0 \end{pmatrix} = i\,k\,\boldsymbol{L} \tag{2.45}$$

or by:

$$\boldsymbol{D} \rightarrow i\,\omega \begin{pmatrix} s_1 & 0 & 0 & 0 & s_3 & s_2 \\ 0 & s_2 & 0 & s_3 & 0 & s_1 \\ 0 & 0 & s_3 & s_2 & s_1 & 0 \end{pmatrix} = i\,w\,\boldsymbol{S} \tag{2.46}$$

From equations 2.3 and 2.27, the strain vector $\boldsymbol{e}$ can be rewritten as:

$$\boldsymbol{e} = \boldsymbol{D}^T \boldsymbol{u} \tag{2.47}$$

Using the differential-operator matrix $\boldsymbol{D}$, the equation of motion 2.1 becomes

$$\boldsymbol{D}\boldsymbol{\sigma} + \boldsymbol{f} = \rho \partial_t^2 \boldsymbol{u} \tag{2.48}$$

Combining equations 2.25, 2.47 and 2.48 we obtain

$$\boldsymbol{D}\Big[\boldsymbol{C}\big(\boldsymbol{D}^T \boldsymbol{u}\big)\Big] + \boldsymbol{f} = \rho \partial_t^2 \boldsymbol{u} \tag{2.49}$$

Substituting equations 2.41 and 2.45 into equation 2.49 and dropping the body force $\boldsymbol{f}$ we obtain

$$k^2\boldsymbol{G}\boldsymbol{u} = \rho\omega^2\boldsymbol{u} \tag{2.50}$$

where

$$\boldsymbol{G} = \boldsymbol{L}\boldsymbol{C}\boldsymbol{L}^T \tag{2.51}$$

is known as the Christoffel matrix.

From equation 2.39 and 2.50 we obtain the so-called Christoffel equation

$$\big(\boldsymbol{G} - \rho v^2\boldsymbol{I}_{(3)}\big)\boldsymbol{U} = 0 \tag{2.52}$$

where $\boldsymbol{I}_{(3)}$ is the 3×3 identity matrix.

The Christoffel matrix $\boldsymbol{G}$ can also be rewritten as follows

$$G_{ik} = c_{ijkl}n_jn_l \tag{2.53}$$

Note that, from the symmetry properties of the stiffness tensor, we have:

$$G_{ik} = c_{ijkl}n_jn_l = c_{klij}n_ln_j = G_{ki} \tag{2.54}$$

which means that Christoffel matrix $\boldsymbol{G}$ is symmetric. In addition, Christoffel matrix $\boldsymbol{G}$ is positive-definite (Tsvankin, 2005).

Note that equation 2.52 is an eigenvalue equation with eigenvalue ρv^2 and eigenvector $\boldsymbol{U}$ for the symmetric 3×3 matrix $\boldsymbol{G}$, and because the Christoffel matrix $\boldsymbol{G}$

is positive definite, the eigenvalues are real and positive.

To find the different eigenvalues, we need to solve the characteristic function

$$\left|\boldsymbol{G} - \rho v^2 \boldsymbol{I}_{(3)}\right| = 0 \tag{2.55}$$

Equation 2.55, known as the dispersion relation, is a third degree polynomial in the variable ρv^2 and has three possible real and positive solutions. This means that to each direction of the slowness $\boldsymbol{s}$, there are three values for ρv^2. One corresponds to the P-wave and the other two to the S-waves. To find the eigenvectors $\boldsymbol{U}$ we need to substitute the eigenvalues in equation 2.52.

Because the Christoffel matrix $\boldsymbol{G}$ is real and symmetric, the corresponding eigenvectors are mutually orthogonal, but they are not necessarily parallel or perpendicular to the slowness $\boldsymbol{s}$. Thus, in general, there are no pure longitudinal and shear waves in anisotropic media. This is why we usually call the fast mode, "quasi-P" (qP) and the two slower modes "quasi-S$_1$" (qS_1) and "quasi-S$_2$" (qS_2) (Tsvankin, 2005).

In the case the Christoffel matrix is non-singular (rank two) we get three distinct eigenvalues ($\rho v_1^2 \neq \rho v_2^2 \neq \rho v_3^2$). To each of the eigenvalues corresponds a distinct polarization direction. In the case the Christoffel matrix is singular with rank one, two of the eigenvalues are equal ($\rho v_1^2 = \rho v_2^2 \neq \rho v_3^2$). In this case of degeneracy, the eigenvectors corresponding to the eigenvalues ρv_1^2 and ρv_2^2 do not have uniquely determined directions within a plane. The eigenvector corresponding to the eigenvalue ρv_3^2, is perpendicular to the plane containing the other two eigenvectors. In the case the Christoffel matrix is singular with rank zero, all the eigenvalues are identical

$(\rho v_1^2 = \rho v_2^2 = \rho v_3^2)$. In this case, all the eigenvectors are not uniquely determined.

2.7 Energy Velocity

The energy velocity vector $\boldsymbol{V}_E$ represents the velocity at which energy propagates and may be defined as the ratio of the mean energy flux vector $\langle \boldsymbol{I} \rangle$ to the mean total energy $\langle E \rangle$, as follows:

$$\boldsymbol{V}_E = \frac{\langle \boldsymbol{I} \rangle}{\langle E \rangle} = \frac{\langle \boldsymbol{I} \rangle}{\langle K \rangle + \langle W \rangle} \tag{2.56}$$

To calculate the energy velocity, we need to calculate the mean of the energy flux and the total energy. For the complex vectors $\boldsymbol{a}$, $\boldsymbol{b}$, $\boldsymbol{A}$ and $\boldsymbol{B}$ and the arbitrary symmetric matrix $\boldsymbol{D}$, where

$$\boldsymbol{a}(\boldsymbol{x}, t) = \boldsymbol{A}(\boldsymbol{x}) e^{\pm i\omega t} \quad \text{and} \quad \boldsymbol{b}(\boldsymbol{x}, t) = \boldsymbol{B}(\boldsymbol{x}) e^{\pm i\omega t} \tag{2.57}$$

the mean over a period T has the following properties:

$$\big\langle \mathrm{Re}\big(\boldsymbol{a}^T\big)\mathrm{Re}\big(\boldsymbol{b}\big)\big\rangle = \frac{1}{2}\mathrm{Re}\big(\boldsymbol{a}^T \boldsymbol{b}^*\big) \tag{2.58}$$

$$\big\langle \mathrm{Re}\big(\boldsymbol{a}^T\big)\mathrm{Re}\big(\boldsymbol{D}\big)\mathrm{Re}\big(\boldsymbol{a}\big)\big\rangle = \frac{1}{2}\mathrm{Re}\big(\boldsymbol{a}^T \boldsymbol{D} \boldsymbol{a}^*\big) \tag{2.59}$$

$$\big\langle \mathrm{Re}\big(\boldsymbol{a}^T\big)\mathrm{Im}\big(\boldsymbol{D}\big)\mathrm{Re}\big(\boldsymbol{a}\big)\big\rangle = \frac{1}{2}\mathrm{Im}\big(\boldsymbol{a}^T \boldsymbol{D} \boldsymbol{a}^*\big) \tag{2.60}$$

where the asterisk denotes the complex conjugate (Carcione, 2001).

Applying equation 2.58 to the energy flux $\boldsymbol{I}$ defined by equation 2.11, we get:

$$\big\langle I_j \big\rangle = -\big\langle \mathrm{Re}(\sigma_{ij})\mathrm{Re}(\dot{u}_i)\big\rangle = -\frac{1}{2}\mathrm{Re}\big(\sigma_{ij}\dot{u}_i^*\big) = -\frac{1}{2}\mathrm{Re}\big(c_{ijkl}u_{k,l}\dot{u}_i^*\big) \tag{2.61}$$

The particle displacement $\boldsymbol{u}$ is given by equation 2.38, namely

$$\boldsymbol{u} = \boldsymbol{U}\, e^{i\omega(\boldsymbol{s}\cdot\boldsymbol{x}-t)} = U\, e^{i\omega(\boldsymbol{s}\cdot\boldsymbol{x}-t)}\, \boldsymbol{d} \tag{2.62}$$

where $\boldsymbol{U} = U\,\boldsymbol{d}$, U is the amplitude of the wave and $\boldsymbol{d}$ is the unit polarization vector. Hence,

$$\begin{aligned} \langle I_j \rangle &= -\frac{1}{2}\mathrm{Re}\big(c_{ijkl} i\,\omega\, U\, s_l\, e^{i\omega(\boldsymbol{s}\cdot\boldsymbol{x}-t)} d_k i\,\omega\, U^*\, e^{-i\omega(\boldsymbol{s}^*\cdot\boldsymbol{x}-t)} d_i^*\big) \\ &= \frac{1}{2}\omega^2 |U|^2\, e^{-2\omega\,\mathrm{Im}(\boldsymbol{s})\cdot\boldsymbol{x}}\, c_{ijkl}\,\mathrm{Re}\big(s_l d_k d_i^*\big) \end{aligned} \tag{2.63}$$

or

$$\langle \boldsymbol{I} \rangle = \frac{1}{2}\omega^2 |U|^2\, e^{-2\omega\,\mathrm{Im}(\boldsymbol{s})\cdot\boldsymbol{x}}\,\mathrm{Re}\big(\boldsymbol{H}^*\boldsymbol{C}\boldsymbol{S}^T\boldsymbol{d}\big) \tag{2.64}$$

where

$$\boldsymbol{H} = \begin{pmatrix} d_1 & 0 & 0 & 0 & d_3 & d_2 \\ 0 & d_2 & 0 & d_3 & 0 & d_1 \\ 0 & 0 & d_3 & d_2 & d_1 & 0 \end{pmatrix} \tag{2.65}$$

If we exclude evanescent waves, and assume $\boldsymbol{d}$ to be real, then we obtain:

$$\langle I_j \rangle = \frac{1}{2}\omega^2 |U|^2 c_{ijkl} s_l d_k d_i \tag{2.66}$$

or

$$\langle \boldsymbol{I} \rangle = \frac{1}{2}\omega^2 |U|^2\, \big(\boldsymbol{H}\boldsymbol{C}\boldsymbol{S}^T\boldsymbol{d}\big) \tag{2.67}$$

Applying equation 2.59 to the strain energy density W defined by equation 2.20, we get:

$$\langle W\rangle = \frac{1}{2}\langle \mathrm{Re}(\boldsymbol{e}^T)\boldsymbol{C}\mathrm{Re}(\boldsymbol{e})\rangle = \frac{1}{4}\mathrm{Re}\big(\boldsymbol{e}^T\boldsymbol{C}\boldsymbol{e}^*\big) \tag{2.68}$$

From equations 2.46 and 2.47, we have

$$\boldsymbol{e} = \boldsymbol{D}^T\boldsymbol{u} = i\,\omega\,\boldsymbol{S}^T\boldsymbol{u} \tag{2.69}$$

Substituting equation 2.69 in 2.68 and using equation 2.62, we obtain:

$$\begin{aligned}\langle W\rangle &= \frac{1}{4}\mathrm{Re}\Big(i\,\omega\,U\,e^{i\omega(\boldsymbol{s}\cdot\boldsymbol{x}-t)}\big(\boldsymbol{S}^T\boldsymbol{d}\big)^T\boldsymbol{C}(-i)\,\omega\,U^*\,e^{-i\omega(\boldsymbol{s}^*\cdot\boldsymbol{x}-t)}\boldsymbol{S}^H\boldsymbol{d}^*\Big)\\ &= \frac{1}{4}\omega^2|U|^2\,e^{-2\omega\,\mathrm{Im}(\boldsymbol{s})\cdot\boldsymbol{x}}\,\mathrm{Re}\Big(\boldsymbol{d}^T\boldsymbol{S}\boldsymbol{C}\boldsymbol{S}^H\boldsymbol{d}^*\Big)\end{aligned} \tag{2.70}$$

If we exclude evanescent waves, and assume $\boldsymbol{d}$ to be real, then we obtain:

$$\langle W\rangle = \frac{1}{4}\rho\omega^2|U|^2 \tag{2.71}$$

The kinetic energy density K defined by equation 2.7, can be written in matrix form as follows:

$$\langle K\rangle = \frac{1}{2}\rho\dot{\boldsymbol{u}}^T\dot{\boldsymbol{u}} \tag{2.72}$$

Applying equation 2.58 to the kinetic energy density K, we obtain:

$$\langle K\rangle = \frac{1}{2}\rho\langle \mathrm{Re}(\dot{\boldsymbol{u}}^T)\mathrm{Re}(\dot{\boldsymbol{u}})\rangle = \frac{1}{4}\rho\,\mathrm{Re}\big(\dot{\boldsymbol{u}}^T\dot{\boldsymbol{u}}^*\big) \tag{2.73}$$

Substituting equation 2.62 in 2.73, we obtain:

$$\begin{aligned}\langle K\rangle &= \frac{1}{4}\rho\,\mathrm{Re}\Big(-i\omega U\, e^{i\omega(\boldsymbol{s}\cdot\boldsymbol{x}-t)}\boldsymbol{d}^T i\omega U^*\, e^{-i\omega(\boldsymbol{s}^*\cdot\boldsymbol{x}-t)}\boldsymbol{d}^*\Big)\\ &= \frac{1}{4}\rho\omega^2|U|^2\, e^{-2\omega\,\mathrm{Im}(\boldsymbol{s})\cdot\boldsymbol{x}}\,\mathrm{Re}\big(\boldsymbol{d}^T\boldsymbol{d}^*\big)\end{aligned} \tag{2.74}$$

If we exclude evanescent waves, and assume $\boldsymbol{d}$ to be real, then we obtain:

$$\langle K\rangle = \frac{1}{4}\rho\omega^2|U|^2 = \langle W\rangle \tag{2.75}$$

Hence, the energy velocity vector is

$$\boldsymbol{V_E} = \frac{2\,\mathrm{Re}\big(\boldsymbol{H}^*\boldsymbol{C}\boldsymbol{S}^T\boldsymbol{d}\big)}{\rho\,\mathrm{Re}\big(\boldsymbol{d}^T\boldsymbol{d}^*\big)+\mathrm{Re}\Big(\boldsymbol{d}^T\boldsymbol{S}\boldsymbol{C}\boldsymbol{S}^H\boldsymbol{d}^*\Big)} \tag{2.76}$$

If we exclude evanescent waves, and assume $\boldsymbol{d}$ to be real, then, from equations 2.67, 2.71, and 2.75, we obtain:

$$\boldsymbol{V_E} = \frac{\langle\boldsymbol{I}\rangle}{2\,\langle K\rangle} = \rho^{-1}\big(\boldsymbol{H}\boldsymbol{C}\boldsymbol{S}^T\boldsymbol{d}\big) \tag{2.77}$$

Note that, Because $\langle K\rangle$ is a scalar and $\langle\boldsymbol{I}\rangle = 2\langle K\rangle\boldsymbol{V_E}$, $\boldsymbol{V_E}$ and $\langle\boldsymbol{I}\rangle$ have the same direction.

2.8 Group Velocity

In anisotropic, homogenous and elastic media, the phase velocity differs in general from the group velocity. The group velocity is of primary importance in the kinematic

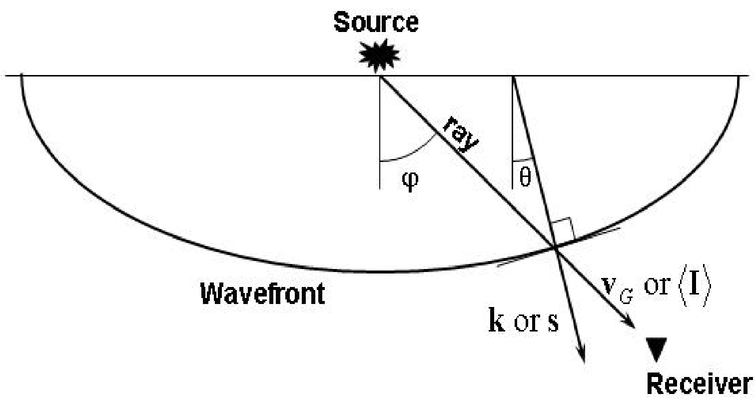

Figure 2.1: Group versus phase velocity

analysis of seismic anisotropy. It is a vector whose magnitude is the wave speed along the raypath and whose direction is aligned with the source-receiver direction as shown in figure 2.1. In isotropic, homogenous and elastic media the group velocity and phase velocity are identical. In the most general form, the group velocity vector can be defined as (Carcione, 2001; Tsvankin, 2005)

$$\boldsymbol{V_G} = \frac{\partial \omega}{\partial k_1}\boldsymbol{i_1} + \frac{\partial \omega}{\partial k_2}\boldsymbol{i_2} + \frac{\partial \omega}{\partial k_3}\boldsymbol{i_3} \tag{2.78}$$

where k_1, k_2 and k_3 are the components of the wave vector $\boldsymbol{k}$, ω is the angular frequency, and $\boldsymbol{i_1}$, $\boldsymbol{i_2}$ and $\boldsymbol{i_3}$ are the the unit coordinate vectors.

From the Christoffel equation 2.50, we have

$$k^2 G_{ik} u_k = \rho\omega^2 u_i \tag{2.79}$$

Substituting the Christoffel matrix 2.53 into 2.79, we obtain

$$k^2 c_{ijkl} n_j n_l u_k = \rho\omega^2 u_i \tag{2.80}$$

From equations 2.39 and 2.62, equation 2.80 becomes

$$c_{ijkl} k_j k_l d_k = \rho\omega^2 d_i \tag{2.81}$$

Differentiating both terms of equation 2.81 with respect to k_n, we get

$$c_{ijkl}\left(k_l \frac{\partial k_j}{\partial k_n} + k_j \frac{\partial k_l}{\partial k_n}\right) d_k = 2\rho\omega \frac{\partial \omega}{\partial k_n} d_i \tag{2.82}$$

Note that $\partial k_j/\partial k_n = \delta_{kn}$. Multiplying the above equation by d_i and summing over i gives

$$c_{ijkl}\Big(k_l \delta_{jn} + k_j \delta_{ln}\Big) d_k d_i = 2\rho\omega \frac{\partial \omega}{\partial k_n} d_i d_i \tag{2.83}$$

If we exclude evanescent waves, and assume $\boldsymbol{d}$ to be real, we have $d_i d_i = 1$ (as d_i is a unit vector). Now we expand and perform the sums involving the Kronecker delta. For the first delta, we sum over j, and for the second, we sum over l. This gives

$$c_{inkl} k_l d_k d_i + c_{ijkn} k_j d_k d_i = 2\rho\omega \frac{\partial \omega}{\partial k_n} \tag{2.84}$$

We now show that the second term on the left is the same as the first term on the left. First, since j is just a dummy summation index, we can replace it with l (as l appears nowhere else in the second term). The second term on the left then becomes

$$c_{ilkn} k_l d_k d_i \tag{2.85}$$

Similarly, we can switch the i and the k as they are also just dummy summation indices. This gives

$$c_{klin} k_l d_i d_k \tag{2.86}$$

Next, we use one of the symmetries of the stress tensor, giving

$$c_{inkl} k_l d_i d_k \tag{2.87}$$

Note that this is now the same as the first term on the left in equation 2.84 above ($d_i d_k = d_k d_i$). We also replace k_l with ωs_l. Therefore, we obtain

$$2c_{inkl} \omega s_l d_i d_k = 2\rho\omega \frac{\partial \omega}{\partial k_n} \tag{2.88}$$

Cancelling the 2ω from both sides, gives

$$c_{inkl} s_l d_i d_k = \rho \frac{\partial \omega}{\partial k_n} \tag{2.89}$$

Finally, this reduces to

$$\frac{1}{\rho} c_{inkl} s_l d_i d_k = \frac{\partial \omega}{\partial k_n} \quad n = 1, 2, 3 \tag{2.90}$$

We can replace n with j now, as n is a free index. This gives

$$\frac{1}{\rho} c_{ijkl} s_l d_i d_k = \frac{\partial \omega}{\partial k_j} \quad j = 1, 2, 3 \tag{2.91}$$

Hence, the group velocity is

$$V_{Gj} = \frac{\partial \omega}{\partial k_j} = \frac{1}{\rho} c_{ijkl} s_l d_i d_k \quad j = 1, 2, 3 \tag{2.92}$$

or

$$\boldsymbol{V_G} = \rho^{-1} \big(\boldsymbol{H C S}^T \boldsymbol{d} \big) \tag{2.93}$$

Note from equations 2.77 and 2.93, that the energy velocity and the group velocity are identical for anisotropic, homogeneous and elastic media.

Chapter 3

Analytical Solution of Scattering Coefficients Problem

The scattering coefficient problem in anisotropic media can be found in Daley and Hron (1977), Graebner (1992), Rüger (2001) and Carcione (2001). In this chapter we are interested in the analytical solution of the scattering coefficient problem in anisotropic media, which will be used later to validate the results obtained numerically in chapter 6. In the first section, we give the solution of the Christoffel equation for isotropic as well as VTI media. In the second section, we review exact scattering formulae for isotropic, VTI and Monoclinic media.

3.1 Solution of the Christoffel Equation

In this section, we are interested in finding the phase velocity and the polarization of body waves in a given medium, which can be obtained by solving the eigenvalue problem of equation 2.52.

3.1.1 Isotropic Media

The Christoffel matrix for isotropic media is given as follows:

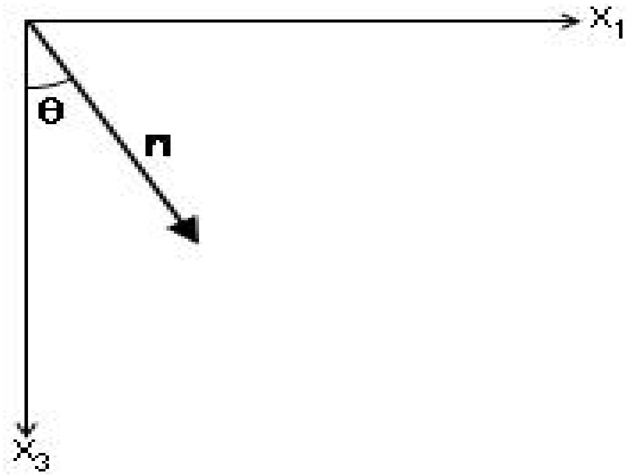

Figure 3.1: Unit vector $\boldsymbol{n}$ for a wave propagating in the $x_1 - x_3$ plane

$$\begin{aligned} G_{11} &= (\lambda + 2\mu)n_1^2 + \mu(n_2^2 + n_3^2), \\ G_{12} &= (\lambda + \mu)n_1 n_2, \\ G_{13} &= (\lambda + \mu)n_1 n_3, \\ G_{22} &= \mu(n_1^2 + n_3^2) + (\lambda + 2\mu)n_2^2, \\ G_{23} &= (\lambda + \mu)n_2 n_3, \\ G_{33} &= \mu(n_1^2 + n_2^2) + (\lambda + 2\mu)n_3^2. \end{aligned} \tag{3.1}$$

For propagation in the $x_1 - x_3$ plane (without loss of generality), $n_2 = 0$, $\boldsymbol{n} = (\sin\theta, 0, \cos\theta)$ (see figure 3.1) and the Christoffel equation can be given as follows:

$$\begin{pmatrix} G_{11} - \rho v^2 & 0 & G_{13} \\ 0 & G_{22} - \rho v^2 & 0 \\ G_{13} & 0 & G_{33} - \rho v^2 \end{pmatrix} \begin{pmatrix} U_1 \\ U_2 \\ U_3 \end{pmatrix} = 0 \tag{3.2}$$

where

$$
\begin{aligned}
G_{11} &= (\lambda + 2\mu)\sin^2\theta + \mu\cos^2\theta \\
G_{13} &= (\lambda + \mu)\sin\theta\cos\theta \\
G_{22} &= \mu \\
G_{33} &= \mu\sin^2\theta + (\lambda + 2\mu)\cos^2\theta
\end{aligned}
\tag{3.3}
$$

We obtain two uncoupled dispersion relations,

$$
\begin{gathered}
\mu\rho v^2 = 0, \\
\mu(\lambda + 2\mu) - (3\mu + \lambda)\rho v^2 + \rho^2 v^4 = 0
\end{gathered}
\tag{3.4}
$$

which gives the phase velocities

$$
\begin{aligned}
v_1 &= \sqrt{\mu/\rho} \\
v_2 &= \sqrt{\mu/\rho} \\
v_3 &= \sqrt{(\lambda + 2\mu)/\rho}
\end{aligned}
\tag{3.5}
$$

Replacing the phase velocities (eigenvalues) in equation 3.2, we obtain the corresponding normalized polarization vectors (eigenvectors) (see figure 3.2).

$$
\begin{aligned}
\boldsymbol{U}^{(1)} &= (0, 1, 0)^T \\
\boldsymbol{U}^{(2)} &= (\cos\theta, 0, -\sin\theta)^T \\
\boldsymbol{U}^{(3)} &= (\sin\theta, 0, \cos\theta)^T
\end{aligned}
\tag{3.6}
$$

The first wave has a polarization given by $\boldsymbol{U}^{(1)} = (0, 1, 0)^T$, which is normal to the $x_1 - x_3$ plane. Hence, this solution describes a pure shear wave, known as an SH-wave. The H denotes a horizontal polarization. The coupled solutions have in-plane polarizations as we can see in figure 3.2. The wave with the polarization $\boldsymbol{U}^{(2)} = (\cos\theta, 0, -\sin\theta)^T$ describes a pure shear wave, know as an SV-wave. The V

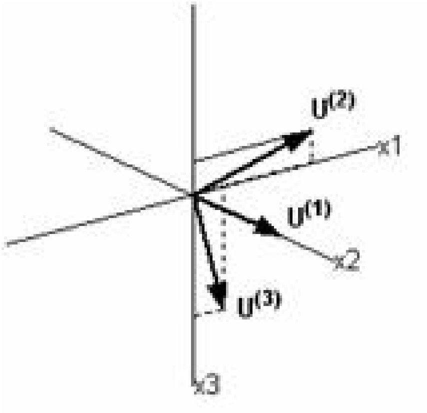

Figure 3.2: Eigenvectors of the Christoffel matrix for a wave propagating in $x_1 - x_3$ plane in an isotropic medium

denotes a vertical polarization (but it has also a non-vanishing in-plane horizontal component). The wave with the polarization $\boldsymbol{U}^{(3)} = (\sin\theta, 0, \cos\theta)^T$ describes a pure P-wave because it is polarized in the wave propagation direction.

From equation 3.5, notice that v_1, the velocity of the SH-wave, is equal to v_2, the velocity of SV-wave. This is referred to as a shear-wave singularity in the language of wave propagation and degeneracy or singularity in the language of mathematics.

3.1.2 VTI Media

In this section, we are going to consider wave propagation in the $x_1 - x_3$ plane, because for VTI media all planes containing the symmetry axis are equivalent (Tsvankin, 2005). Hence, the Christoffel equation is given as follows:

$$\begin{pmatrix} G_{11}-\rho v^2 & 0 & G_{13} \\ 0 & G_{22}-\rho v^2 & 0 \\ G_{13} & 0 & G_{33}-\rho v^2 \end{pmatrix} \begin{pmatrix} U_1 \\ U_2 \\ U_3 \end{pmatrix} = 0 \tag{3.7}$$

where

$$\begin{aligned} G_{11} &= c_{11}\sin^2\theta + c_{55}\cos^2\theta \\ G_{13} &= (c_{13}+c_{55})\sin\theta\cos\theta \\ G_{22} &= c_{66}\sin^2\theta + c_{55}\cos^2\theta \\ G_{33} &= c_{55}\sin^2\theta + c_{33}\cos^2\theta \end{aligned} \tag{3.8}$$

which gives us two uncoupled dispersion relations (Carcione, 2001),

$$\begin{gathered} c_{66}\sin^2\theta + c_{55}\cos^2\theta - \rho v^2 = 0, \\ (c_{11}\sin^2\theta + c_{55}\cos^2\theta - \rho v^2)(c_{33}\cos^2\theta + c_{55}\sin^2\theta - \rho v^2) - (c_{13}+c_{55})^2\sin^2\theta\cos^2\theta = 0 \end{gathered} \tag{3.9}$$

The solution of equation 3.9 will give the following phase velocities

$$\begin{aligned} v_1(\theta) &= \sqrt{(c_{66}\sin^2\theta + c_{55}\cos^2\theta)/\rho} \\ v_2(\theta) &= \sqrt{(c_{11}\sin^2\theta + c_{33}\cos^2\theta + c_{55} - C)/(2\rho)} \\ v_3(\theta) &= \sqrt{(c_{11}\sin^2\theta + c_{33}\cos^2\theta + c_{55} + C)/(2\rho)} \end{aligned} \tag{3.10}$$

where $C = \sqrt{[(c_{11}-c_{55})\sin^2\theta + (c_{55}-c_{33})\cos^2\theta]^2 + 4[(c_{13}+c_{55})\sin\theta\cos\theta]^2}$ (Carcione, 2001).

Replacing the phase velocity v_1 in equation 3.7, we obtain the normalized polarization vector

$$\boldsymbol{U}^{(1)} = (0,1,0)^T \tag{3.11}$$

which describes a horizontally polarized pure shear wave, i.e. SH-wave. Note that the first dispersion relation in equation 3.9, can be rewritten as

$$\frac{\sin^2\theta/v_1^2}{\rho/c_{66}} + \frac{\cos^2\theta/v_1^2}{\rho/c_{55}} = 1 \tag{3.12}$$

which means that the slowness curve for an SH-wave is an an ellipse with semi-axis ρ/c_{66} in the horizontal direction and ρ/c_{55} in the vertical direction (Carcione, 2001).

The normalized polarizations for the two coupled waves with velocities v_2 and v_3 can be given from equation 3.7 as follows

$$\begin{aligned}
\boldsymbol{U}^{(2)} &= \left(\sqrt{(G_{33}-\rho v_2^2)/(G_{11}+G_{33}-2\rho v_2^2)}, 0, \sqrt{(G_{11}-\rho v_2^2)/(G_{11}+G_{33}-2\rho v_2^2)}\right) \\
\boldsymbol{U}^{(3)} &= \left(\sqrt{(G_{33}-\rho v_2^2)/(G_{11}+G_{33}-2\rho v_3^2)}, 0, \sqrt{(G_{11}-\rho v_3^2)/(G_{11}+G_{33}-2\rho v_3^2)}\right)
\end{aligned} \tag{3.13}$$

where v_2 and v_3 are defined in 3.10 and $\boldsymbol{G}$ is the Christoffel matrix as defined in equation 3.7 (Carcione, 2001).

The phase velocities for the special case where the wave propagates along the x_3-axis, can be easily found by substituting with $\theta = 0$ in equation 3.10,

$$\begin{aligned}
v_1(\theta = 0) &= \sqrt{c_{55}/\rho} \\
v_2(\theta = 0) &= \sqrt{c_{55}/\rho} \\
v_3(\theta = 0) &= \sqrt{c_{33}/\rho}
\end{aligned} \tag{3.14}$$

and the polarization vectors can be found by substituting $\theta = 0$ in 3.14,

$$\begin{aligned}
\boldsymbol{U}^{(1)} &= (0, 1, 0)^T \\
\boldsymbol{U}^{(2)} &= (1, 0, 0)^T \\
\boldsymbol{U}^{(3)} &= (0, 0, 1)^T
\end{aligned} \tag{3.15}$$

which means that for the polarization vector $\boldsymbol{U}^{(2)} = (1,0,0)^T$ we have a pure shear SV-wave with a horizontal in-plane polarization and for the polarization vector $\boldsymbol{U}^{(3)} = (0,0,1)^T$ we have a pure P-wave polarized in the direction of propagation.

Notice from equation 3.14, that the SV- and SH-waves have the same vertical velocity, meaning that we have a shear-wave singularity for $\theta = 0$.

The phase velocities for the special case where the wave propagates along the x_1-axis, can be easily found by substituting $\theta = 90^o$ in equation 3.10,

$$\begin{aligned} v_1(\theta = 90^o) &= \sqrt{c_{66}/\rho} \\ v_2(\theta = 90^o) &= \sqrt{c_{55}/\rho} \\ v_3(\theta = 90^o) &= \sqrt{c_{11}/\rho} \end{aligned} \tag{3.16}$$

and the polarization vectors can be found by substituting $\theta = 90^o$ in 3.14,

$$\begin{aligned} \boldsymbol{U}^{(1)} &= (0,1,0)^T \\ \boldsymbol{U}^{(2)} &= (0,0,1)^T \\ \boldsymbol{U}^{(3)} &= (1,0,0)^T \end{aligned} \tag{3.17}$$

which means that for the polarization vector $\boldsymbol{U}^{(2)} = (0,0,1)^T$ we have a pure shear SV-wave with a vertical in-plane polarization and for the polarization vector $\boldsymbol{U}^{(3)} = (1,0,0)^T$ we have a pure P-wave polarized in the direction of propagation. The $x_1 - x_2$ plane of a VTI medium is a plane of isotropy and equations 3.16 and 3.17 are valid for any wave propagation direction in the horizontal plane. Notice from equation 3.16, that the velocities of the SV- and SH-waves are different, which produces what is known as shear-wave splitting (Tsvankin, 2005).

For waves traveling with oblique propagation angles, the polarization directions are no longer parallel and perpendicular to the wave propagation direction for the P- and SV-waves respectively, which means that the waves are no longer pure waves and instead we call them quasi-P (qP) and quasi-SV (qSV).

3.2 Scattering Coefficients of Plane Waves

In this section, we are interested in finding the scattering coefficients resulting from a plane wave of the form 2.38 propagating in the $x_1 - x_3$ plane, incident from an upper medium on a plane boundary between two elastic media. The sign convention adopted in this work is the one used by Aki and Richards (1980), which chooses the directions of the polarization vectors so that their horizontal components are in the same direction as the horizontal slowness component (Rüger, 2001).

The computation of reflection and transmission coefficients is based on two physical principles known as the kinematic and dynamic boundary conditions. The kinematic boundary conditions state that the sum of displacements are equal across the interface and the dynamic boundary conditions state that the sum of stress components are equal across the interface. These are sometimes referred to as welded-contact boundary conditions.

3.2.1 Isotropic Media

An incident P-wave propagating in the $x_1 - x_3$ plane, will generate two transmitted and two reflected waves upon arrival into the plane interface ($x_3 = 0$) (see figure 3.3). The upper medium is isotropic and is defined by its P-wave propagation velocity α_1, S-wave propagation velocity β_1 and density ρ_1. The lower medium is isotropic and is defined by its P-wave propagation velocity α_2, S-wave propagation velocity β_2 and density ρ_2. The angles θ_1, φ_1, θ_2, and φ_2 are the angles between the P-wave and S-wave propagation direction and the x_3-axis for the upper and lower media, respectively. The particle displacement of the incident P-wave with unit amplitude, is given as follows

$$\boldsymbol{u}_P^I = U_P^I \begin{pmatrix} \sin\theta_1 \\ 0 \\ \cos\theta_1 \end{pmatrix} e^{i\omega((\sin\theta_1/\alpha_1)\, x_1 + (\cos\theta_1/\alpha_1)\, x_3 - t)} \tag{3.18}$$

The two generated reflected waves are given as follows

$$\boldsymbol{u}_P^R = U_P^R \begin{pmatrix} \sin\theta_1 \\ 0 \\ -\cos\theta_1 \end{pmatrix} e^{i\omega((\sin\theta_1/\alpha_1)\, x_1 - (\cos\theta_1/\alpha_1)\, x_3 - t)} \tag{3.19}$$

$$\boldsymbol{u}_S^R = U_S^R \begin{pmatrix} \cos\varphi_1 \\ 0 \\ \sin\varphi_1 \end{pmatrix} e^{i\omega((\sin\varphi_1/\beta_1)\, x_1 - (\cos\varphi_1/\beta_1)\, x_3 - t)} \tag{3.20}$$

where U_P^I is the the amplitude of the incident P-wave, and U_P^R and U_S^R are the amplitudes of the reflected P-wave and S-wave, respectively.

The two generated transmitted waves are given as follows

$$\boldsymbol{u}_P^T = U_P^T \begin{pmatrix} \sin\theta_2 \\ 0 \\ \cos\theta_2 \end{pmatrix} e^{i\omega((\sin\theta_2/\alpha_2)\, x_1 + (\cos\theta_2/\alpha_2)\, x_3 - t)} \tag{3.21}$$

$$\boldsymbol{u}_S^T = U_S^T \begin{pmatrix} \cos\varphi_2 \\ 0 \\ -\sin\varphi_2 \end{pmatrix} e^{i\omega((\sin\varphi_2/\beta_2)\, x_1 + (\cos\varphi_2/\beta_2)\, x_3 - t)} \tag{3.22}$$

where U_P^T and U_S^T are the amplitudes of the transmitted P-wave and S-wave, respectively.

For welded-contact, the kinematic and dynamic boundary conditions are written as follows:

$$\begin{gathered} \boldsymbol{u}_P^I + \boldsymbol{u}_P^R + \boldsymbol{u}_S^R = \boldsymbol{u}_P^T + \boldsymbol{u}_S^T \\ (\boldsymbol{\Sigma}_P^I + \boldsymbol{\Sigma}_P^R + \boldsymbol{\Sigma}_S^R) \cdot \boldsymbol{n} = (\boldsymbol{\Sigma}_P^T + \boldsymbol{\Sigma}_S^T) \cdot \boldsymbol{n} \end{gathered} \tag{3.23}$$

where $\boldsymbol{n}$ is a unit vector normal to the interface and $\boldsymbol{\Sigma}$ is defined as follows:

$$\boldsymbol{\Sigma} = \begin{pmatrix} \sigma_{11} & \sigma_{12} & \sigma_{13} \\ \sigma_{12} & \sigma_{22} & \sigma_{23} \\ \sigma_{13} & \sigma_{23} & \sigma_{33} \end{pmatrix} \tag{3.24}$$

Equations 3.23 will produce a system of four equations and four unknowns, i.e. the reflection and transmission coefficients. The scattering coefficients for the P-wave incident from the upper medium are (Aki and Richards, 1980; Krebes, 2001):

$$\begin{gathered} R_{PP} = U_P^R/U_P^I = [(b\xi_1 - c\xi_2)F - (a + d\xi_1\eta_2)Hp^2]D^{-1} \\ R_{PS} = U_S^R/U_P^I = -2\xi_1 p(\alpha_1/\beta_1)(ab + cd\xi_2\eta_2)D^{-1} \\ T_{PP} = U_P^T/U_P^I = 2\rho_1\xi_1(\alpha_1/\alpha_2)FD^{-1} \\ T_{PS} = U_S^T/U_P^I = 2\rho_1\xi_1(\alpha_1/\beta_2)pFD^{-1} \end{gathered} \tag{3.25}$$

where

$$
\begin{gathered}
a=\gamma_2-\gamma_1,\ b=\gamma_2+\chi_1 p,\ c=\gamma_1+\chi_2 p,\ d=2(\rho_2\beta_2^2-\rho_1\beta_1^2),\\
\chi_i=2\rho_i\beta_i^2 p,\ \gamma_i=\rho_i(1-2\beta_i^2p^2),\ \xi_i=\cos\theta_i/\alpha_i,\ \eta_i=\cos\varphi_i/\beta_i,\ i=1,2\\
E=b\xi_1+c\xi_2,\ F=b\eta_1+c\eta_2,\ G=a-d\xi_1\eta_2,\ H=a-d\xi_2\eta_1,\\
D=EF+GHp^2
\end{gathered}
\tag{3.26}
$$

Aki and Richards (1980) derived expressions for all reflection and transmission coefficients in isotropic media and they presented the solution in the following convenient matrix from:

$$\boldsymbol{M}\boldsymbol{R}=\boldsymbol{N} \tag{3.27}$$

where

$$
\boldsymbol{M}=\begin{pmatrix}
-\alpha_1 p & -\cos\varphi_1 & \alpha_2 p & \cos\varphi_2\\
\cos\theta_1 & -\beta_1 p & \cos\theta_2 & -\beta_2 p\\
2\rho_1\beta_1^2 p\cos\theta_1 & \rho_1\beta_1(1-2\beta_1^2p^2) & 2\rho_2\beta_2^2 p\cos\theta_2 & \rho_2\beta_2(1-2\beta_2^2p^2)\\
-\rho_1\alpha_1(1-2\beta_1^2p^2) & 2\rho_1\beta_1^2 p\cos\varphi_1 & \rho_2\alpha_2(1-2\beta_2^2p^2) & -2\rho_2\beta_2^2 p\cos\varphi_2
\end{pmatrix},
\tag{3.28}
$$

$$
\boldsymbol{N}=\begin{pmatrix}
\alpha_1 p & \cos\varphi_1 & -\alpha_2 p & -\cos\varphi_2\\
\cos\theta_1 & -\beta_1 p & \cos\theta_2 & -\beta_2 p\\
2\rho_1\beta_1^2 p\cos\theta_1 & \rho_1\beta_1(1-2\beta_1^2p^2) & 2\rho_2\beta_2^2 p\cos\theta_2 & \rho_2\beta_2(1-2\beta_2^2p^2)\\
\rho_1\alpha_1(1-2\beta_1^2p^2) & -2\rho_1\beta_1^2 p\cos\varphi_1 & -\rho_2\alpha_2(1-2\beta_2^2p^2) & 2\rho_2\beta_2^2 p\cos\varphi_2
\end{pmatrix}
\tag{3.29}
$$

and

$$
\boldsymbol{R}=\begin{pmatrix}
\grave{P}\acute{P} & \grave{S}\acute{P} & \acute{P}\acute{P} & \acute{S}\acute{P}\\
\grave{P}\acute{S} & \grave{S}\acute{S} & \acute{P}\acute{S} & \acute{S}\acute{S}\\
\grave{P}\grave{P} & \grave{S}\grave{P} & \acute{P}\grave{P} & \acute{S}\grave{P}\\
\grave{P}\grave{S} & \grave{S}\grave{S} & \acute{P}\grave{S} & \acute{S}\grave{S}
\end{pmatrix}
\tag{3.30}
$$

The notations "`" and "´" represent downgoing and upgoing waves respectively. Hence, for example, $\acute{S}\grave{P}$ represent the reflection coefficient of a P-wave resulting from an S-wave incident from the lower medium.

3.2.2 VTI Media

The analytic solution of the scattering coefficients problem for VTI media was studied in great detail by many authors (e.g. Daley and Hron (1977), Graebner (1992) and Rüger (2001)).

The following is a summary of Graebner's (1992) solution of the scattering coefficients problem for VTI media, which was described in Rüger (2001). The scattering coefficients given by the vector $\boldsymbol{R} = \left(R_P, R_{PS}, T_P, T_{PS}\right)^T$, resulting from a P-wave propagating in the $x_1 - x_3$ plane can be obtained by solving the following linear system:

$$\boldsymbol{M}\boldsymbol{R} = \boldsymbol{b} \tag{3.31}$$

where

$$\boldsymbol{M} = \begin{pmatrix} l_\alpha^{(1)} & p\,l_\alpha^{(1)} c_{13}^{(1)} + q_\alpha^{(1)} m_\alpha^{(1)} c_{33}^{(1)} & m_\alpha^{(1)} & c_{55}^{(1)}(q_\alpha^{(1)} l_\alpha^{(1)} + p\,m_\alpha^{(1)}) \\ m_\beta^{(1)} & p\,m_\beta^{(1)} c_{13}^{(1)} - q_\beta^{(1)} l_\beta^{(1)} c_{33}^{(1)} & -l_\beta^{(1)} & c_{55}^{(1)}(q_\beta^{(1)} m_\beta^{(1)} - p\,l_\beta^{(1)}) \\ -l_\alpha^{(2)} & -(p\,l_\alpha^{(2)} c_{13}^{(2)} + q_\alpha^{(2)} m_\alpha^{(2)} c_{33}^{(2)}) & m_\alpha^{(2)} & c_{55}^{(2)}(q_\alpha^{(2)} l_\alpha^{(2)} + p\,m_\alpha^{(2)}) \\ -m_\beta^{(2)} & -(p\,m_\beta^{(2)} c_{13}^{(2)} - q_\beta^{(2)} l_\beta^{(2)} c_{33}^{(2)}) & -l_\beta^{(2)} & c_{55}^{(2)}(q_\beta^{(2)} m_\beta^{(2)} - p l_\beta^{(2)}) \end{pmatrix}^T \tag{3.32}$$

(Note that there is a typo in the elements m_{ij} in Rüger (2001).)

and

$$\boldsymbol{b} = \left(l_\alpha^{(1)}, p\,l_\alpha^{(1)} c_{13}^{(1)} + q_\alpha^{(1)} m_\alpha^{(1)} c_{33}^{(1)}, m_\alpha^{(1)}, c_{55}^{(1)}(q_\alpha^{(1)} l_\alpha^{(1)} + p\,m_\alpha^{(1)})\right)^T \tag{3.33}$$

with

$$\begin{aligned} l_\alpha &= \sqrt{(a_{33}\, q_\alpha^2 + a_{55}\, p^2 - 1)/(a_{11}\, p^2 + a_{55}\, q_\alpha^2 - 1 + a_{33}\, q_\alpha^2 + a_{55}\, p^2 - 1)} \\ m_\alpha &= \sqrt{(a_{11}\, p^2 + a_{55}\, q_\alpha^2 - 1)/(a_{11}\, p^2 + a_{55}\, q_\alpha^2 - 1 + a_{33}\, q_\alpha^2 + a_{55}\, p^2 - 1)} \\ l_\beta &= \sqrt{(a_{11}\, p^2 + a_{55}\, q_\beta^2 - 1)/(a_{11}\, p^2 + a_{55}\, q_\beta^2 - 1 + a_{33}\, q_\beta^2 + a_{55}\, p^2 - 1)} \\ m_\beta &= \sqrt{(a_{33}\, q_\beta^2 + a_{55}\, p^2 - 1)/(a_{11}\, p^2 + a_{55}\, q_\beta^2 - 1 + a_{33}\, q_\beta^2 + a_{55}\, p^2 - 1)} \end{aligned} \tag{3.34}$$

where q_α and q_β are the vertical slowness of the P-wave and S-wave respectively.

3.2.3 Monoclinic Media

The scattering coefficient problem becomes simpler if we restrict ourselves to the case where the incidence plane coincides with the symmetry plane of the upper and lower media, because an incident qP-wave or qSV-wave will generate reflected and transmitted qP and qSV-waves, and an incident SH-wave will generate reflected and transmitted SH-waves. Carcione (2001), provided analytic formulae for reflected and transmitted SH-waves resulting from an incident SH-wave traveling in the plane of symmetry of a monoclinic medium, as follows:

$$R = \frac{Z^{(1)} - Z^{(2)}}{Z^{(1)} + Z^{(2)}}, \qquad T = \frac{2Z^{(1)}}{Z^{(1)} + Z^{(2)}} \tag{3.35}$$

where

$$Z^{(i)} = \pm\sqrt{\rho^{(i)} c_{44}^{(i)} - \left(c_{44}^{(i)} c_{66}^{(i)} - \left(c_{46}^{(i)}\right)^2\right) s_1^2}, \quad i = 1, 2 \tag{3.36}$$

The index i in equation 3.36 is the index of the medium. The $+$ sign in equation 3.36 corresponds to downward propagating waves and the $-$ sign corresponds to upward propagating waves. The horizontal slowness s_1 is equal for all waves (Snell's law) and can be given as a function of the incidence angle θ^I and the phase velocity v as follows:

$$s_1 = \sin\theta^I / v(\theta^I) \tag{3.37}$$

where

$$v(\theta) = \sqrt{\frac{1}{\rho}\big(c_{44}\cos^2\theta + c_{66}\sin^2\theta + c_{46}\sin(2\theta)\big)} \tag{3.38}$$

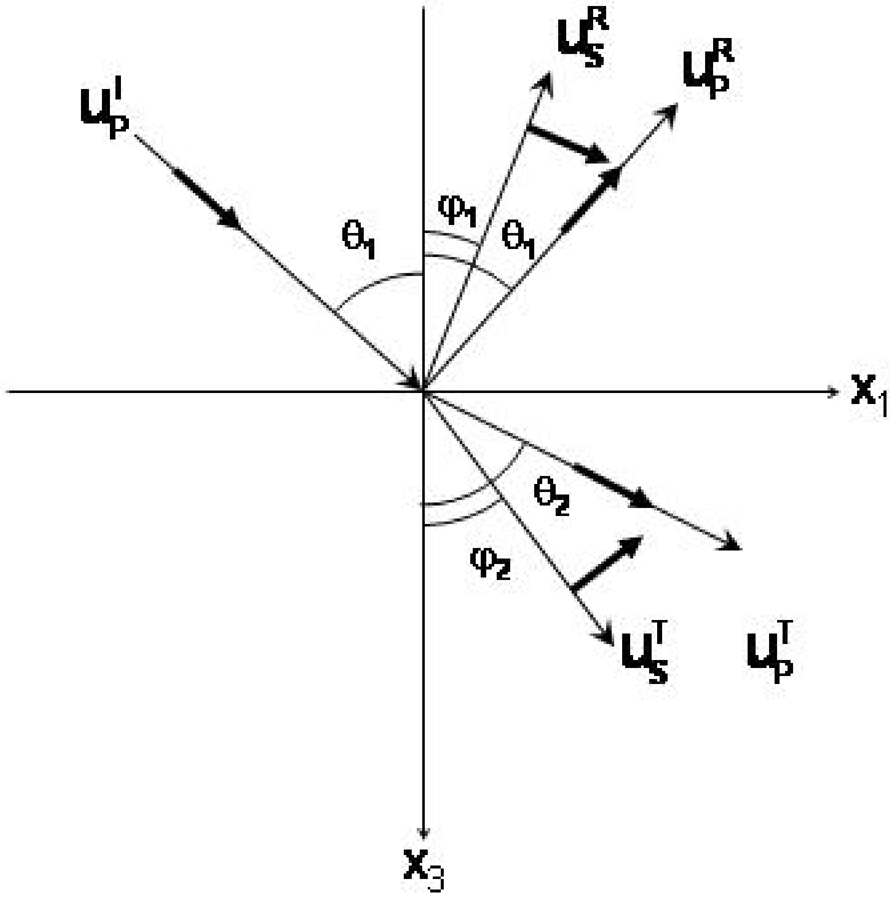

Figure 3.3: Scattering coefficients generated from a P-wave propagating in the $x_1 - x_3$ plane of an isotropic medium. The thick lines indicate the unit vectors for each wave mode

Chapter 4

Numerical Solution of Scattering Coefficients Problem

In this chapter we present the theory behind the program TAVRT which stands for "Tilted Anisotropic Viscoelastic Reflection and Transmission". The theory behind TAVRT as well as the code was developed by Professor Edward S. Krebes. Despite its name, TAVRT does not yet treat the viscoelastic case as it stands. It has also not yet been fully tested (and modified if necessary) for all possible anisotropic cases.

4.1 Scattering Coefficients for Generally Anisotropic Media

Let us consider a plane wave of the form given by equation 2.38, incident from an anisotropic upper (lower) medium on a plane horizontal boundary to an anisotropic lower (upper) medium. The incident wave will generate three transmitted and three reflected waves. Each medium can be generally anisotropic (with up to 21 medium parameters) and can be oriented (tilted) in any arbitrary direction. Note that there are six different possibilities for the incident wave: the incident wave can be either in the upper medium or in the lower medium and it can be either qP-wave, qSV-wave or qSH-wave. We will set up the problem by incorporating all possible incident waves, to save ourselves some work. To solve the system for a given incident wave, we set the amplitude of the remaining incident waves to zero.

The particle displacement $\boldsymbol{u}$ for each wave has the form given by equation 2.38, namely:

$$\boldsymbol{u} = \boldsymbol{U}\, e^{i\omega(\boldsymbol{s}\cdot\boldsymbol{x}-t)} = U\, e^{i\omega(\boldsymbol{s}\cdot\boldsymbol{x}-t)}\, \boldsymbol{d} \tag{4.1}$$

where $\boldsymbol{U} = U\,\boldsymbol{d}$, is the polarization vector, U is the amplitude of the wave and $\boldsymbol{d}$ is the unit polarization vector. Each wave has a different amplitude U, unit polarization direction d and slowness s. The naming convention for the different waves is according to figure 4.1.

For welded contact, the boundary conditions are the continuity of the displacement and stress across the interface:

$$\sum_{i=1}^{4}(-1)^i\left(\boldsymbol{u}_{qP}^{(i)} + \boldsymbol{u}_{qSV}^{(i)} + \boldsymbol{u}_{qSH}^{(i)}\right) = 0 \tag{4.2}$$

$$\sum_{i=1}^{4}(-1)^i\left(\boldsymbol{\Sigma}_{qP}^{(i)} + \boldsymbol{\Sigma}_{qSV}^{(i)} + \boldsymbol{\Sigma}_{qSH}^{(i)}\right)\cdot\boldsymbol{n} = 0 \tag{4.3}$$

where $\boldsymbol{n} = (0,0,1)^T$ is a unit vector normal to the interface and $\boldsymbol{\Sigma}$ is defined as follows:

$$\boldsymbol{\Sigma} = \begin{pmatrix} \sigma_{11} & \sigma_{12} & \sigma_{13} \\ \sigma_{12} & \sigma_{22} & \sigma_{23} \\ \sigma_{13} & \sigma_{23} & \sigma_{33} \end{pmatrix} \tag{4.4}$$

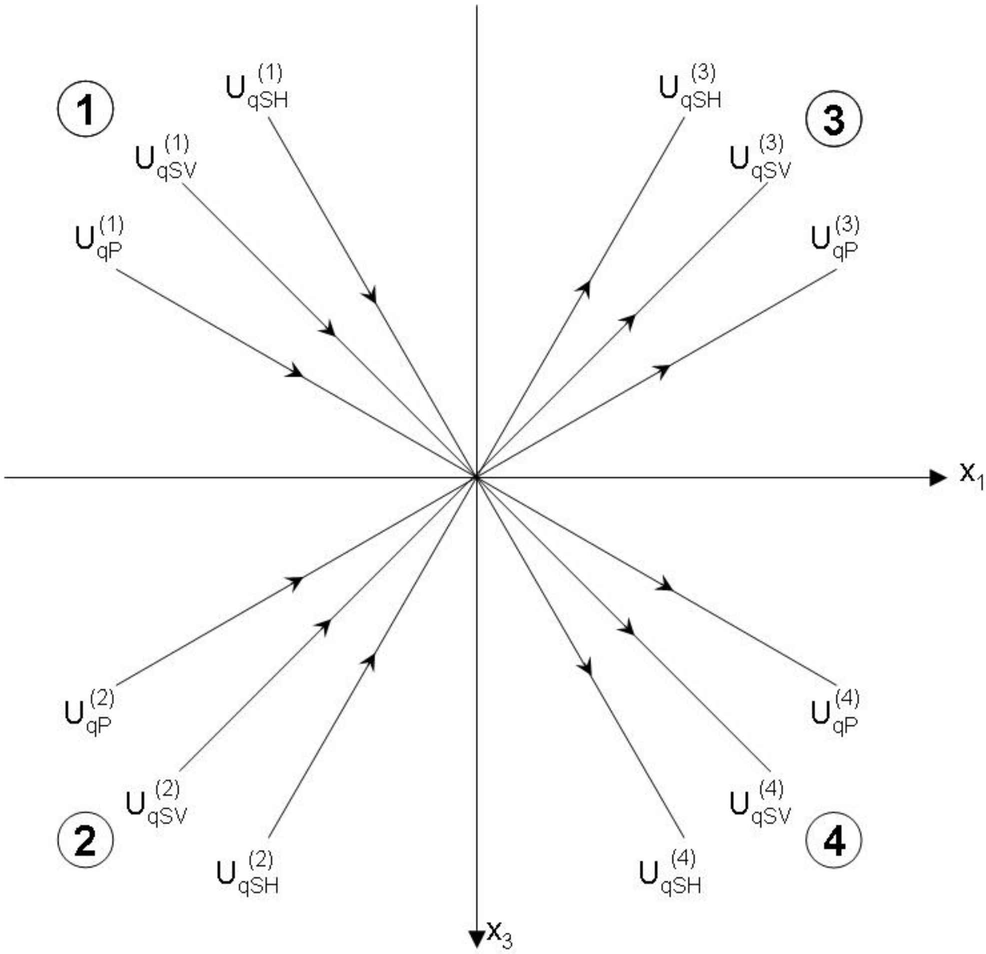

Figure 4.1: Reflection and transmission of an incident qP, qSV or qSH-wave from the upper or lower medium in a generally anisotropic medium

Equation 4.3 only involves σ_{13}, σ_{23} and σ_{33}, because

$$\boldsymbol{\Sigma} \cdot \boldsymbol{n} = \begin{pmatrix} \sigma_{11} & \sigma_{12} & \sigma_{13} \\ \sigma_{12} & \sigma_{22} & \sigma_{23} \\ \sigma_{13} & \sigma_{23} & \sigma_{33} \end{pmatrix} \begin{pmatrix} 0 \\ 0 \\ 1 \end{pmatrix} = \begin{pmatrix} \sigma_{13} \\ \sigma_{23} \\ \sigma_{33} \end{pmatrix} \tag{4.5}$$

with

$$\sigma_{i3} = c_{i3kl}\, i\omega s_l u_k, \quad i = 1, 2, 3 \tag{4.6}$$

Snell's law implies that all slowness vectors lie in the plane formed by the slowness vector of the incident wave and the normal to the interface which means, in our case (figure 4.1), that $s_2 = 0$ for all waves. Moreover, the projections of the slowness vectors on the interface coincide, which means in our case, that

$$\begin{gathered} s_{1\,qP}^{(1)} = s_{1\,qP}^{(2)} = s_{1\,qP}^{(3)} = s_{1\,qP}^{(4)} = s_{1\,qSV}^{(1)} = s_{1\,qSV}^{(2)} = s_{1\,qSV}^{(3)} = \\ s_{1\,qSV}^{(4)} = s_{1\,qSH}^{(1)} = s_{1\,qSH}^{(2)} = s_{1\,qSH}^{(3)} = s_{1\,qSH}^{(4)} \equiv s_1 \end{gathered} \tag{4.7}$$

This is just Snell's law. From equation 4.6 and Snell's law (with $s_2 = 0$), we can write the tangential stress components as follows:

$$\sigma_i = i\omega U h_i, \quad i = 3, 4, 5 \tag{4.8}$$

where σ_3, σ_4 and σ_5 are the third, fourth and fifth elements of the stress column vector (2.26), and where

$$h_i = c_{i1} s_1 d_1 + c_{i3} s_3 d_3 + c_{i4} s_3 d_2 + c_{i5}(s_1 d_3 + s_3 d_1) + c_{i6} s_1 d_2 \tag{4.9}$$

Note that the complex exponential is not present in equation 4.8 because it cancels out when Snell's law is applied at the interface. Together, equations 4.2 and 4.3 will produce the following system of six equations:

$$\begin{cases} \sum_{i=1}^{4}(-1)^i\left(u_{k\,qP}^{(i)} + u_{k\,qSV}^{(i)} + u_{k\,qSH}^{(i)}\right) = 0, \quad k = 1,2,3 \\ \sum_{i=1}^{4}(-1)^i\left(\sigma_{l\,qP}^{(i)} + \sigma_{l\,qSV}^{(i)} + \sigma_{l\,qSH}^{(i)}\right) = 0, \quad l = 3,4,5 \end{cases} \tag{4.10}$$

where σ_i is defined in equation 4.8.

From equations 4.7 and 4.8, the system of equations 4.10 becomes:

$$\begin{cases} \sum_{i=1}^{4}(-1)^i\left(U_{qP}^{(i)}d_{k\,qP}^{(i)} + U_{qSV}^{(i)}d_{k\,qSV}^{(i)} + U_{qSH}^{(i)}d_{k\,qSH}^{(i)}\right) = 0, \quad k = 1,2,3 \\ \sum_{i=1}^{4}(-1)^i\left(U_{qP}^{(i)}h_{l\,qP}^{(i)} + U_{qSV}^{(i)}h_{l\,qSV}^{(i)} + U_{qSH}^{(i)}h_{l\,qSH}^{(i)}\right) = 0, \quad l = 3,4,5 \end{cases} \tag{4.11}$$

which can be written more explicitly as follows:

$$\boldsymbol{A}\,\boldsymbol{x} = \boldsymbol{B}\,\boldsymbol{y} \tag{4.12}$$

where

$$\boldsymbol{A} = \begin{pmatrix} -d_{1\,qP}^{(3)} & -d_{1\,qSV}^{(3)} & -d_{1\,qSH}^{(3)} & d_{1\,qP}^{(4)} & d_{1\,qSV}^{(4)} & d_{1\,qSH}^{(4)} \\ -d_{2\,qP}^{(3)} & -d_{2\,qSV}^{(3)} & -d_{2\,qSH}^{(3)} & d_{2\,qP}^{(4)} & d_{2\,qSV}^{(4)} & d_{2\,qSH}^{(4)} \\ -d_{3\,qP}^{(3)} & -d_{3\,qSV}^{(3)} & -d_{3\,qSH}^{(3)} & d_{3\,qP}^{(4)} & d_{3\,qSV}^{(4)} & d_{3\,qSH}^{(4)} \\ -h_{1\,qP}^{(3)} & -h_{1\,qSV}^{(3)} & -h_{1\,qSH}^{(3)} & h_{1\,qP}^{(4)} & h_{1\,qSV}^{(4)} & h_{1\,qSH}^{(4)} \\ -h_{2\,qP}^{(3)} & -h_{2\,qSV}^{(3)} & -h_{2\,qSH}^{(3)} & h_{2\,qP}^{(4)} & h_{2\,qSV}^{(4)} & h_{2\,qSH}^{(4)} \\ -h_{3\,qP}^{(3)} & -h_{3\,qSV}^{(3)} & -h_{3\,qSH}^{(3)} & h_{3\,qP}^{(4)} & h_{3\,qSV}^{(4)} & h_{3\,qSH}^{(4)} \end{pmatrix}, \ \boldsymbol{x} = \begin{pmatrix} U_{qP}^{(3)} \\ U_{qSV}^{(3)} \\ U_{qSH}^{(3)} \\ U_{qP}^{(4)} \\ U_{qSV}^{(4)} \\ U_{qSH}^{(4)} \end{pmatrix} \tag{4.13}$$

$$
\boldsymbol{B} = \begin{pmatrix}
d^{(1)}_{1\,qP} & d^{(1)}_{1\,qSV} & d^{(1)}_{1\,qSH} & -d^{(2)}_{1\,qP} & -d^{(2)}_{1\,qSV} & -d^{(2)}_{1\,qSH} \\
d^{(1)}_{2\,qP} & d^{(1)}_{2\,qSV} & d^{(1)}_{2\,qSH} & -d^{(2)}_{2\,qP} & -d^{(2)}_{2\,qSV} & -d^{(2)}_{2\,qSH} \\
d^{(1)}_{3\,qP} & d^{(1)}_{3\,qSV} & d^{(1)}_{3\,qSH} & -d^{(2)}_{3\,qP} & -d^{(2)}_{3\,qSV} & -d^{(2)}_{3\,qSH} \\
h^{(1)}_{1\,qP} & h^{(1)}_{1\,qSV} & h^{(1)}_{1\,qSH} & -h^{(2)}_{1\,qP} & -h^{(2)}_{1\,qSV} & -h^{(2)}_{1\,qSH} \\
h^{(1)}_{2\,qP} & h^{(1)}_{2\,qSV} & h^{(1)}_{2\,qSH} & -h^{(2)}_{2\,qP} & -h^{(2)}_{2\,qSV} & -h^{(2)}_{2\,qSH} \\
h^{(1)}_{3\,qP} & h^{(1)}_{3\,qSV} & h^{(1)}_{3\,qSH} & -h^{(2)}_{3\,qP} & -h^{(2)}_{3\,qSV} & -h^{(2)}_{3\,qSH}
\end{pmatrix}, \; \boldsymbol{y} = \begin{pmatrix}
U^{(1)}_{qP} \\ U^{(1)}_{qSV} \\ U^{(1)}_{qSH} \\ U^{(2)}_{qP} \\ U^{(2)}_{qSV} \\ U^{(2)}_{qSH}
\end{pmatrix} \tag{4.14}
$$

For example, for an incident P-wave from the upper medium, the array $\boldsymbol{y}$ will be given as follows:

$$
\boldsymbol{y} = (1, 0, 0, 0, 0, 0)^T \tag{4.15}
$$

and the right hand side of equation 4.12, namely $\boldsymbol{B}\,\boldsymbol{y}$, will be given as follows:

$$
\boldsymbol{B}\,\boldsymbol{y} = (d^{(1)}_{1\,qP}, d^{(1)}_{2\,qP}, d^{(1)}_{3\,qP}, h^{(1)}_{1\,qP}, h^{(1)}_{2\,qP}, h^{(1)}_{3\,qP})^T \tag{4.16}
$$

The scattering coefficients given by the vector $\boldsymbol{x} = \left(U^{(3)}_{qP}, U^{(3)}_{qSV}, U^{(3)}_{qSH}, U^{(4)}_{qP}, U^{(4)}_{qSV}, U^{(4)}_{qSH}\right)^T$ resulting from an incident P-wave from the upper medium, can be obtained by solving the following linear system:

$$
\begin{pmatrix}
-d^{(3)}_{1\,qP} & -d^{(3)}_{1\,qSV} & -d^{(3)}_{1\,qSH} & d^{(4)}_{1\,qP} & d^{(4)}_{1\,qSV} & d^{(4)}_{1\,qSH} \\
-d^{(3)}_{2\,qP} & -d^{(3)}_{2\,qSV} & -d^{(3)}_{2\,qSH} & d^{(4)}_{2\,qP} & d^{(4)}_{2\,qSV} & d^{(4)}_{2\,qSH} \\
-d^{(3)}_{3\,qP} & -d^{(3)}_{3\,qSV} & -d^{(3)}_{3\,qSH} & d^{(4)}_{3\,qP} & d^{(4)}_{3\,qSV} & d^{(4)}_{3\,qSH} \\
-h^{(3)}_{1\,qP} & -h^{(3)}_{1\,qSV} & -h^{(3)}_{1\,qSH} & h^{(4)}_{1\,qP} & h^{(4)}_{1\,qSV} & h^{(4)}_{1\,qSH} \\
-h^{(3)}_{2\,qP} & -h^{(3)}_{2\,qSV} & -h^{(3)}_{2\,qSH} & h^{(4)}_{2\,qP} & h^{(4)}_{2\,qSV} & h^{(4)}_{2\,qSH} \\
-h^{(3)}_{3\,qP} & -h^{(3)}_{3\,qSV} & -h^{(3)}_{3\,qSH} & h^{(4)}_{3\,qP} & h^{(4)}_{3\,qSV} & h^{(4)}_{3\,qSH}
\end{pmatrix}
\begin{pmatrix}
U^{(3)}_{qP} \\ U^{(3)}_{qSV} \\ U^{(3)}_{qSH} \\ U^{(4)}_{qP} \\ U^{(4)}_{qSV} \\ U^{(4)}_{qSH}
\end{pmatrix}
=
\begin{pmatrix}
d^{(1)}_{1\,qP} \\ d^{(1)}_{2\,qP} \\ d^{(1)}_{3\,qP} \\ h^{(1)}_{1\,qP} \\ h^{(1)}_{2\,qP} \\ h^{(1)}_{3\,qP}
\end{pmatrix}
\tag{4.17}
$$

4.2 Arbitrary Tilt Angles

The TAVRT program handles anisotropic media with arbitrary tilt angles. One of the most common ways of describing 3D rotations is by using Euler's angles (ϕ, θ, ψ) (Goldstein, 1980). Starting from the cartesian coordinate system (x_1, x_2, x_3), the first rotation is a rotation about the x_3-axis by the angle ϕ. Denoting the new coordinate system by (x'_1, x'_2, x'_3), the second rotation is a rotation about the x'_2-axis (the line of nodes) by the angle θ. Denoting the new coordinate system by (x''_1, x''_2, x''_3), the third rotation is a rotation about the x''_3-axis by the angle ψ. The new coordinate system is denoted by (x'''_1, x'''_2, x'''_3) (see figure 4.2).

Notice that Euler's angles (ϕ, θ, ψ) described here to specify the rotation of the coordinate system (x'''_1, x'''_2, x'''_3) relative to the coordinate system (x_1, x_2, x_3), can be found with variations in the literature. Note that we have used the x'_2-axis as the second axis of rotation and the line of nodes, unlike Goldstein (1980) who uses x'_1-axis.

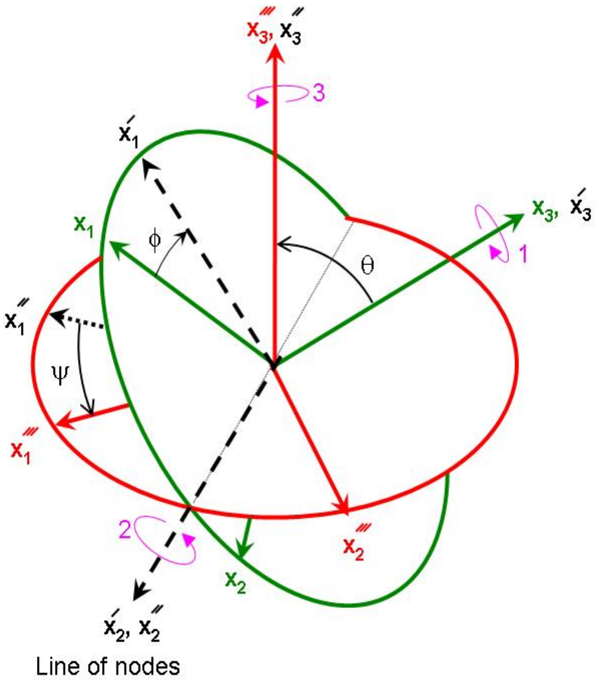

Figure 4.2: The definition of the Euler angles (ϕ, θ, ψ) that relate the un-tilted coordinate system (x''', y''', z''') to the tilted coordinate system (x, y, z)

TAVRT assumes that the stiffness matrix $\boldsymbol{C'''}$ for the medium is known in the (x_1''', x_2''', x_3''') system and computes the stiffness matrix $\boldsymbol{C}$ in the (x_1, x_2, x_3) system.

Figure 4.3 was produced by TAVRT. It depicts the comparison between P1P1 scattering coefficient versus angle of incidence of a VTI over isotropic interface and P1P1 scattering coefficient versus angle of incidence of a tilted VTI over isotropic interface. The tilt is given by the following Euler angles: $(\phi = 15^o, \theta = 30^o, \psi = 45^o)$. The model parameters are given in table 4.1.

Table 4.1: Model parameters used for constructing figure 4.3

Parameter	Upper Medium	Lower Medium
V_{P0}	3.00	3.50
V_{S0}	2.00	2.70
ρ	2.50	2.70
ϵ	0.10	0.00
δ	0.10	0.00
γ	0.10	0.00

Velocities in km/s and density in g/cm^3

4.3 Solution of the Christoffel Equation

4.3.1 Calculation of Vertical Slownesses

The vertical slowness s_3 components for each wave can be obtained by solving the dispersion relation (2.55), which can be rewritten, using equations 2.39 and 2.53, as follows:

$$\left| c_{ijkl} s_j s_l - \rho \delta_{ij} \right| = 0 \tag{4.18}$$

or

$$\left| \boldsymbol{S} \boldsymbol{C} \boldsymbol{S}^T - \rho I_{(3)} \right| = 0 \tag{4.19}$$

where

$$\boldsymbol{S} = \begin{pmatrix} s_1 & 0 & 0 & 0 & s_3 & 0 \\ 0 & 0 & 0 & s_3 & 0 & s_1 \\ 0 & 0 & s_3 & 0 & s_1 & 0 \end{pmatrix} \tag{4.20}$$

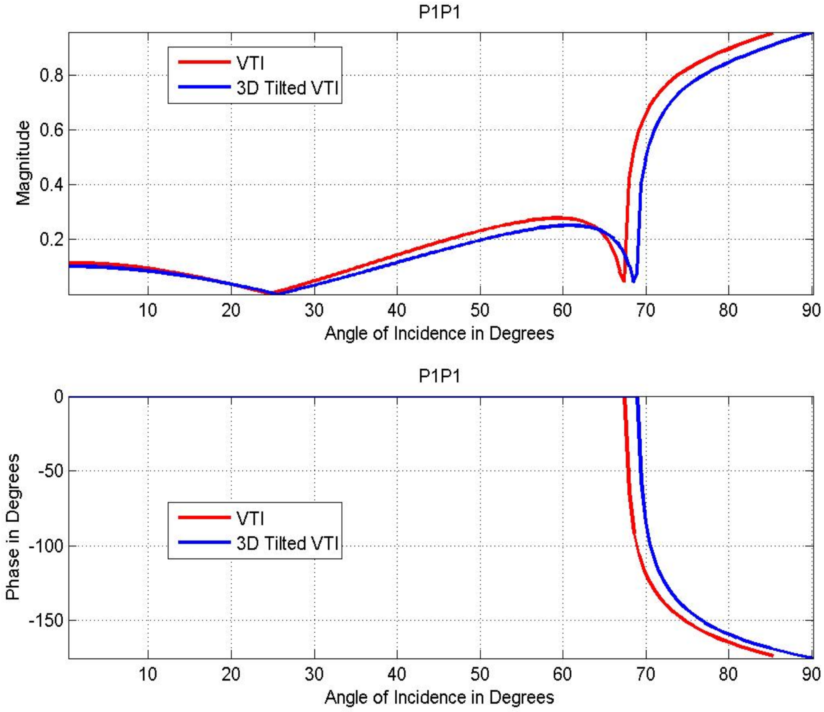

Figure 4.3: A comparison between P1P1 scattering coefficient versus angle of incidence of a VTI over isotropic interface and P1P1 scattering coefficient versus angle of incidence of a tilted ($\phi = 30^o, \theta = 30^o, \psi = 45^o$) VTI over isotropic interface. The model parameters are given in table 4.1.

Equation 4.19 is a sixth degree polynomial of s_3 and by solving it we get 6 solutions: 3 upgoing qP, qSV and qSH waves and 3 downgoing qP, qSV and qSH waves. The distinction between upgoing and downgoing waves is based on the rule that the energy flux vector $\boldsymbol{I}$ should be pointing towards the incidence medium for a reflected wave and to the transmission medium for a transmitted wave (Carcione, 2001). To calculate the energy flux vector $\boldsymbol{I}$, we need first to calculate the unit polarization vector $\boldsymbol{d}$ as we can see from equation 2.63. The solutions of the dispersion relation (4.19) can be either real or complex. The sign of the imaginary part of the complex solutions should be chosen so that the amplitude decays exponentially with distance (Carcione, 2001). These types of waves are known as evanescent waves. An evanescent wave has an energy flux vector $\boldsymbol{I}$ parallel to the interface (Carcione, 2001).

4.3.2 Degeneracy

If two or more of the 6 vertical slownesses s_3 obtained in section 4.3.1 are the same, degeneracy exists. For example, the isotropic case is degenerate for all input ray parameter values (the qSH and qSV wave speeds are the same) and the VTI case is degenerate at ray parameter $s_1 = 0$ (the qSH and qSV vertical wave speeds are the same). The program checks for degeneracy and skips the computations for scattering coefficients for ray parameter (s_1) values resulting in degenerate s_3 values.

4.3.3 Calculation of Unit Polarization Vectors

The Christoffel equation (2.52) can be rewritten, using equations 2.39 and 2.53, as follows:

$$\left(\boldsymbol{S}\hat{\boldsymbol{C}}\boldsymbol{S}^T - I_{(3)}\right)\boldsymbol{U} = 0 \tag{4.21}$$

where $\hat{\boldsymbol{C}}$ is the density-normalized stiffness matrix.

For each value of the vertical slownesses s_3 obtained in section 4.3.1, we solve the eigenvector problem of equation 4.21. We obtain three eigenvalues and eigenvectors. In theory, the only correct eigenvalue is 1 and the other eigenvalues need to be rejected because they correspond to other wave types with the same slowness direction. We select the eigenvector that corresponds to the eigenvalue equal to 1. The unit polarization vector $\boldsymbol{d}$ can be then obtained by normalizing the eigenvector $\boldsymbol{U}$. Notice that the sign of the polarization vectors have not been specified yet and to do this we need to calculate the energy flux vector.

4.4 Wave Types Determination

We have seen in section 4.3.1 that by solving the dispersion relation (4.18), we get six solutions for the vertical component of the slowness s_3. In this section, we are interested in determining the wave types corresponding to each vertical slowness value among the six possible solutions.

The six solutions of equation 4.19 correspond to an upgoing and a downgoing qP-wave, an upgoing and a downgoing qSV-wave, and an upgoing and a downgoing qSH-wave. The qP-waves are characterized by having the closest unit polarization vectors to the slowness vector and hence they have the highest cosine of the angle between the unit polarization and the slowness vectors. The qSV-waves are characterized by having the closest unit polarization vectors to the normal to the slowness vector and hence they have the highest cosine of the angle between the unit polarization and the normal to the slowness vectors. The qSH-waves are characterized by having the closest unit polarization vectors to the x_2-axis and hence they have the highest cosine of the angle between the unit polarization vector and the x_2-axis.

The energy flux vector can be calculated using equation 2.63. It is clear from this

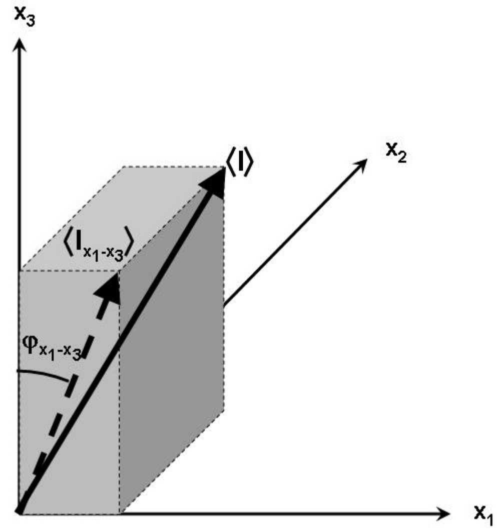

Figure 4.4: Mean Energy Flux Vector $\langle \boldsymbol{I} \rangle$

equation that even with a wrong sign for the polarization vector we get the correct energy flux vector. The energy flux vector has in general an x_2 component, i.e., it is not always in the $x_1 - x_3$ plane (see figure 4.4).

Let $\varphi_{x_1-x_3}$ be the angle in the $x_1 - x_3$ plane made by the $x_1 - x_3$ projection of the mean energy flux vector(see figure 4.4). An upgoing wave would have an angle $\varphi_{x_1-x_3}$ between $-\pi/2$ and $\pi/2$, a downgoing wave would have an angle $\varphi_{x_1-x_3}$ between $\pi/2$ and $3\pi/2$ and an evanescent wave would have an angle $\varphi_{x_1-x_3}$ equal to $-\pi/2$ or $\pi/2$ (see figure 4.5).

The sign of the polarization vector of qP-wave is chosen so that the cosine of

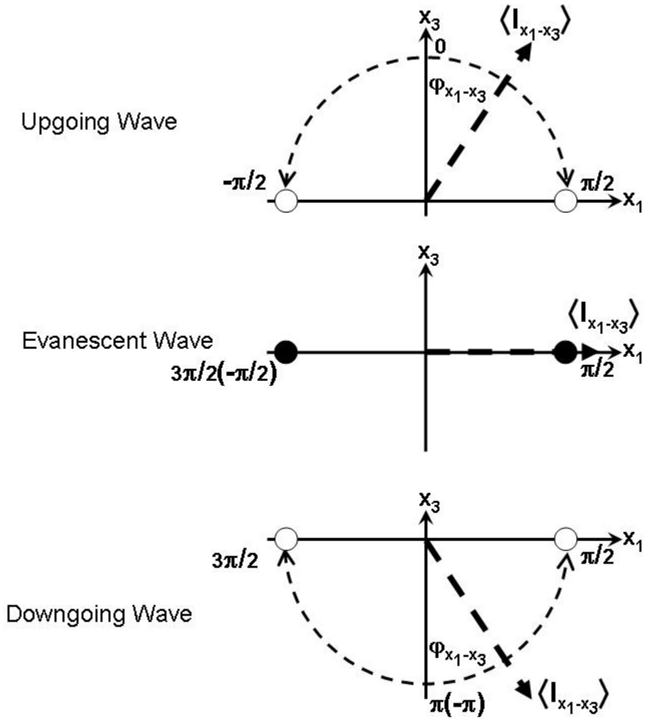

Figure 4.5: Distinguishing Upgoing, Downgoing and Evanescent Waves

the angle between the unit polarization and the slowness vectors is positive (see figure 4.6).

The sign of the polarization vector of qSV-wave is chosen so that the cross product of the slowness with the polarization vector has a positive (negative) x_2 component for waves with upgoing (downgoing) energy flux. This rule assumes that the x_3 axis is pointing upwards (see figure 4.7).

The sign of the polarization vector of qSH-wave is chosen so that it has a negative x_2 component if the x_3 axis is pointing upwards and a positive x_2 component if the x_3 axis is pointing downwards.

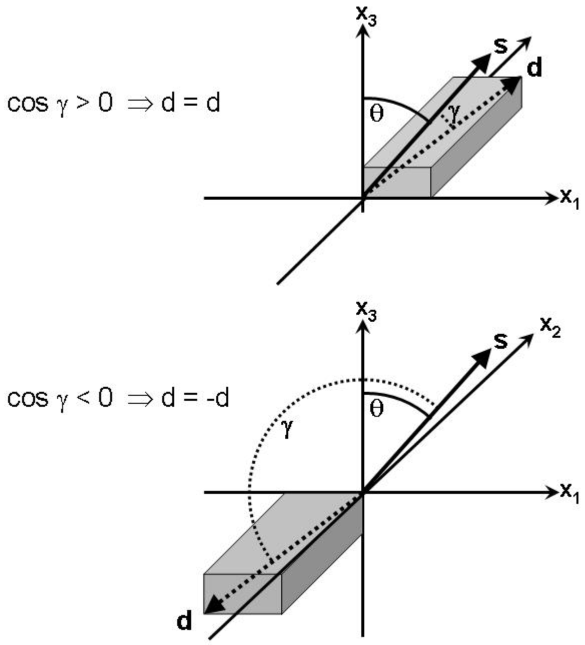

Figure 4.6: qP-Wave Unit Vector Sign Determination

4.5 True Incidence Angles Check

If the phase angle corresponding to a given ray parameter (s_1) for an incident wave is between -90^o and 90^o but the ray angle (or energy angle) is not, then the wave is not really an incident wave, and the given ray parameter value (or phase angle of incidence) should not be included in the plots of the scattering coefficients for that incident wave. At the same time, if the phase angle is not between -90^o and 90^o, but the ray angle is within it, then the wave is a true incident wave, and should be included in the plots. The program computes which ray parameter values correspond to true incident waves, so that the proper plots can be produced.

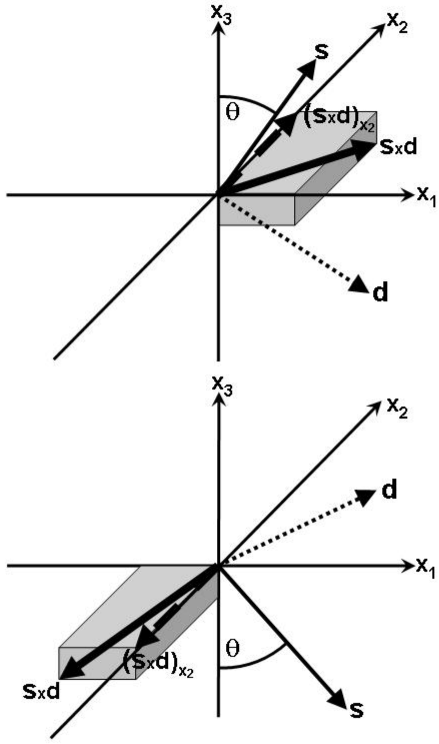

Figure 4.7: qSV-Wave Unit Vector Sign Determination

4.6 TAVRT Algorithm

The main steps involved in TAVRT program can be summarized in the flowchart given in figure 4.9.

4.7 Outputs

In addition to the scattering coefficients, the program outputs:

- The vertical component of the slowness s_3 for all twelve waves (see figure 4.1) corresponding to three downgoing waves (qP, qSV and qSH) in medium 1

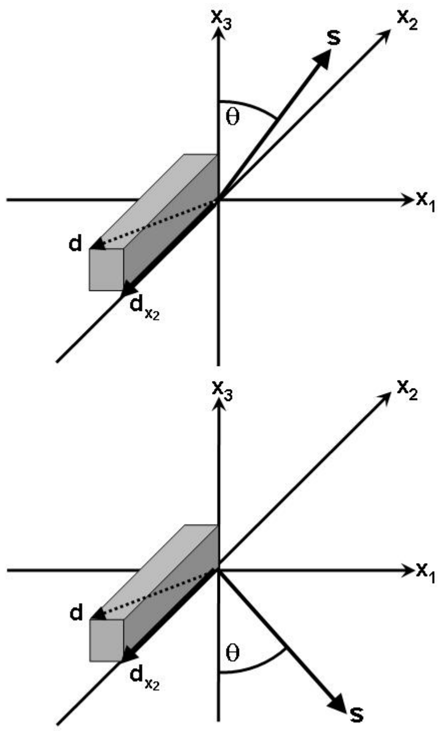

Figure 4.8: qSH-Wave Unit Vector Sign Determination

representing incident waves, three upgoing waves (qP, qSV and qSH) in medium 2 representing incident waves, three upgoing waves (qP, qSV and qSH) in medium 1 and three downgoing waves in medium 2 representing scattered waves.

- The energy velocity (ray or group velocity) vector as well as its magnitude.

- The angle, in degrees, that the energy velocity makes with the $x_1 - x_3$-plane, i.e., the angle between the energy velocity and its projection onto the $x_1 - x_3$-plane.

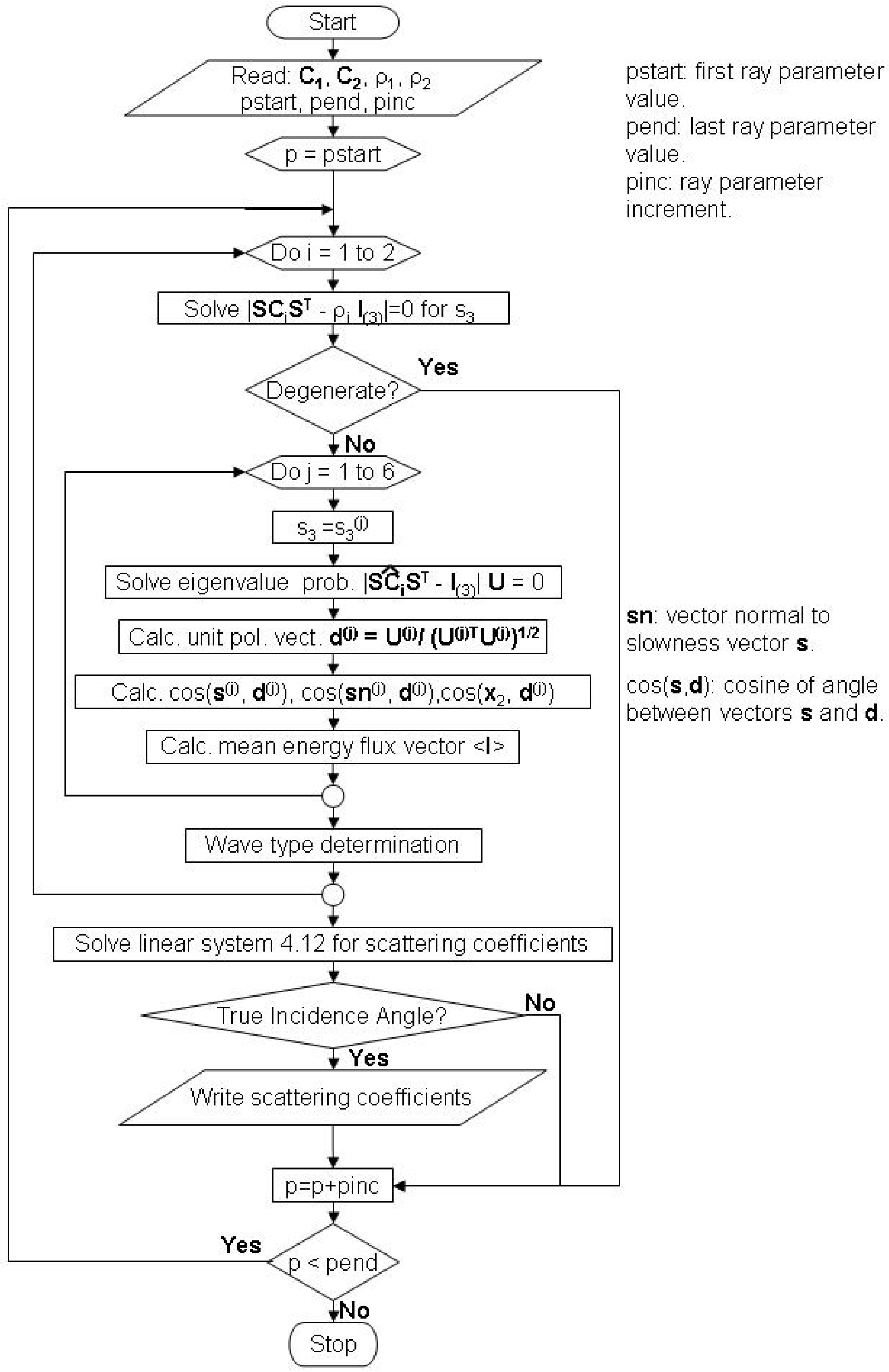

Figure 4.9: TAVRT Flowchart

- The angle, in degrees, made in the $x_1 - x_3$-plane by the projection of the energy velocity onto the $x_1 - x_3$-plane.

- The phase angle in degrees.

- The magnitude of the phase velocity.

- The phase-energy angle, i.e., the angle, in degrees, between the phase velocity and the energy velocity.

- The components of the complex unit polarization vector (which gives the direction of particle motion).

Using these outputs, one can produce, for example, the following plots:

- Any one of the scattering coefficients versus phase angle.

- Any one of the scattering coefficients versus the $x_1 - x_3$ projection of the energy (ray or group) angle.

- The slowness diagram which is the cross-plot of the horizontal component of the slowness s_1 and the vertical component of the slowness s_3.

- A 3D plot of a scattering coefficient versus the ray direction. The vertical axis would be the amplitude axis, and the two horizontal axes would be the two angles required to specify the ray direction (which does not necessarily lie in the $x_1 - x_3$-plane)

4.8 Graphical User Interface (GUI)

In order to facilitate the testing of TAVRT program I created a graphical user interface (GUI) (see figure 4.10) with the following main capabilities:

1. The media parameters can be entered for a given experiment either by filling the stiffness matrices or by entering Thomsen's parameters, then computing the corresponding stiffness matrices.

2. Experiments can be imported and exported.

3. The upper and/or lower stiffness matrix can be rotated, flipped or cleared.

4. The magnitude and phase spectra of a given scattering coefficients can be displayed versus ray parameter or phase angle.

5. The media parameters can be modified to eliminate degeneracy.

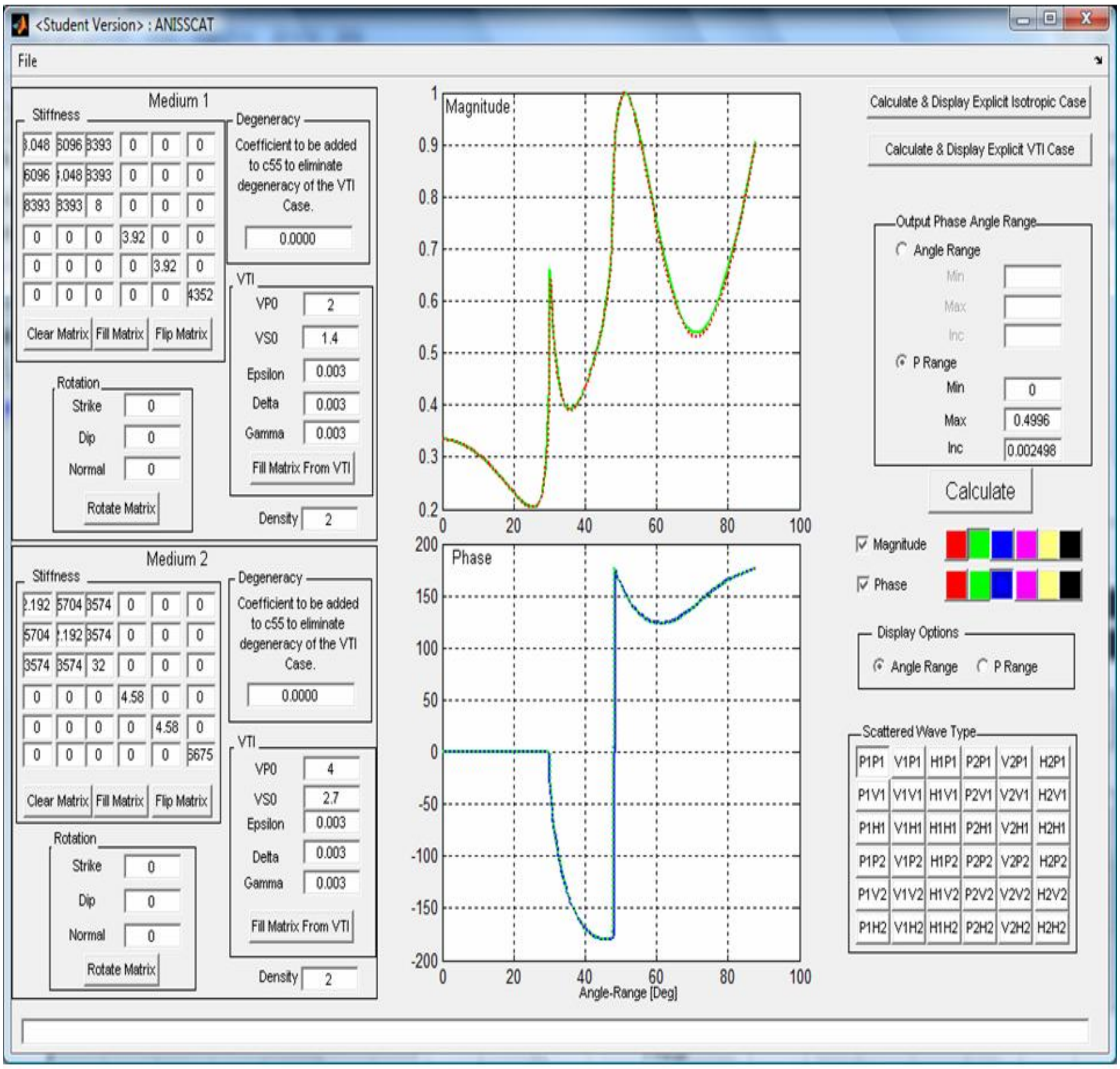

Figure 4.10: TAVRT GUI

Chapter 5

Investigation of the Effect of Tilt on the Scattering Coefficients

In this chapter we are going to investigate the effect of tilt on the scattering coefficients of an SH-wave propagating in a VTI-medium. We first start by deriving analytical formulae for the reflection and transmission coefficients of an SH-wave propagating on a VTI medium tilted with an angle φ about the x_2-axis (see figure 5.1). We then give some examples to help understand the effect of tilt on the SH-wave reflection and transmission coefficients.

5.1 Stiffness Matrix for Tilted VTI Media

A VTI medium refers to a medium represented by the stiffness matrix given by equation 2.29, with the symmetry axis along the x_3-axis. By performing a rotation with an angle φ about the x_2-axis of the coordinate system, the medium becomes tilted VTI as can be seen in figure 5.1. From equation 2.35, the corresponding transformation matrix is given by

$$\boldsymbol{M} = \begin{pmatrix} \cos^2\varphi & 0 & \sin^2\varphi & 0 & -\sin 2\varphi & 0 \\ 0 & 1 & 0 & 0 & 0 & 0 \\ \sin^2\varphi & 0 & \cos^2\varphi & 0 & \sin 2\varphi & 0 \\ 0 & 0 & 0 & \cos\varphi & 0 & \sin\varphi \\ \frac{1}{2}\sin 2\varphi & 0 & -\frac{1}{2}\sin 2\varphi & 0 & \cos 2\varphi & 0 \\ 0 & 0 & 0 & -\sin\varphi & 0 & \cos\varphi \end{pmatrix} \tag{5.1}$$

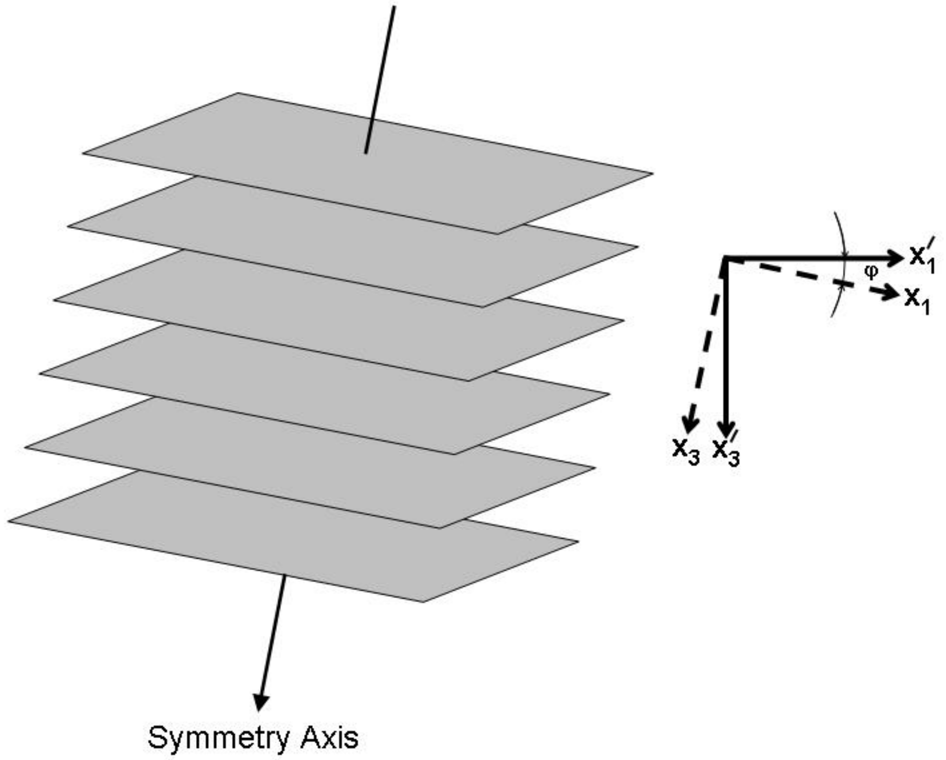

Figure 5.1: Tilted VTI medium with an angle φ about the x_2-axis

Using equation 5.1, the stiffness matrix in the new system is given by

$$\boldsymbol{C}' = \begin{pmatrix} c'_{11} & c'_{12} & c'_{13} & 0 & c'_{15} & 0 \\ c'_{12} & c'_{22} & c'_{23} & 0 & c'_{25} & 0 \\ c'_{13} & c'_{23} & c'_{33} & 0 & c'_{35} & 0 \\ 0 & 0 & 0 & c'_{44} & 0 & c'_{46} \\ c'_{15} & c'_{25} & c'_{35} & 0 & c'_{55} & 0 \\ 0 & 0 & 0 & c'_{46} & 0 & c'_{66} \end{pmatrix} \tag{5.2}$$

where

$$
\begin{gathered}
c'_{11} = (c_{11} + c_{33} - 2c_{13})\cos^4\varphi + 2(c_{13} - c_{33})\cos^2\varphi - c_{55}\cos^2 2\varphi + c_{33} + c_{55} \\
c'_{12} = (c_{11} - c_{13} - 2c_{66})\cos^2\varphi + c_{13} \\
c'_{13} = (2c_{13} - c_{11} - c_{33})\cos^4\varphi + (c_{11} + c_{33} - 2c_{13})\cos^2\varphi + c_{55}\cos^2 2\varphi + c_{13} - c_{55} \\
c'_{15} = \tfrac{1}{2}\sin 2\varphi\Big((c_{11} - 2c_{13} + c_{33})\cos^2\varphi - 2c_{55}\cos 2\varphi + c_{13} - c_{33}\Big) \\
c'_{22} = c_{11} \\
c'_{23} = (c_{13} - c_{11} + 2c_{66})\cos^2\varphi + c_{11} - 2c_{66} \\
c'_{25} = -\tfrac{1}{2}(c_{13} - c_{11} + 2c_{66})\sin 2\varphi \\
c'_{33} = (c_{11} + c_{33} - 2c_{13})\cos^4\varphi + 2(c_{13} - c_{11})\cos^2\varphi - 2c_{55}\cos^2 2\varphi + c_{11} + c_{55} \\
c'_{35} = -\tfrac{1}{2}\sin 2\varphi\Big((c_{11} - 2c_{13} + c_{33})\cos^2\varphi - 2c_{55}\cos 2\varphi - c_{11} + c_{13}\Big) \\
c'_{44} = (c_{55} - c_{66})\cos^2\varphi + c_{66} = c_{55}\cos^2\varphi + c_{66}\sin^2\varphi \\
c'_{46} = (c_{66} - c_{55})\sin\varphi\cos\varphi \\
c'_{55} = \tfrac{1}{4}\Big((2c_{13} - c_{11} - c_{33} + 4c_{55})\cos^2 2\varphi + c_{11} - 2c_{13} + c_{33}\Big) \\
c'_{66} = (c_{66} - c_{55})\cos^2\varphi + c_{55}
\end{gathered}
\tag{5.3}
$$

I have checked that these are correct by comparing them with the numerical results from TAVRT.

5.2 Solution of the Christoffel Equation for Tilted VTI Media

The Christoffel equation for a tilted VTI medium can be given as follows:

$$
\begin{pmatrix} G'_{11} - \rho v^2 & G'_{12} & G'_{13} \\ G'_{12} & G'_{22} - \rho v^2 & G'_{23} \\ G'_{13} & G'_{23} & G'_{33} - \rho v^2 \end{pmatrix} \begin{pmatrix} U'_1 \\ U'_2 \\ U'_3 \end{pmatrix} = 0 \tag{5.4}
$$

where

$$
\begin{aligned}
G'_{11} &= c'_{11}n'^2_1 + c'_{66}n'^2_2 + c'_{55}n'^2_3 + 2c'_{15}n'_1n'_3 \\
G'_{22} &= c'_{66}n'^2_1 + c'_{22}n'^2_2 + c'_{44}n'^2_3 + 2c'_{46}n'_1n'_3 \\
G'_{33} &= c'_{55}n'^2_1 + c'_{44}n'^2_2 + c'_{33}n'^2_3 + 2c'_{35}n'_1n'_3 \\
G'_{23} &= (c'_{44} + c'_{23})n'_2n'_3 + (c'_{25} + c'_{46})n'_1n'_2 \\
G'_{13} &= c'_{15}n'^2_1 + c'_{46}n'^2_2 + c'_{35}n'^2_3 + (c'_{13} + c'_{55})c'_{35}n'_1n'_3 \\
G'_{12} &= (c'_{46} + c'_{25})n'_2n'_3 + (c'_{12} + c'_{66})n'_1n'_2
\end{aligned}
\tag{5.5}
$$

For propagation in the $x_1 - x_3$-plane ($n'_2 = 0$), the stiffness matrix becomes

$$
\begin{pmatrix} G'_{11} - \rho v^2 & 0 & G'_{13} \\ 0 & G'_{22} - \rho v^2 & 0 \\ G'_{13} & 0 & G'_{33} - \rho v^2 \end{pmatrix} \begin{pmatrix} U'_1 \\ U'_2 \\ U'_3 \end{pmatrix} = 0 \tag{5.6}
$$

where

$$
\begin{aligned}
G'_{11} &= c'_{11}n'^2_1 + 2c'_{15}n'_1n'_3 \\
G'_{22} &= c'_{66}n'^2_1 + c'_{44}n'^2_3 + 2c'_{46}n'_1n'_3 \\
G'_{33} &= c'_{55}n'^2_1 + c'_{33}n'^2_3 + 2c'_{35}n'_1n'_3 \\
G'_{23} &= 0 \\
G'_{13} &= c'_{15}n'^2_1 + c'_{35}n'^2_3 + (c'_{13} + c'_{55})c'_{35}n'_1n'_3 \\
G'_{12} &= 0
\end{aligned}
\tag{5.7}
$$

We obtain the following two uncoupled dispersion relations:

$$
\begin{aligned}
G'_{22} - \rho v^2 &= 0, \\
(G'_{11} - \rho v^2)(G'_{33} - \rho v^2) - G'^2_{13} &= 0
\end{aligned}
\tag{5.8}
$$

From equation 5.6, we can see that the first equation of 5.8 has a displacement $u' = (0, u'_2, 0)^T$, which describes a horizontally polarized pure shear wave, i.e. SH-wave. The phase velocity of the SH-wave can be given as follows:

$$
v = \sqrt{\frac{1}{\rho}\Big(c'_{66}n'^2_1 + c'_{44}n'^2_3 + 2c'_{46}n'_1n'_3\Big)} \tag{5.9}
$$

where $n'_1 = \sin\theta$ and $n'_3 = \cos\theta$.

For the case of no tilt ($\varphi = 0$), equation 5.9 becomes

$$v = \sqrt{\frac{1}{\rho}\Big(c_{66}\sin^2\theta + c_{55}\cos^2\theta\Big)} \tag{5.10}$$

since $c'_{66} = c_{66}$, $c'_{44} = c_{55}$, and $c'_{46} = 0$ for $\varphi = 0$, which is, as expected, identical to the phase velocity of an SH-wave traveling in a VTI medium (3.10).

The first equation of 5.8 can be rewritten as follows:

$$c'_{44}{s'}_3^2 + 2c'_{46}{s'}_1{s'}_3 + c'_{66}{s'}_1^2 - \rho = 0 \tag{5.11}$$

Solving equation 5.11 for ${s'}_3$, we get 2 solutions:

$$\begin{aligned} {s'}_3{}^{(1)} &= \tfrac{1}{c'_{44}}\Big(- c'_{46}{s'}_1 + \sqrt{{c'_{46}}^2{s'}_1^2 - c'_{44}(c'_{66}{s'}_1^2 - \rho)}\Big) \\ {s'}_3{}^{(2)} &= \tfrac{1}{c'_{44}}\Big(- c'_{46}{s'}_1 - \sqrt{{c'_{46}}^2{s'}_1^2 - c'_{44}(c'_{66}{s'}_1^2 - \rho)}\Big) \end{aligned} \tag{5.12}$$

For an x_3-axis pointing downward, the solution ${s'}_3{}^{(1)}$ corresponds to downward propagating waves while the solution ${s'}_3{}^{(2)}$ corresponds to upward propagating waves.

5.3 Scattering Coefficients for Tilted VTI Media

The particle displacement of the incident, reflected and transmitted SH-waves propagating in a tilted VTI medium can be written as (see figure 5.2)

$$\begin{aligned} {u'}_2^I &= e^{i\omega({s'}_1{x'}_1 + {s'}_3^I{x'}_3 - t)} \\ {u'}_2^R &= Re^{i\omega({s'}_1{x'}_1 + {s'}_3^R{x'}_3 - t)} \\ {u'}_2^T &= Te^{i\omega({s'}_1{x'}_1 + {s'}_3^T{x'}_3 - t)} \end{aligned} \tag{5.13}$$

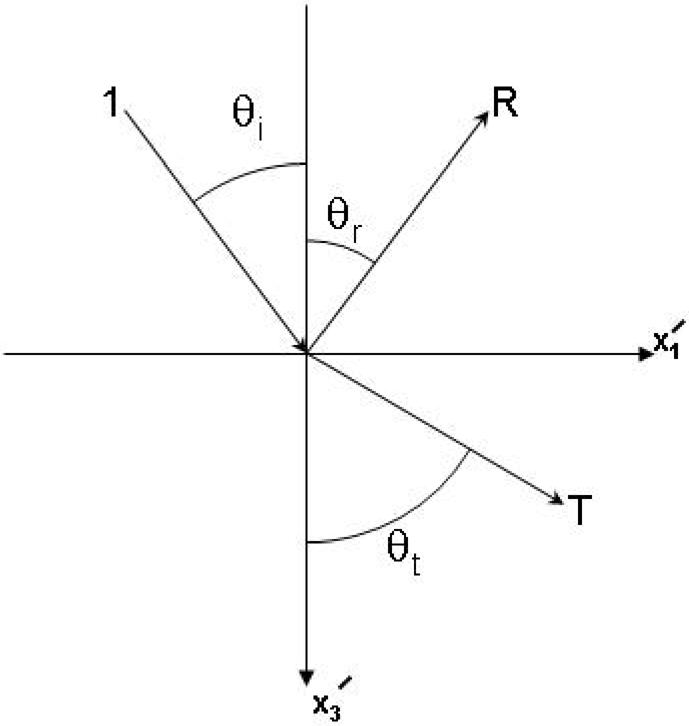

Figure 5.2: Scattering Coefficients of an SH wave. The positive direction of particle motion is the positive x'_2 direction (out of the page).

where R and T are the reflection and transmission coefficients, respectively.

From the stress-strain relation (2.2), we have the x'_2 component of the stress of the incident, reflected and transmitted SH-waves in a tilted VTI medium can be written as

$$\begin{aligned} \sigma'^{I}_{23} &= i\omega u'^{I}_{2}({c'_{2321}}^{(1)} s'_1 + {c'_{2323}}^{(1)} s'^{I}_{3}) \\ \sigma'^{R}_{23} &= i\omega u'^{R}_{2}({c'_{2321}}^{(1)} s'_1 + {c'_{2323}}^{(1)} s'^{R}_{3}) \\ \sigma'^{T}_{23} &= i\omega u'^{T}_{2}({c'_{2321}}^{(2)} s'_1 + {c'_{2323}}^{(2)} s'^{T}_{3}) \end{aligned} \tag{5.14}$$

or

$$
\begin{aligned}
\sigma'^{I}_{4} &= i\omega u'^{I}_{2}(c'^{(1)}_{46} s'_1 + c'^{(1)}_{44} s'^{I}_{3}) \\
\sigma'^{R}_{4} &= i\omega u'^{R}_{2}(c'^{(1)}_{46} s'_1 + c'^{(1)}_{44} s'^{R}_{3}) \\
\sigma'^{T}_{4} &= i\omega u'^{T}_{2}(c'^{(2)}_{46} s'_1 + c'^{(2)}_{44} s'^{T}_{3})
\end{aligned}
\tag{5.15}
$$

using Voigt notation.

The boundary conditions states that u'_2 and σ'_4 are continuous across the boundary ($x'_3 = 0$), i.e.,

$$
\begin{aligned}
\left[u'^{I}_{2} + u'^{R}_{2}\right]_{x'_3=0} &= \left[u'^{T}_{2}\right]_{x'_3=0} \\
\left[\sigma'^{I}_{4} + \sigma'^{R}_{4}\right]_{x'_3=0} &= \left[\sigma'^{T}_{4}\right]_{x'_3=0}
\end{aligned}
\tag{5.16}
$$

Substituting equations 5.13 and 5.15 into equation 5.16, we get

$$
\begin{aligned}
T &= 1 + R \\
Z^T T &= Z^I + Z^R R
\end{aligned}
\tag{5.17}
$$

where $Z = c'_{46} s'_1 + c'_{44} s'_3$.

The system of equations 5.17, has the following solution:

$$
R = \frac{Z^I - Z^T}{Z^T - Z^R}, \quad T = \frac{Z^I - Z^R}{Z^T - Z^R} \tag{5.18}
$$

The dispersion relation can be given for the incident wave as follows

$$
c'_{44} s'^{I\,2}_{3} + 2c'_{46} s'_1 s'^{I}_{3} + c'_{66} s'^{2}_{1} - \rho = 0 \tag{5.19}
$$

and it can be given for the reflected wave as follows

$$c'_{44}{s'}_3^{R\,2} + 2c'_{46}{s'}_1{s'}_3^{R} + c'_{66}{s'}_1^{2} - \rho = 0 \tag{5.20}$$

Subtracting equation 5.20 from equation 5.19, we get

$$2c'_{46}{s'}_1({s'}_3^{I} - {s'}_3^{R}) + c'_{44}({s'}_3^{I\,2} - {s'}_3^{R\,2}) = 0 \tag{5.21}$$

In general, $({s'}_3^{I} - {s'}_3^{R}) \neq 0$, then equation 5.21 becomes

$$2c'_{46}{s'}_1 + c'_{44}({s'}_3^{I} + {s'}_3^{R}) = 0 \tag{5.22}$$

which means that

$$Z^R = -Z^I \tag{5.23}$$

and hence the reflection and transmission coefficients become

$$R = \frac{Z^I - Z^T}{Z^I + Z^T}, \quad T = \frac{2Z^I}{Z^I + Z^T} \tag{5.24}$$

The angle of incidence can be defined as follows:

$$\theta_i = \arctan\left(\frac{{s'}_1}{{s'}_3^{I}}\right) \tag{5.25}$$

and because the incident wave propagates downwards, we have

$$\theta_i = \arctan\left(\frac{s'_1}{\frac{1}{c'_{44}}\Big(-c'_{46}s'_1 + \sqrt{{c'_{46}}^2 s'^2_1 - c'_{44}(c'_{66}s'^2_1 - \rho)}\Big)}\right) \tag{5.26}$$

The angle of reflection can be defined as follows:

$$\theta_r = \arctan\left(\frac{s'_1}{s'^R_3}\right) \tag{5.27}$$

and because the reflected wave propagates upwards, we have

$$\theta_r = \arctan\left(\frac{s'_1}{\frac{1}{c'_{44}}\Big(-c'_{46}s'_1 - \sqrt{{c'_{46}}^2 s'^2_1 - c'_{44}(c'_{66}s'^2_1 - \rho)}\Big)}\right) \tag{5.28}$$

In general, equations 5.27 and 5.28 are not equal, i.e., the angle of incidence is not equal to the angle of reflection in tilted VTI media.

5.4 Ray Angle

True incidence angles correspond to ray (group) angles between -90 and 90^o and only the phase angles corresponding to these angles should be used for plotting scattering coefficients. For a ray (group) angle between -90 and 90^o, the phase angle could be outside of this range and vice versa.

We have seen from section 2.8, that the energy velocity and the group velocity are identical for anisotropic, homogeneous and elastic media. We have seen also from section 2.8, that the energy velocity and the mean energy density $\langle \boldsymbol{I} \rangle$, have the same direction. Hence to calculate the ray angle, we need to calculate the the mean energy density $\langle \boldsymbol{I} \rangle$. Using equation 2.67, the mean energy density for a tilted VTI medium can be given as follows

$$\langle \boldsymbol{I} \rangle = \frac{1}{2}\omega^2 |U|^2 \left(s_1' c_{66}' + s_3' c_{46}', 0, s_1' c_{46}' + s_3' c_{44}' \right)^T \tag{5.29}$$

From equation 5.29, the ray angle can be defined as follows

$$\phi = \arctan \left(\frac{s_1' c_{46}' + s_3' c_{44}'}{s_1' c_{66}' + s_3' c_{46}'} \right) \tag{5.30}$$

5.5 Examples

In this section we are going to give some examples to illustrate the effect of tilt on the scattering coefficients of an SH-wave propagating in a VTI-medium.

Based on the theory developed in this chapter, I implemented a program that calculates explicitly the exact SH reflection and transmission coefficients for interfaces between two tilted VTI media with angles φ_1 and φ_2 about the x_2-axis (figure 5.1).

Figures 5.3 and 5.4 show the SH-wave reflection and transmission coefficients, respectively, as a function of incidence and tilt angles for a boundary between a tilted VTI medium and an isotropic medium. The tilt is measured with respect to the x_2-axis in the clockwise direction. The model parameters are given in table 5.1.

From figures 5.3 and 5.4, we can see that the reflection and transmission coefficients vary with tilt. Figures 5.5 and 5.6 are a zoom in of figures 5.3 and 5.4, respectively. From figure 5.5 we can see that the magnitude of the reflection coefficient decrease with increasing tilt angle and from figure 5.6 we can see that the magnitude of the transmission coefficient increase with increasing tilt angle.

Table 5.1: Model parameters used for constructing figures 5.3 through **??**

Parameter	Upper Medium	Lower Medium
V_{P0}	3.00	3.50
V_{S0}	2.00	2.70
ρ	2.50	2.70
ϵ	0.10	0.00
δ	0.10	0.00
γ	0.10	0.00

Velocities in km/s and density in g/cm^3

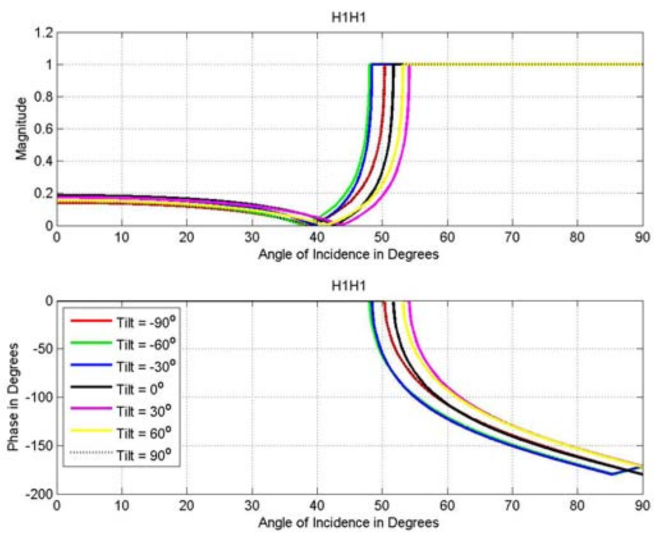

Figure 5.3: H1H1 Scattering Coefficient vs. Incidence Angle and Tilt. Upper Medium is Tilted VTI and Lower Medium is Isotropic. The model parameters are given in table 5.1.

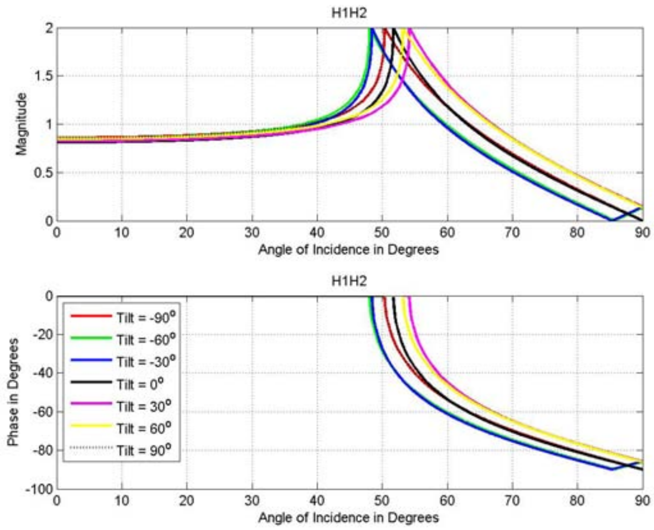

Figure 5.4: H1H2 Scattering Coefficient vs. Incidence Angle and Tilt. Upper Medium is Tilted VTI and Lower Medium is Isotropic. The model parameters are given in table 5.1.

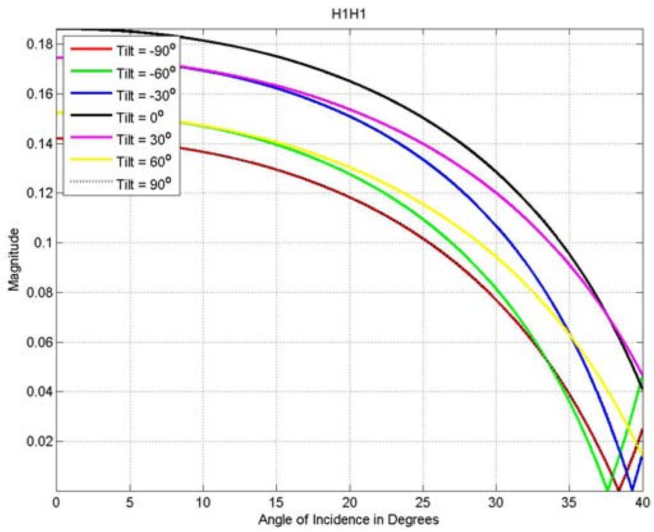

Figure 5.5: Zoom in of figure 5.3.

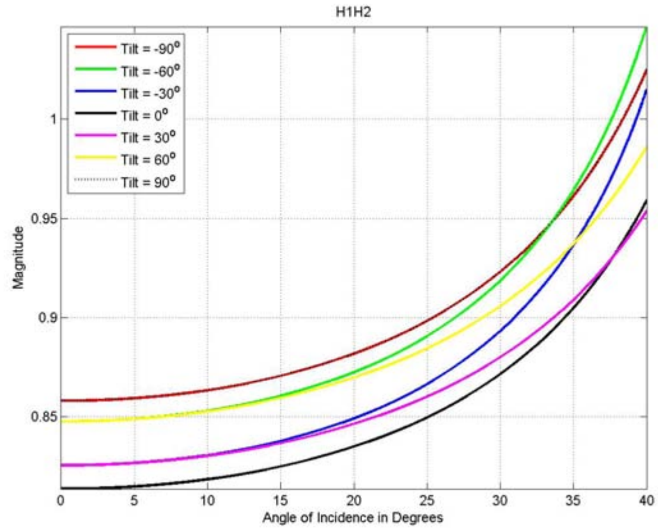

Figure 5.6: Zoom in of figure 5.4.

Notice from figures 5.3 and 5.4, that the angles of incidence (phase angles) beyond 85^o and tilt angles -30^o and -60^o correspond to non-physical rays. To confirm this, we plot the ray angle versus phase angle in figure 5.7, from which we can see that, in fact, the corresponding ray angles are greater than 90^o and the corresponding rays are non-physical.

Figures 5.8 and 5.9 show the SH-wave reflection and transmission coefficients, respectively, as a function of incidence and tilt angles for a boundary between two tilted VTI media. The tilt is measured with respect to the x_2-axis in the clockwise direction. The model parameters are given in table 5.2.

From figures 5.8 and 5.9, we can see that the reflection and transmission coefficients are unaffected by the sign of the tilt angle of the lower medium. Notice that in both figures, only reflection and transmission coefficients for physical rays have

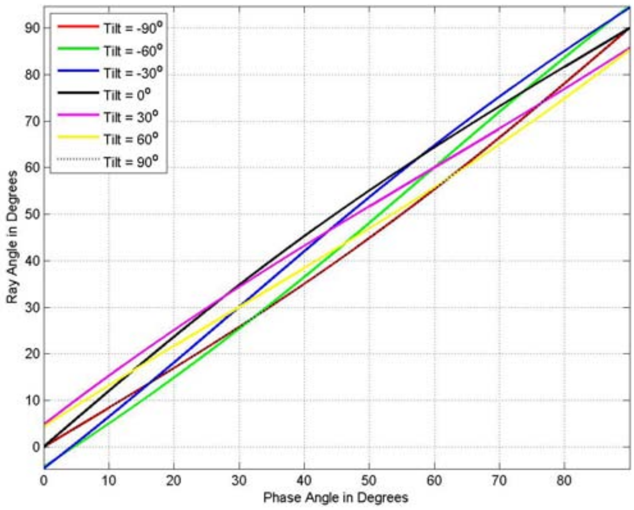

Figure 5.7: Ray vs. Phase Angle. Upper Medium is Tilted VTI and Lower Medium is Isotropic. The model parameters are given in table 5.1.

Table 5.2: Model parameters used for constructing figures 5.8 and 5.9

Parameter	Upper Medium	Lower Medium
V_{P0}	3.00	3.50
V_{S0}	2.00	2.70
ρ	2.50	2.70
ϵ	0.10	0.20
δ	0.10	0.20
γ	0.10	0.20

Velocities in km/s and density in g/cm^3

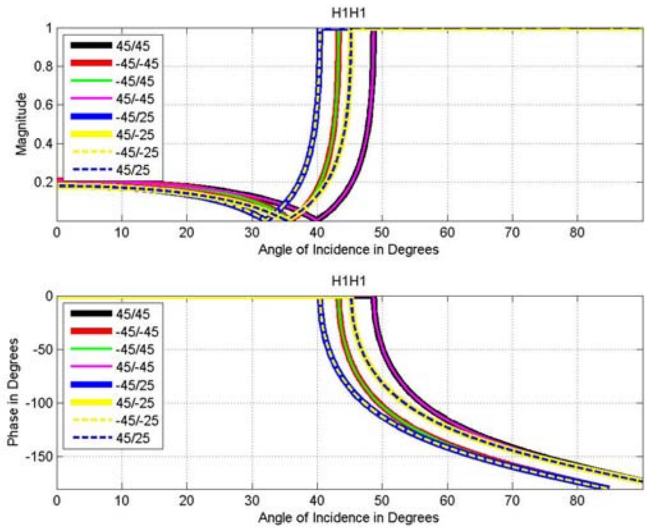

Figure 5.8: H1H1 Scattering Coefficient vs. Incidence Angle and Tilt. Both Media are Tilted VTI. The model parameters are given in table 5.2.

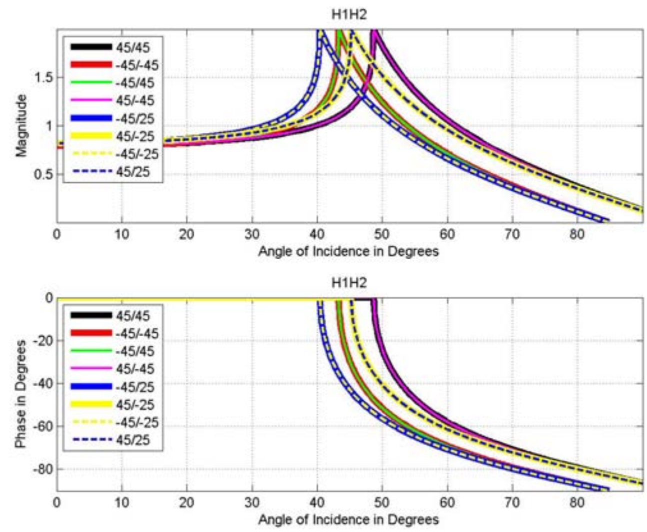

Figure 5.9: H1H2 Scattering Coefficient vs. Incidence Angle and Tilt. Both Media are Tilted VTI. The model parameters are given in table 5.2.

been plotted.

Chapter 6

Comparison Between Numerical and Formula Based Scattering Coefficients

In this chapter I am going to compare between numerical (TAVRT) and formula based scattering coefficients. The comparison is done for isotropic, VTI, tilted VTI, and monoclinic media.

For HTI media, the comparison is done between the results obtained by the program TAVRT and those obtained by the Seismic Unix program refRealAziHTI (Rüger, 2001; Stockwell, 1997) which computes the exact scattering coefficients numerically for interfaces between two HTI media having the same symmetry plane.

The program TAVRT does not include degenerate cases, when the shear wave speeds of the media involved are the same in a given direction. The code simply skips these angles which do not cause problems as they are few and sparse. Interpolation will suffice to fill in these gaps in the reflection and transmission coefficient curves. One other possible solution is to slightly change some appropriate medium parameters without changing the general behavior of the medium to avoid the degeneracy.

6.1 Isotropic Media

Isotropic media are degenerate for all input ray parameter values and to make TAVRT work we need to modify the medium parameters so that the medium becomes

Table 6.1: Model parameters used for constructing figures 6.1 through 6.16

Parameter	Upper Medium	Lower Medium
V_P	2.50	3.60
V_S	1.40	2.08
ρ	2.00	2.00

Velocities in km/s and density in g/cm^3

slightly anisotropic to eliminate the degeneracy. This can be achieved by replacing Thomsen parameters ϵ, δ and γ by a small number, say 0.003 instead of zero, for example.

Based on section 3.2.1, I implemented a program that calculates the exact scattering coefficients for interfaces between two isotropic media. Figures 6.1 through 6.16 show the comparison between the scattering coefficients obtained by the formula based program and the numerical program (TAVRT). The model parameters are given in table 6.1.

From these figures we can see that the scattering coefficients calculated explicitly based on formulae agree very well with the numerical results computed with TAVRT.

6.2 VTI Media

VTI media are degenerate in the vertical direction ($p = 0$), because the qSH and qSV wave speeds are the same. To remove the degeneracy, we need to modify slightly

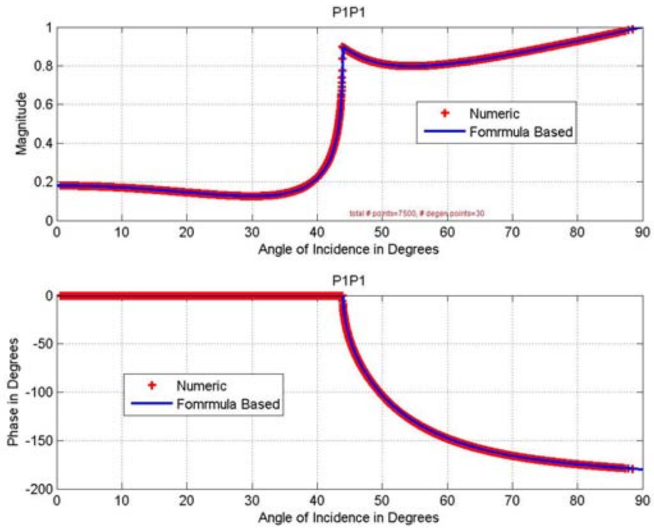

Figure 6.1: P1P1 scattering coefficient versus angle of incidence of an isotropic/isotropic interface. The model parameters are given in table 6.1.

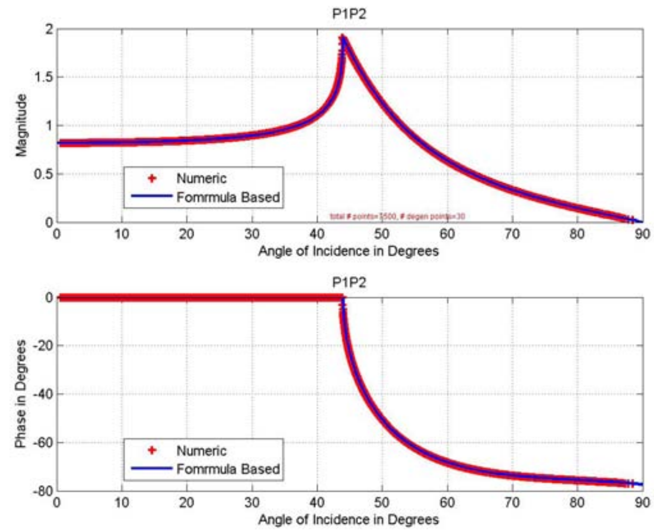

Figure 6.2: P1P2 scattering coefficient versus angle of incidence of an isotropic/isotropic interface. The model parameters are given in table 6.1.

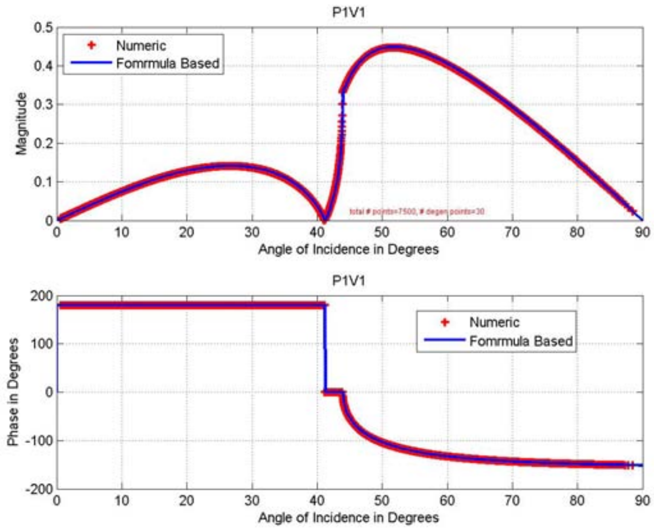

Figure 6.3: P1V1 scattering coefficient versus angle of incidence of an isotropic/isotropic interface. The model parameters are given in table 6.1.

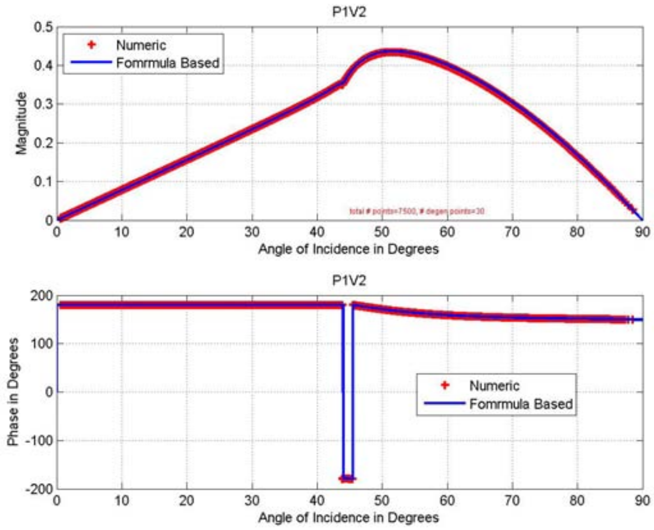

Figure 6.4: P1V2 scattering coefficient versus angle of incidence of an isotropic/isotropic interface. The model parameters are given in table 6.1.

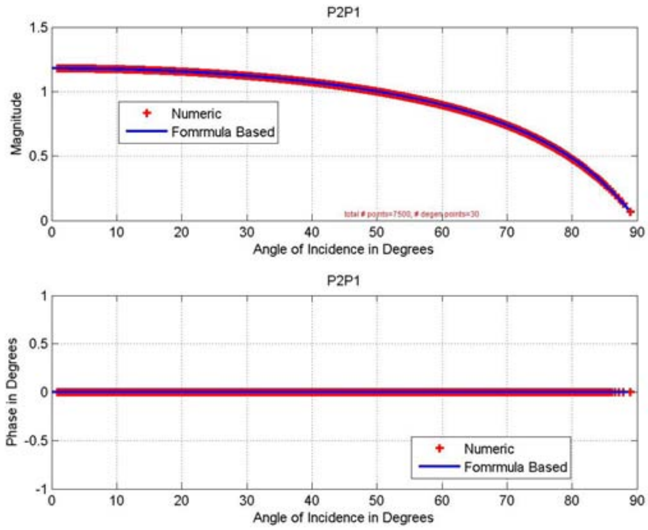

Figure 6.5: P2P1 scattering coefficient versus angle of incidence of an isotropic/isotropic interface. The model parameters are given in table 6.1.

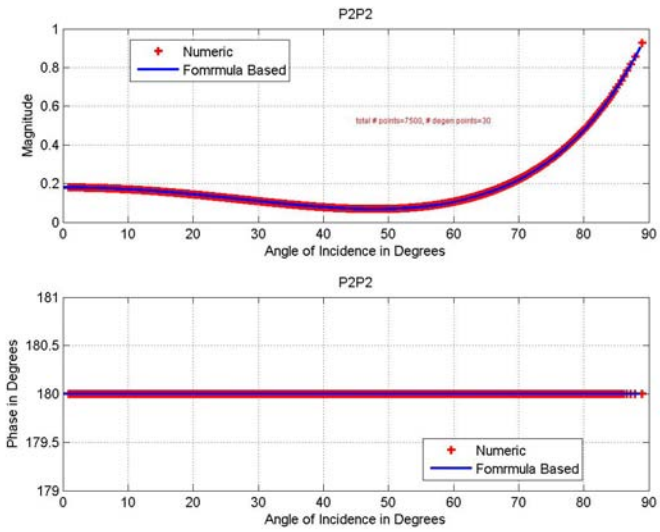

Figure 6.6: P2P2 scattering coefficient versus angle of incidence of an isotropic/isotropic interface. The model parameters are given in table 6.1.

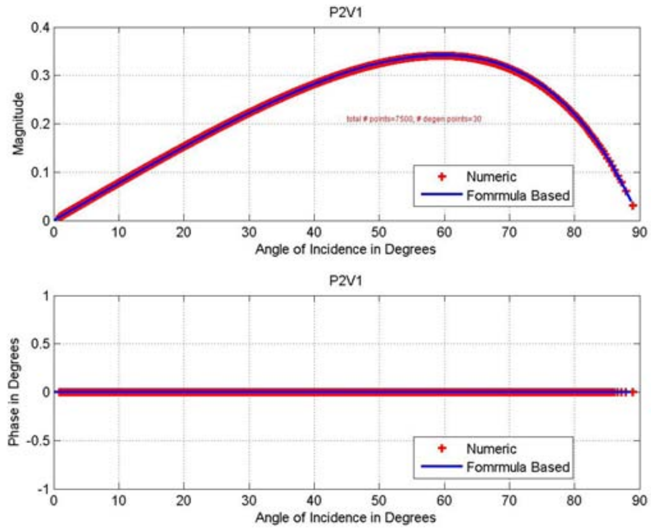

Figure 6.7: P2V1 scattering coefficient versus angle of incidence of an isotropic/isotropic interface. The model parameters are given in table 6.1.

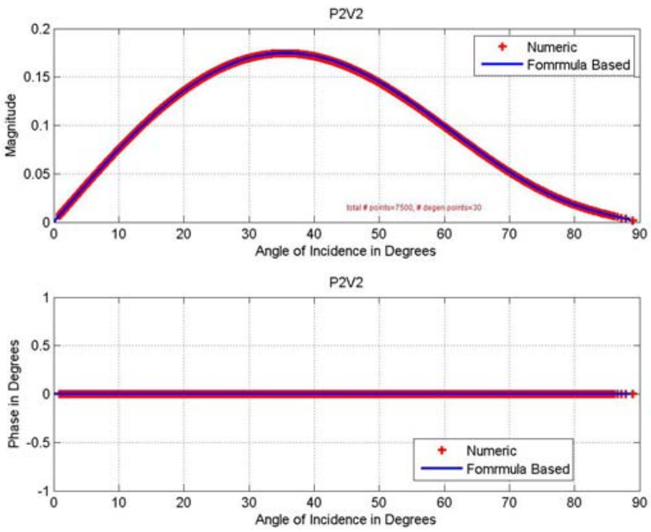

Figure 6.8: P2V2 scattering coefficient versus angle of incidence of an isotropic/isotropic interface. The model parameters are given in table 6.1.

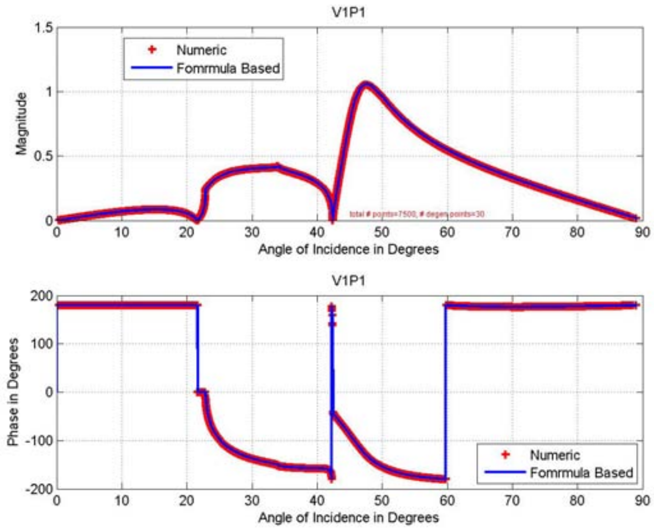

Figure 6.9: V1P1 scattering coefficient versus angle of incidence of an isotropic/isotropic interface. The model parameters are given in table 6.1.

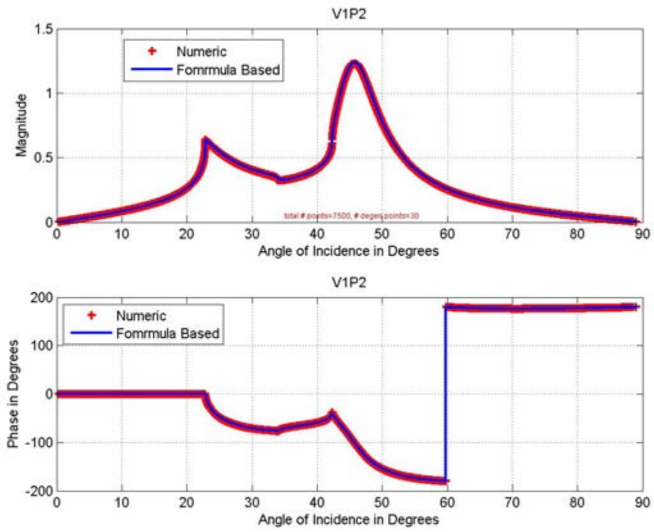

Figure 6.10: V1P2 scattering coefficient versus angle of incidence of an isotropic/isotropic interface. The model parameters are given in table 6.1.

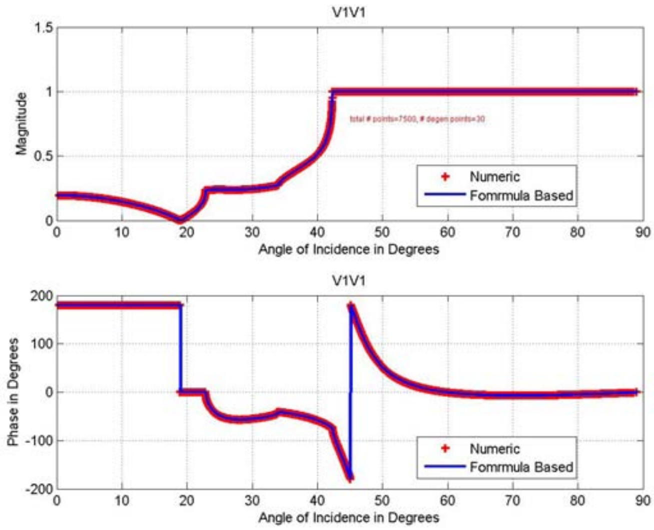

Figure 6.11: V1V1 scattering coefficient versus angle of incidence of an isotropic/isotropic interface. The model parameters are given in table 6.1.

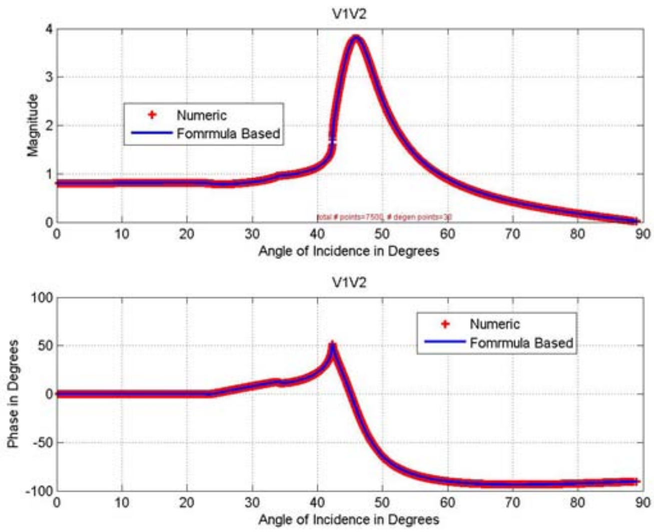

Figure 6.12: V1V2 scattering coefficient versus angle of incidence of an isotropic/isotropic interface. The model parameters are given in table 6.1.

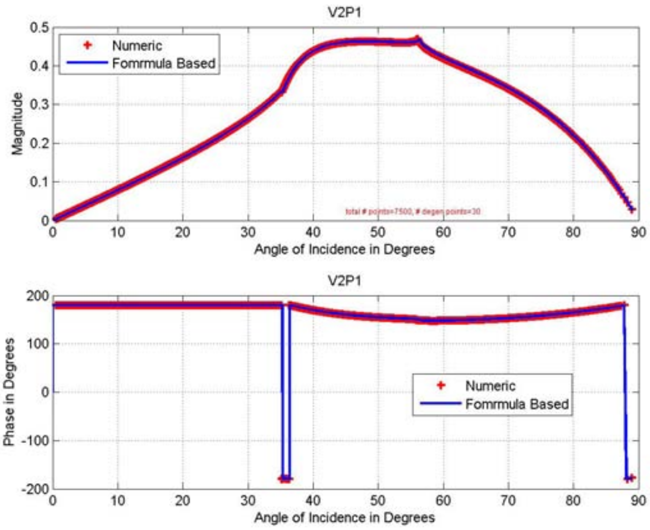

Figure 6.13: V2P1 scattering coefficient versus angle of incidence of an isotropic/isotropic interface. The model parameters are given in table 6.1.

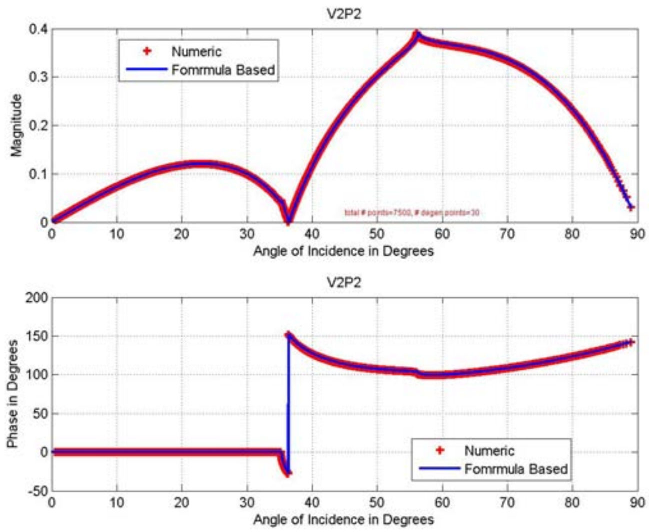

Figure 6.14: V2P2 scattering coefficient versus angle of incidence of an isotropic/isotropic interface. The model parameters are given in table 6.1.

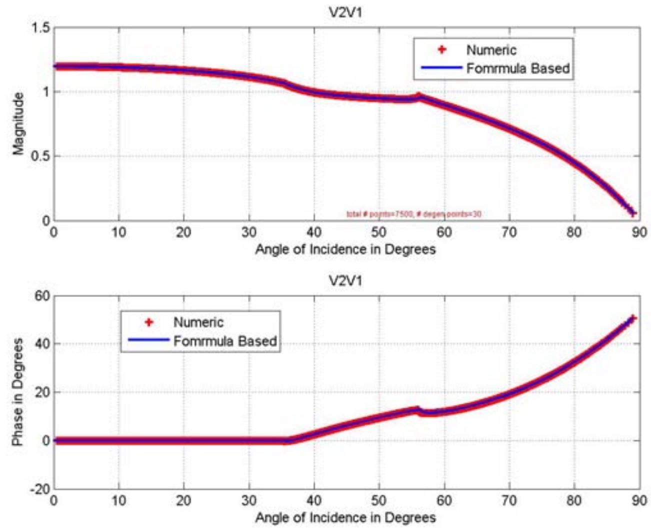

Figure 6.15: V2V1 scattering coefficient versus angle of incidence of an isotropic/isotropic interface. The model parameters are given in table 6.1.

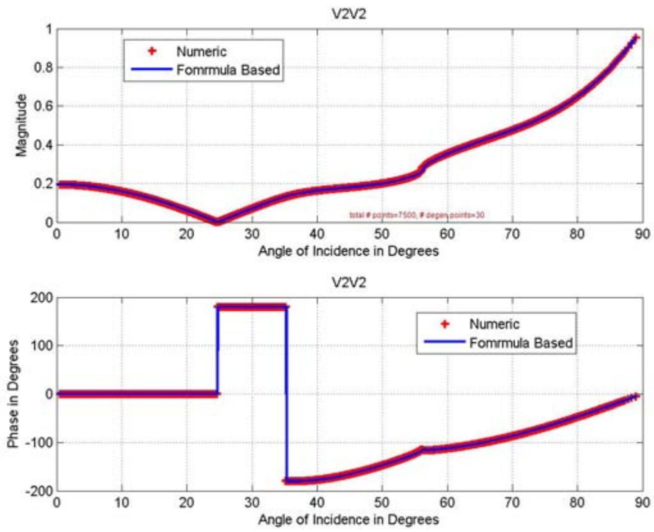

Figure 6.16: V2V2 scattering coefficient versus angle of incidence of an isotropic/isotropic interface. The model parameters are given in table 6.1.

Table 6.2: Model parameters used for constructing figures 6.17 through 6.20

Parameter	Upper Medium	Lower Medium
V_{P0}	3.30	4.20
V_{S0}	1.70	2.70
ρ	2.35	2.49
ϵ	0.10	0.00
δ	0.10	0.00

Velocities in km/s and density in g/cm^3

some appropriate medium parameters so that the medium is nearly the same but more anisotropic. For example, we can replace c_{55} with, say $c_{55} \times 1.001$.

Based on section 3.2.2, I implemented a program that calculates the exact scattering coefficients for interfaces between two VTI media. Figures 6.17 through 6.20 depict the comparison between the scattering coefficients obtained by the formula based program and the numerical program (TAVRT). The model parameters are given in table 6.2.

From these figures we can see that the scattering coefficients calculated based on formulae agree very well with the numerical results computed with TAVRT.

6.3 Tilted VTI Media

Based on chapter 5, I implemented a program that calculates the exact SH reflection and transmission coefficients for interfaces between two tilted VTI media with

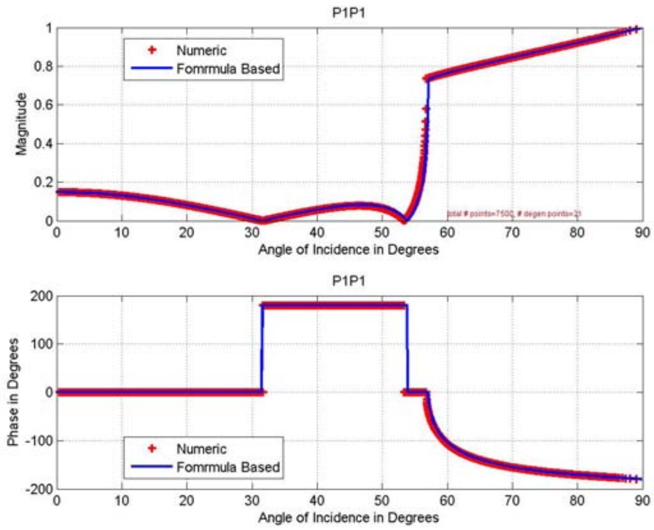

Figure 6.17: P1P1 scattering coefficient versus angle of incidence of a VTI/isotropic interface. The model parameters are given in table 6.2.

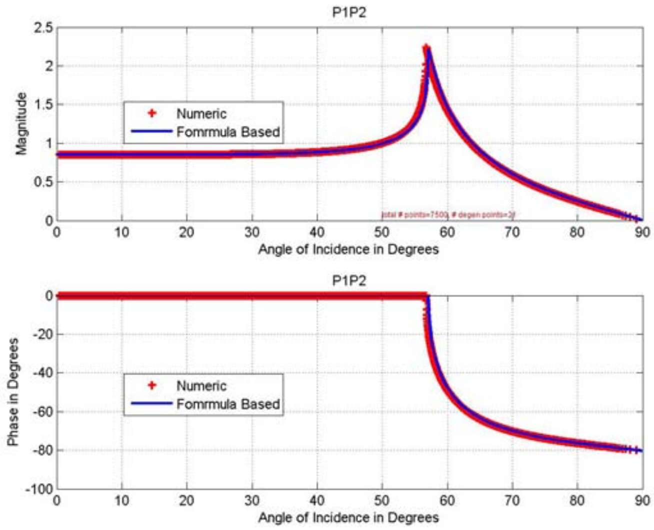

Figure 6.18: P1P2 scattering coefficient versus angle of incidence of a VTI/isotropic interface. The model parameters are given in table 6.2.

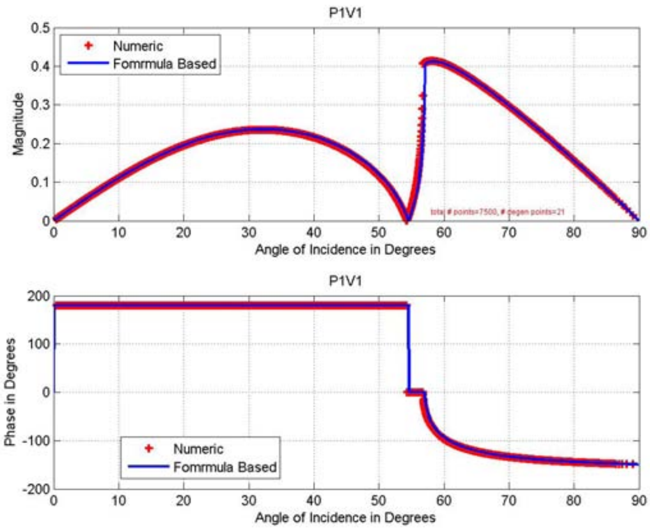

Figure 6.19: P1V1 scattering coefficient versus angle of incidence of a VTI/isotropic interface. The model parameters are given in table 6.2.

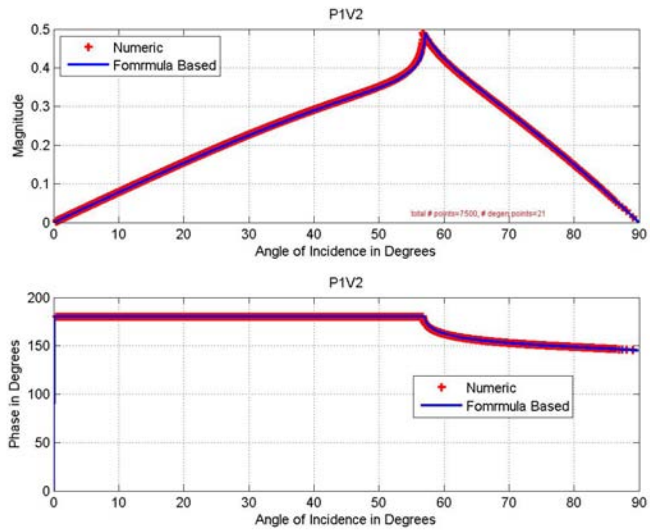

Figure 6.20: P1V2 scattering coefficient versus angle of incidence of a VTI/isotropic interface. The model parameters are given in table 6.2.

Table 6.3: Model parameters used for constructing figures 6.21 through 6.28

Parameter	Upper Medium	Lower Medium
V_{P0}	3.00	3.50
V_{S0}	2.00	2.70
ρ	2.50	2.70
ϵ	0.10	0.00
δ	0.10	0.00
γ	0.10	0.00

Velocities in km/s and density in g/cm^3

angles φ_1 and φ_2 about the x_2-axis (figure 5.1). Figures 6.21 through 6.28 depict the comparison between the scattering coefficients obtained by the formula based program and the numerical program (TAVRT). The model parameters are given in table 6.3.

From these figures we can see that the scattering coefficients calculated based on formulae agree very well with the numerical results computed with TAVRT.

6.4 HTI Media

In this section I am going to compare the results obtained numerically by the program TAVRT with the results obtained numerically by the Seismic Unix program refRealAziHTI (Rüger, 2001; Stockwell, 1997) that calculates the exact scattering coefficients for a boundary between to HTI media having the same symmetry axis direction. For a given incident wave mode, phase angle, and azimuth angle,

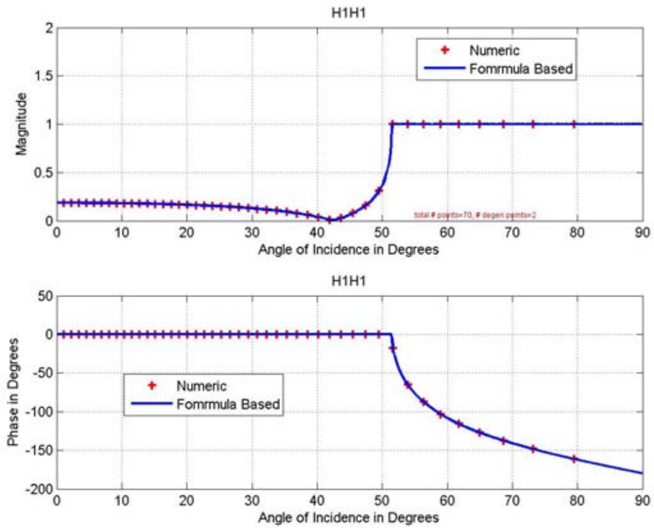

Figure 6.21: H1H1 scattering coefficient versus angle of incidence of a tilted (0^o) VTI over isotropic interface. The model parameters are given in table 6.3.

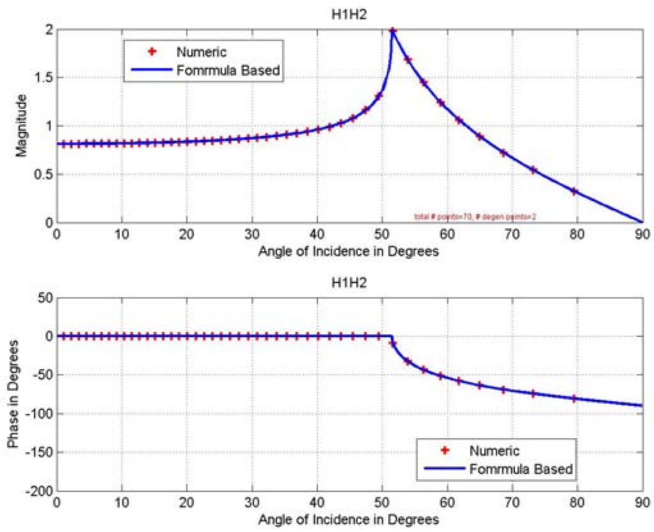

Figure 6.22: H1H2 scattering coefficient versus angle of incidence of a tilted (0^o) VTI over isotropic interface. The model parameters are given in table 6.3.

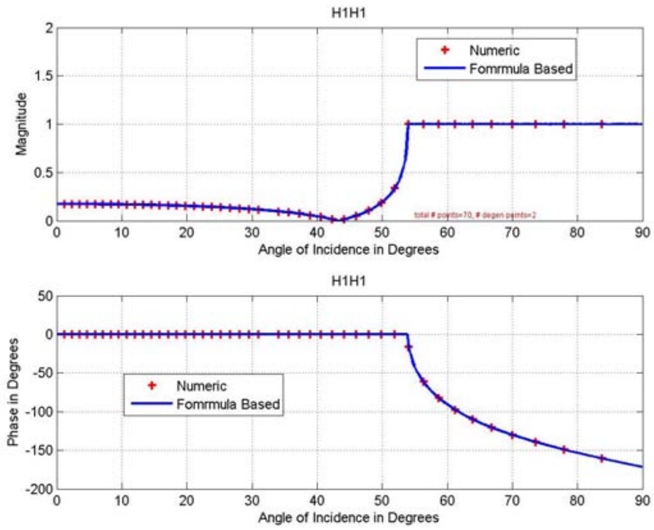

Figure 6.23: H1H1 scattering coefficient versus angle of incidence of a tilted (30^o) VTI over isotropic interface. The model parameters are given in table 6.3.

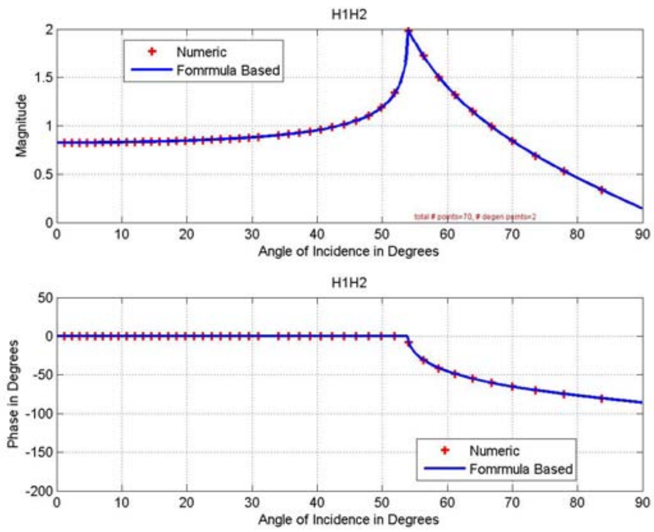

Figure 6.24: H1H2 scattering coefficient versus angle of incidence of a tilted (30^o) VTI over isotropic interface. The model parameters are given in table 6.3.

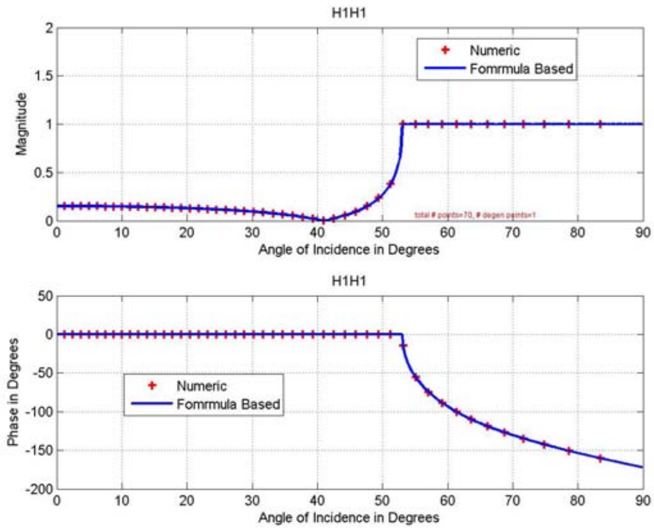

Figure 6.25: H1H1 scattering coefficient versus angle of incidence of a tilted (60^o) VTI over isotropic interface. The model parameters are given in table 6.3.

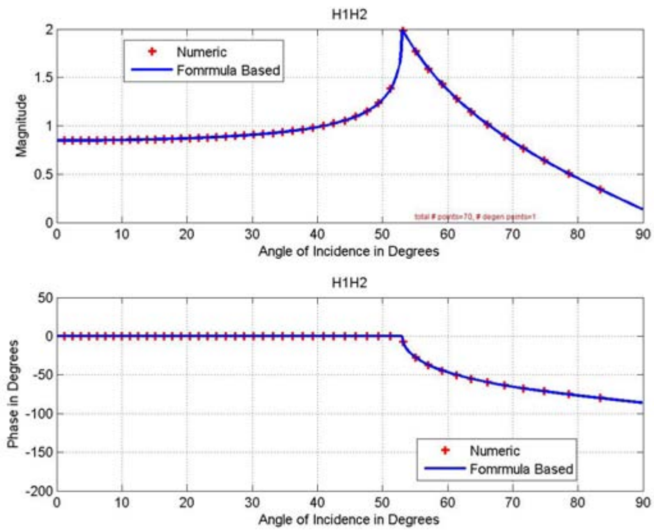

Figure 6.26: H1H2 scattering coefficient versus angle of incidence of a tilted (60^o) VTI over isotropic interface. The model parameters are given in table 6.3.

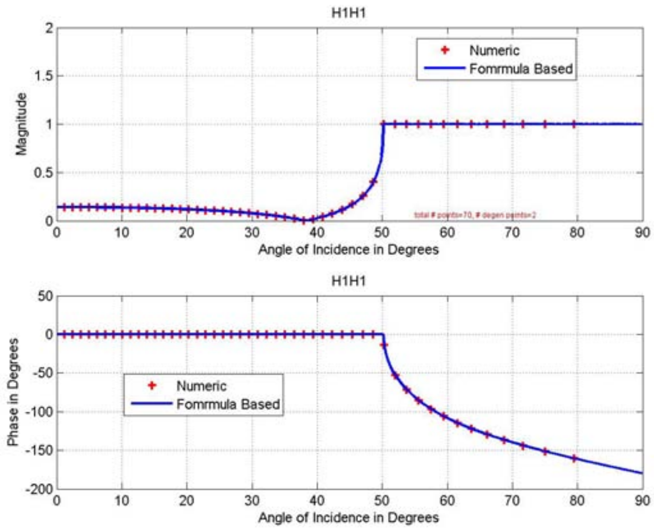

Figure 6.27: H1H1 scattering coefficient versus angle of incidence of a tilted (90^o) VTI over isotropic interface. The model parameters are given in table 6.3.

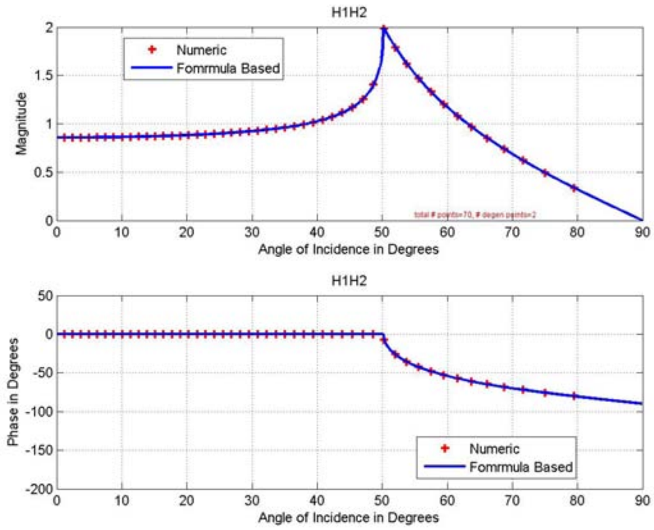

Figure 6.28: H1H2 scattering coefficient versus angle of incidence of a tilted (90^o) VTI over isotropic interface. The model parameters are given in table 6.3.

Table 6.4: Model parameters used for constructing figure 6.29

Parameter	Upper Medium	Lower Medium
V_{P0}	2.260	2.370
V_{S0}	1.428	1.360
ρ	2.600	2.700
ϵ	0.000	0.050
δ	0.000	0.020
γ	0.000	0.100

Velocities in km/s and density in g/cm^3

refRealAziHTI starts by computing the phase velocity and the horizontal slowness. Then the Christoffel equation is used to determine the vertical slowness components which will be sorted to determine the different wave modes. The next step of the algorithm would be to calculate the polarization vectors. The final step would be to solve the system resulting from applying the welded contact boundary conditions to the interface for the scattering coefficients.

Figures 6.29 depicts the P-wave reflection coefficient as a function of incidence and azimuthal angles of an isotropic/HTI interface obtained by refRealAziHTI and by TAVRT. The model parameters are given in table 6.4.

From figure 6.29 we can see that the scattering coefficient calculated based on the two numerical programs refRealAziHTI and TAVRT agree very well with each other.

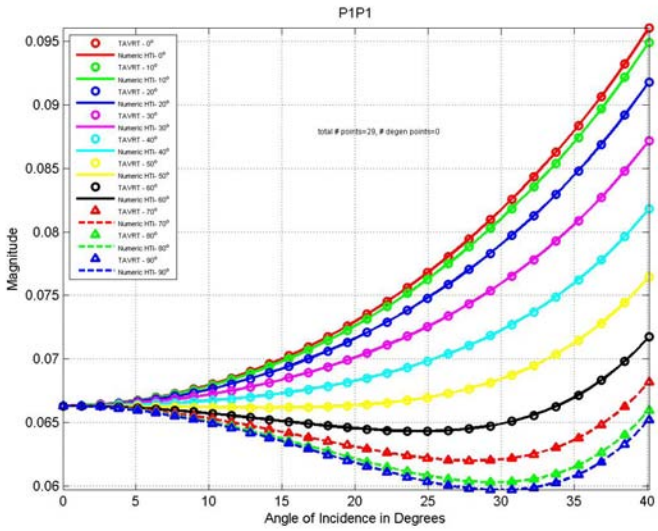

Figure 6.29: H1H1 scattering coefficient of an isotropic/HTI interface. The model parameters are given in table 6.4.

6.5 Monoclinic Media

Based on section 3.2.3, I implemented a program that calculates the exact SH-wave scattering coefficients for interfaces between two monoclinic media. Figures 6.30 and 6.31 depict the comparison between the scattering coefficients obtained by the formula based program and the numerical program (TAVRT). The model parameters are given in table 6.5.

From these figures we can see that the scattering coefficients calculated based on formulae agree very well with the numerical results computed with TAVRT.

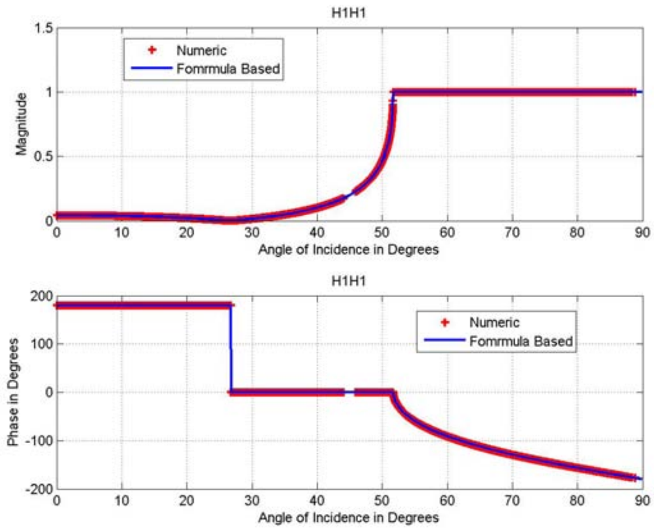

Figure 6.30: H1H1 scattering coefficient of an isotropic/monoclinic interface. The model parameters are given in table 6.5.

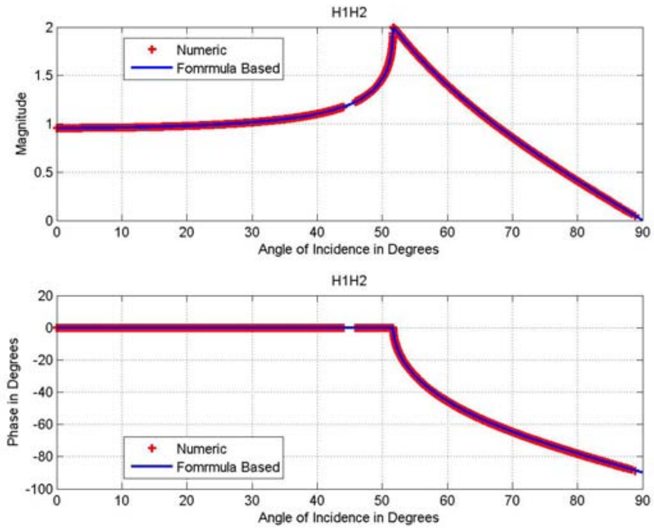

Figure 6.31: H1H2 scattering coefficient of an isotropic/monoclinic interface. The model parameters are given in table 6.5.

Table 6.5: Model parameters used for constructing figures 6.30 and 6.31

Parameter	Upper Medium	Lower Medium
c_{44}	10.00	11.00
c_{46}	0.00	-7.00
c_{66}	10.00	22.00
ρ	2.500	2.700

Stiffness elements in GPa and density in g/cm^3

Chapter 7

Conclusion and Possible Extensions

7.1 Conclusion

The program TAVRT was tested for isotropic, VTI and monoclinic anisotropic media. The results matched very well the results of the scattering coefficients formulae found in the literature. TAVRT was also tested for the HTI case and the results matched very well the results of the Seismic Unix program refRealAziHTI (Rüger, 2001; Stockwell, 1997) which computes the exact scattering coefficients numerically for interfaces between two HTI media having the same symmetry plane.

The results of the derived SH-wave scattering coefficients formulae for an interface between two tilted VTI media with angles φ_1 and φ_2 about the x_2-axis (figure 5.1) matched very well the results of the program TAVRT.

The program TAVRT can be used to check the validity of new derived exact and approximate scattering coefficients and group velocity formulae. It can also be used to analyze very complex anisotropic media.

For tilted VTI media, the scattering coefficients vary with tilt, but they are unaffected by the sign of the tilt angle of the lower medium, i.e., the scattering coefficients for an interface between two tilted VTI media with angles φ_1 and φ_2 and the scattering coefficients for an interface between two tilted VTI media with angles φ_1 and $-\varphi_2$ are equal.

For tilted VTI media, and pre-critical angle of incidence, the magnitude of the reflection coefficient decreases as the absolute value of the tilt angle of the upper medium φ_1 increases and the magnitude of the transmission coefficient increases as the absolute value of the tilt angle of the upper medium φ_1 increases.

In general, the angle of incidence and the angle of reflection are different for tilted VTI media.

7.2 Possible Extensions

The program TAVRT has some provisions to treat the anelastic (viscoelastic) case for dissipative media, but is not fully developed. More work is needed to make it fully operational.

Although, slightly modifying the medium parameters, to avoid degeneracy works well, a more rigorous mathematical investigation is desirable to overcome the problem.

Currently, TAVRT expects horizontal slowness values s_1 as input and can be extended to accept phase and ray angles of incidence as well. However, phase and ray angles that correspond to the horizontal slowness values s_1 are computed in the program, and can be used to make plots of scattering coefficients against phase or ray angles.

Scattering coefficients formulae for arbitrary tilt angles (not only about the x_2-axis) can be derived for the SH-wave propagating in tilted VTI media as well as deriving scattering formulae for a P-wave and SV-wave propagating in tilted VTI media.

References

Aki, K., and Richards, P. G., 1980, Quantitative seismology: Theory and methods, volume 1: W. H. Freeman and Co.

Backus, G. E., 1962, Long-wave elastic anisotropy produced by horizontal layering: Journal of Geophysical Research, **67**, 4427–4440.

Bakulin, A., Grechka, V., and Tsvankin, I., 2000b, Estimation of fracture parameters from reflection seismic data. part ii: Fractured models with orthorhombic symmetry: Geophysics, **65**, 1803–1817.

Carcione, J. M., 2001, Wave fields in real media: Wave propagation in anisotropic, anelastic and porous media: PERGAMON.

Daley, P. F., and Hron, F., 1977, Reflection and transmission coefficients for transversely isotropic solids: Bull. Seis. Soc. Am., **67**, 661–675.

Goldstein, H., 1980, Classical mechanics: Addison-Wesley.

Graebner, M., 1992, Plane-wave reflection and transmission coefficients for a transversely isotropic solid (short note): Geophysics, **57**, 1512–1519.

Krebes, E. S., 2001, Seismic theory and methods - course notes, second edition: University of Calgary.

Mavko, G., Mukerji, T., and Dvorken, J., 2003, The rock physics handbook: Tools for seismic analysis in porous media: Cambridge University Press.

Rüger, A., 2001, Reflection coefficients and azimuthal AVO analysis in anisotropic media: Society of Exploration Geophysicists.

Slawinski, M. A., 2003, Seismic waves and rays in elastic media: PERGAMON.

Stockwell, J. W. J., 1997, Free software in education: A case study of CWP/SU: Seismic unix: The Leading Edge, **16**, 1045–1049.

Thomsen, L., 1986, Weak elastic anisotropy: Geophysics, **51(10)**, 1954–1966.

Thomsen, L., 2002, Understanding seismic anisotropy in exploration and exploitation: SEG 2002 Distinguished Instructor Short Course.

Tsvankin, I., 2005, Seismic signatures and analysis of reflection data in anisotropic media: ELSEVIER.

Appendix A

Calculation of Vertical Slownesses

In this appendix I present explicitly the sixth degree polynomial of s_3. Equation 4.19 of the main text, can be rewritten as follows:

$$\left|\boldsymbol{S}\boldsymbol{A}\boldsymbol{S}^T - I_{(3)}\right| = 0 \tag{A.1}$$

where $\boldsymbol{A}$ is the density normalized stiffness matrix.

Using MATLAB's symbolic math, the sixth degree polynomial of s_3 is

$$A + B\, s_3 + C\, s_3^2 + D\, s_3^3 + E\, s_3^4 + F\, s_3^5 + G\, s_3^6 = 0 \tag{A.2}$$

where

$$\begin{aligned}
A &= -c_{35}^2\, c_{44} + 2 * c_{34}\, c_{35}\, c_{45} - c_{33}\, c_{45}^2 - c_{34}^2\, c_{55} + c_{33}\, c_{44}\, c_{55} \\
B &= 2 * \Big[- c_{15}\, c_{34}^2 + c_{14}\, c_{34}\, c_{35} + c_{15}\, c_{33}\, c_{44} - c_{13}\, c_{35}\, c_{44} - c_{14}\, c_{33}\, c_{45} \\
&\quad + c_{13}\, c_{34}\, c_{45} + c_{35}\, c_{36}\, c_{45} - c_{35}^2\, c_{46} - c_{34}\, c_{36}\, c_{55} + c_{33}\, c_{46}\, c_{55} \\
&\quad + c_{34}\, c_{35}\, c_{56} - c_{33}\, c_{45}\, c_{56} \Big] s_1
\end{aligned}$$

$$
\begin{aligned}
C &= c_{34}^2 + c_{35}^2 - c_{33}\,c_{44} + c_{45}^2 - (c_{33} + c_{44})\,c_{55} \\
&+ \Big[- c_{14}^2\,c_{33} - c_{11}\,c_{34}^2 + 2 * c_{16}\,c_{34}\,c_{35} - 4 * c_{15}\,c_{34}\,c_{36} \\
&- c_{13}^2\,c_{44} + c_{11}\,c_{33}\,c_{44} + 2 * c_{15}\,c_{35}\,c_{44} - 2 * c_{16}\,c_{33}\,c_{45} \\
&- 2 * c_{15}\,c_{34}\,c_{45} + 2 * c_{13}\,c_{36}\,c_{45} + 2 * c_{13}\,c_{45}^2 + 4 * c_{15}\,c_{33}\,c_{46} \\
&- 4 * c_{13}\,c_{35}\,c_{46} - c_{36}^2\,c_{55} - 2 * c_{13}\,c_{44}\,c_{55} + 2 * c_{13}\,c_{34}\,c_{56} \\
&+ 2 * c_{35}\,c_{36}\,c_{56} - c_{33}\,c_{56}^2 + 2 * c_{14}\,(c_{35}\,(c_{36} - c_{45}) \\
&+ c_{34}\,(c_{13} + c_{55}) - c_{33}\,c_{56}) - c_{35}^2\,c_{66} + c_{33}\,c_{55}\,c_{66} \Big] s_1^2 \\
D &= 2 * \Big[c_{35}\,(c_{13} - c_{44}) - c_{15}\,(c_{33} + c_{44}) + c_{34}\,(c_{36} + c_{45}) \\
&- c_{46}\,(c_{33} + c_{55}) + c_{45}\,(c_{14} + c_{56}) \Big] s_1 - 2 \Big[c_{14}^2\,c_{35} \\
&+ c_{11}\,c_{34}\,c_{36} - c_{16}\,c_{35}\,c_{36} + c_{15}\,c_{36}^2 - c_{11}\,c_{35}\,c_{44} \\
&+ c_{11}\,c_{34}\,c_{45} + c_{16}\,c_{35}\,c_{45} + c_{15}\,c_{36}\,c_{45} + c_{13}^2\,c_{46} \\
&- c_{11}\,c_{33}\,c_{46} - 2 * c_{15}\,c_{35}\,c_{46} - c_{16}\,c_{34}\,c_{55} + c_{16}\,c_{33}\,c_{56} \\
&+ c_{15}\,c_{34}\,c_{56} + c_{14}\,(c_{16}\,c_{33} - c_{15}\,c_{34} - c_{13}\,(c_{36} + c_{45}) \\
&- c_{36}\,c_{55} + c_{35}\,c_{56}) - c_{15}\,c_{33}\,c_{66} + c_{13}\,(-c_{16}\,c_{34} + c_{15}\,c_{44} \\
&+ 2 * c_{46}\,c_{55} - (c_{36} + 2 * c_{45})\,c_{56} + c_{35}\,c_{66}) \Big] s_1^3
\end{aligned}
$$

$$
\begin{aligned}
E &= c_{33} + c_{44} + c_{55} + \Big[c_{13}^2 + c_{14}^2 - 2*c_{15}\,c_{35} - c_{11}\,(c_{33} + c_{44}) \\
&\quad +2*c_{16}\,c_{45} + (c_{36} + c_{45})^2 - 4*(c_{15} + c_{35})\,c_{46} + 2*c_{13}\,c_{55} \\
&\quad -c_{44}\,c_{55} + 2*(c_{14} + c_{34})\,c_{56} + c_{56}^2 - (c_{33} + c_{55})\,c_{66}\Big]s_1^2 \\
&\quad +\Big[-c_{16}^2\,c_{33} - c_{11}\,c_{36}^2 - c_{15}^2\,c_{44} - 2*c_{11}\,c_{36}\,c_{45} \\
&\quad -c_{11}\,c_{45}^2 - 4*c_{13}\,c_{15}\,c_{46} + 4*c_{11}\,c_{35}\,c_{46} - c_{14}^2\,c_{55} \\
&\quad +c_{11}\,c_{44}\,c_{55} - 2*c_{11}\,c_{34}\,c_{56} - 2*c_{15}\,c_{36}\,c_{56} + 2*c_{13}\,c_{56}^2 \\
&\quad +2*c_{14}\,(c_{15}\,(c_{36} + c_{45}) + c_{13}\,c_{56}) + 2*c_{16}\,(c_{15}\,c_{34} \\
&\quad +c_{13}\,(c_{36} + c_{45}) + c_{36}\,c_{55} - c_{35}\,(2\,c_{14} + c_{56})) - c_{13}^2\,c_{66} \\
&\quad +c_{11}\,c_{33}\,c_{66} + 2*c_{15}\,c_{35}\,c_{66} - 2*c_{13}\,c_{55}\,c_{66}\Big]s_1^4 \\
F &= 2*\Big[c_{15} + c_{35} + c_{46}\Big]s_1 \\
&\quad +2*\Big[c_{13}\,c_{15} + c_{14}\,c_{16} - c_{11}\,(c_{35} + c_{46}) - c_{46}\,c_{55} \\
&\quad +(c_{16} + c_{36} + c_{45})\,c_{56} - (c_{15} + c_{35})\,c_{66}\Big]s_1^3 \\
&\quad +2*\Big[-c_{16}^2\,c_{35} - c_{15}^2\,c_{46} + c_{16}\,(c_{15}\,(c_{36} + c_{45}) - c_{14}\,c_{55} \\
&\quad +c_{13}\,c_{56}) + c_{15}\,(c_{14}\,c_{56} - c_{13}\,c_{66}) + c_{11}\,(c_{46}\,c_{55} \\
&\quad -(c_{36} + c_{45})\,c_{56} + c_{35}\,c_{66})\Big]s_1^5 \\
G &= -1 + \Big[c_{11} + c_{55} + c_{66}\Big]s_1^2 \\
&\quad +\Big[c_{15}^2 + c_{16}^2 - c_{11}\,c_{55} + c_{56}^2 - (c_{11} + c_{55})\,c_{66}\Big]s_1^4 \\
&\quad +\Big[-c_{16}^2\,c_{55} + 2*c_{15}\,c_{16}\,c_{56} - c_{11}\,c_{56}^2 - c_{15}^2\,c_{66} + c_{11}\,c_{55}\,c_{66}\Big]s_1^6
\end{aligned}
$$